

University of Natural Resources and Life Sciences, Vienna

Department of Water, Atmosphere and Environment

Institute of Hydraulics and Rural Water Management

Head: Univ.Prof. DI Dr. Willibald Loiskandl



Supervisor

Univ.Prof. DI Dr. Willibald Loiskandl, Institute of Hydraulics and Rural Water Management

Advisory board

Ass.Prof. DI Dr. Peter Cepuder, Institute of Hydraulics and Rural Water Management

Ass.Prof. DI Dr. Gerhard Kammerer, Institute of Hydraulics and Rural Water Management

Ao.Univ.Prof. DI Dr. Josef Eitzinger, Institute of Meteorology

Ao.Univ.Prof.i.R. Dr. Franz Konecny, Institute of Mathematics

Performance assessment of selected devices for monitoring soil water balance components with respect to agricultural water management

DI Reinhard Nolz

Dissertation to obtain the academic degree of Dr. nat. techn. at the University of Natural Resources and Life Sciences, Vienna

Vienna, February 2013

Acknowledgement

As this thesis has greatly benefitted from some wonderful teamwork, I would like to thank all my colleagues from the Institute of Hydraulics and Rural Water Management. Above all, I am most grateful to my supervisor Prof. Willibald Loiskandl and advisors Dr. Peter Cepuder and Dr. Gerhard Kammerer for their generous advice, help and support. I also want to thank my colleagues Dr. Margarita Himmelbauer, Dr. Gerlinde Scholl, and DI Stefan Strohmeier for fruitful discussions about scientific issues and beyond; Friedrich Forster and Karl Haigner for field work; DI(FH) Martina Faulhammer and Christian Paulsen for the work in the laboratory; and Wolfgang Sokol for the technical assistance.

I would like to express my gratitude to Dr. Josef Eitzinger, Dr. Herbert Formayer, Wolfgang Laube, and Dr. Erich Mursch-Radlgruber from the Institute of Meteorology for scientific advice and technical support.

I also want to thank Dr. Franz Konecny from the Institute of Mathematics for scientific advice.

I thank our colleagues at the experimental site in Groß-Enzersdorf, in particular Susanne Stickler, for maintaining the lysimeter facility; and Franz Gansberger for maintaining the wireless monitoring network.

I gratefully acknowledge the staff members of Adcon Telemetry, especially Martin Hackl and Philip Vatter for technical support.

Finally, I thank all the known and anonymous reviewers for their helpful comments.

This work is lovingly dedicated to my family.

Abstract

Knowledge about the water cycle and its components is crucial for various environmental topics, in particular agricultural water management. Lysimeters and soil water status sensors are frequently used for water balance studies. In order to obtain valuable data, measurement systems should be state-of-the-art regarding configuration and data management. There are two main objectives of this thesis, the performance assessment of: (1) a weighing lysimeter facility and (2) selected soil water sensors integrated into a remote monitoring network.

(1) The weighing lysimeter facility in Groß-Enzersdorf (Austria) operates with a lever-arm-counterbalance-weighing system. Experiments have shown that the weighing system itself is subject to mechanical oscillations and that disturbances such as wind gusts significantly decrease measuring accuracy. The measuring accuracy for a wind velocity $<5 \text{ m}\cdot\text{s}^{-1}$ was approximately $\pm 0.4 \text{ kg}$ (equivalent to $\pm 0.14 \text{ mm}$ water ponding), at higher wind velocities the accuracy was about three times lower. By using data from special measurements, theoretical verification was obtained to improve the accuracy by modifying the averaging process, which is applied on raw data before they are stored. As alternative data processing is required to smoothen data severely affected by wind, a natural cubic approximation spline and a basic piecewise sigmoid function were tested on a representative dataset including noisy weighing data. The sigmoid function was straightforward to fit and gave sound results of typical diurnal variations of evapotranspiration, but its application was restricted to datasets of single days without rainfall. The spline function performed generally better on the entire dataset, but it was necessary to make a time-consuming adjustment to the smoothing factor in several cases.

(2) Two types of matric potential sensors (Watermark and MPS-1), and two multi-sensor capacitance probes for measuring soil water content (AquaCheck and EnviroSCAN) were evaluated. A general calibration function was determined for the Watermark sensors using pressure plate apparatus. The advantage of a general calibration function is that single sensors of a monitoring system can be exchanged easily. However, a sensor-specific calibration is recommended for increased measurement accuracy. For the MPS-1, sensor-specific calibrations became essential due to very high inter-sensor-variability. The MPS-1 were also calibrated in a pressure plate apparatus, and four different calibration functions were set up and evaluated. During a drying experiment in a thin soil layer, both sensor types delivered water potential measurements in a range from 10 kPa to 600 kPa. At pressures higher 130 kPa the Watermark sensors responded significantly slower than the MPS-1, probably due to reaching equilibrium status faster with the thin ceramic disk of the MPS-1. A pairwise comparison of AquaCheck and EnviroSCAN readings in the respective depth showed considerable variations between single sensors of the AquaCheck probe despite factory normalization. Since soil type was the same within the profile, it is recommended to improve sensor normalization or perform sensor-specific calibrations. Furthermore, AquaCheck readings were more overly sensitive to irrigation and rainfall, possibly due to a tendency for preferential flow along the probe due to the specific installation method.

Keywords: accuracy, calibration, data management, lysimeter, soil water sensors, matric potential, water content, field, laboratory, measurement

Kurzfassung

Die Kenntnis des Wasserhaushalts und seiner Komponenten ist für viele Umweltthemen, vor allem im Bereich landeskulturelle Wasserwirtschaft, von großer Bedeutung. Sehr häufig kommen für Wasserbilanzstudien Lysimeter und Bodenwassersensoren zum Einsatz. Um brauchbare Daten zu erhalten sollten Messsysteme in Bezug auf Ausstattung und Datenmanagement auf dem neusten Stand der Technik sein. Die beiden Hauptziele dieser Arbeit waren die Leistungsbewertung (1) einer Lysimeteranlage und (2) ausgewählter Bodenwassersensoren, welche in ein Netzwerk zur Fernüberwachung integriert wurden.

(1) Die Lysimeteranlage in Groß-Enzersdorf (Österreich) arbeitet mit einem Hebelarm-Gegengewichts-Wiegesystem. Experimente haben gezeigt, dass das Wiegesystem mechanischen Schwingungen unterworfen ist, und dass Störungen, zum Beispiel durch Windböen verursachte, die Messgenauigkeit deutlich verringern. Die Messgenauigkeit für Windgeschwindigkeiten $< 5 \text{ m}\cdot\text{s}^{-1}$ betrug ungefähr $\pm 0,4 \text{ kg}$ (entspricht einer Wasserhöhe von $\pm 0,14 \text{ mm}$), bei höheren Windgeschwindigkeiten war die Genauigkeit etwa dreimal geringer. Anhand von speziellen Messdaten wurde versucht, die Messgenauigkeit durch Modifikation des Mittelungsverfahrens, welches zur Glättung der Rohdaten vor deren Speicherung verwendet wird, zu verbessern. Für stark beeinflusste Wiegedaten ist jedoch eine alternative Datenaufbereitung der Rohdaten erforderlich. In diesem Zusammenhang wurden eine polynomische Splinefunktion und eine stückweise Sigmoidfunktion an einer repräsentativen Datenreihe mit verrauschten Wiegedaten getestet. Die Sigmoidfunktion konnte gut angepasst werden und lieferte brauchbare Ergebnisse von typischen Tagesgängen der Verdunstung, wobei aber die Anpassung nur an einzelnen Tagen ohne Niederschlag möglich war. Die Splinefunktion konnte problemlos an die gesamte Datenreihe angepasst werden, jedoch musste der Glättungsfaktor in einigen Fällen zeitaufwendig nachjustiert werden.

(2) Zwei Arten von Matrixpotenzialsensoren (Watermark und MPS-1) und zwei kapazitative Rohrsonden zur Wasseranteilmessung (AquaCheck und EnviroSCAN) wurden evaluiert. Für die Watermark Sensoren wurde mittels Druckplattenapparat eine generelle Kalibrierfunktion ermittelt. Der Vorteil dieser allgemeinen Kalibrierfunktion ist, dass einzelne Sensoren in einem Netzwerk problemlos ausgetauscht werden können. Zur Minimierung des Messfehlers empfiehlt sich jedoch eine sensorspezifische Kalibrierung. Für den MPS-1 erwies sich aufgrund der großen Unterschiede zwischen den Sensoren eine sensorspezifische Kalibrierung als notwendig. Die MPS-1 Sensoren wurden ebenfalls mittels Druckplattenapparat kalibriert; als Ergebnis dabei wurden vier verschiedene Kalibrierfunktionen aufgestellt und evaluiert. Während eines Austrocknungsexperiments in einer dünnen Bodenschicht lieferten beide Sensortypen Matrixpotenzialwerte zwischen 10 kPa und 600 kPa. Bei Drücken größer 130 kPa reagierten die Watermark Sensoren deutlich langsamer als die MPS-1, wahrscheinlich weil sich in der dünnen Keramikscheibe des MPS-1 der Gleichgewichtszustand schneller einstellt. Der paarweise Vergleich von AquaCheck und EnviroSCAN Messwerten in der entsprechenden Tiefe zeigte, dass sich die einzelnen Sensoren der AquaCheck Sonde trotz Werksnormalisierung unterschiedlich verhielten. Da die Bodenart innerhalb des Messprofils die gleiche war, können diese

Unterschiede nur durch Verbesserung der Normalisierung oder durch sensorspezifische Kalibrierung ausgeglichen werden. Darüber hinaus reagierten AquaCheck Messungen sehr stark auf Bewässerung und Regen, da sich vermutlich aufgrund der Einbaumethode spezielle Fließwege entlang des Sondenrohres ausgebildet haben.

Schlüsselwörter: Messgenauigkeit, Kalibrierung, Datenmanagement, Lysimeter, Bodenwassersensor, Matrixpotenzial, Wasseranteil, Feld, Labor, Messung

Content

1	Structure of the thesis.....	1
1.1	List of papers.....	1
2	General introduction	2
3	Overall objectives and overview.....	4
4	Interpretation of lysimeter weighing data affected by wind	6
4.1	Introduction.....	7
4.2	Materials and methods	8
4.2.1	Measurement accuracy regarding wind effects	10
4.2.2	Oscillation behavior	11
4.2.3	Mechanical performance of the system.....	11
4.2.4	Averaging procedure	11
4.3	Results and discussion	12
4.3.1	Measurement accuracy regarding wind effects	12
4.3.2	Oscillation behavior	15
4.3.3	Mechanical performance of the system.....	16
4.3.4	Averaging procedure	17
4.4	Conclusions	19
4.5	References	20
5	Improving interpretation of lysimeter weighing data	22
5.1	Introduction.....	23
5.2	Materials and methods	24
5.2.1	Data acquisition and water balance	24
5.2.2	Data management	25
5.2.3	Fitting smoothing functions	27
5.3	Results and discussion	27
5.4	Conclusions	34
5.5	References	34
6	Calibrating soil water potential sensors integrated into a wireless monitoring network ..	36
6.1	Introduction.....	37
6.2	Materials and methods	39

6.2.1	Sensor setup	39
6.2.2	Sensor calibration	40
6.2.3	Evaluation of calibrations	43
6.2.4	Comparison of sensors	43
6.3	Results and discussion	44
6.3.1	Watermark calibration	44
6.3.2	MPS-1 test.....	46
6.3.3	MPS-1 calibration	46
6.3.4	Evaluation of the calibrations	50
6.3.5	Comparison of sensors	50
6.4	Conclusions	51
6.5	References	52
7	Comparison of EnviroSCAN and AquaCheck capacitance probe for multi-depth soil water monitoring	56
7.1	Introduction and objectives	57
7.2	Materials and methods	57
7.3	Results and discussion	59
7.4	Conclusions	64
7.5	References	64
8	Weather data as basis for calculating reference evapotranspiration on an irrigation trial plot within a vineyard	66
8.1	Introduction.....	67
8.2	Materials and methods	67
8.3	Results and discussion	69
8.4	Conclusions	73
8.5	References	73
9	Remote monitoring of a novel irrigation system in a vineyard.....	74
9.1	Introduction.....	75
9.2	Materials and methods	75
9.3	Results and discussion	77
9.4	Conclusions	79
9.5	References	80

10	Summary.....	81
10.1	Performance assessment of a weighing lysimeter facility and evaluation of adapted interpretation tools with respect to enhanced data management.....	81
10.2	Performance assessment of approved as well as novel soil water sensors integrated into a remote monitoring network.....	82
10.3	Performance assessment of a field weather station with respect to estimation of evapotranspiration.....	83
10.4	Performance assessment of the serviceability of a sophisticated remote monitoring station for irrigation management	84
11	General references	85
12	List of tables	88
13	List of figures.....	89

1 Structure of the thesis

This cumulative dissertation consists of 13 chapters. A general introduction in chapter 2 provides an overview on monitoring of water balance components, particularly soil water status, as key topic of the work, leading over to the overall objectives of the thesis in chapter 3. The subsequent independent chapters 4 to 9 contain six papers that were published either in a scientific journal or in conference proceedings. These chapters represent the central part of the doctoral thesis as regards content, while the other chapters build a framework that is completed with a summary in chapter 10, general references in chapter 11, and a list of tables and figures in chapter 12 and 13, respectively.

1.1 List of papers

Nolz R., Kammerer G., Cepuder P., 2013. Interpretation of lysimeter weighing data affected by wind. *Journal of Plant Nutrition and Soil Science*. doi 10.1002/jpln.201200342 (in press) [SCI]

(Chapter 4)

Nolz R., Kammerer G., Cepuder P., 2013. Improving interpretation of lysimeter weighing data. *Journal for Land Management, Food and Environment (Die Bodenkultur)* (accepted)

(Chapter 5)

Nolz R., Kammerer G., Cepuder P., 2013. Calibrating soil water potential sensors integrated into a wireless monitoring network. *Agricultural Water Management* 116, 12-20. doi 10.1016/j.agwat.2012.10.002 [SCI]

(Chapter 6)

Nolz R., 2012. Comparison of Enviroscan and Aquacheck capacitance probe for multi-depth soil water monitoring. In: A. Celkova, Institute of Hydrology SAS (Ed.), 20th Int. Poster Day: Transport of water, chemicals and energy in the soil-plant-atmosphere system, Nov. 2012, Bratislava, Slovakia, 496-503. [Conf. Proc.]

(Chapter 7)

Nolz R., Cepuder P., 2011. Weather data as basis for calculating reference evapotranspiration on an irrigation trial plot within a vineyard. In: Stredova H., Roznovsky J., Litschmann T. (Eds.), Int. conference on microclimate and mesoclimate of landscape structures and anthropogenic environment, Feb. 2011, Skalní mlýn, Czech Republic [Conf. Proc.]

(Chapter 8)

Nolz R., Himmelbauer M., Cepuder P., Loiskandl W., 2010. Remote monitoring of a novel irrigation system in a vineyard. In: A. Celkova, Institute of Hydrology SAS (Ed.), 18th Int.

Poster Day: Transport of water, chemicals and energy in the soil-plant-atmosphere system, Nov. 2010, Bratislava, Slovakia, 393-398. [Conf. Proc.]

(Chapter 9)

2 General introduction

Water is vital for all forms of life on earth. Conservation and protection of water resources with respect to quality and quantity provide a basis for human health, welfare, and livelihood. Agriculture plays an important role in this regard, for it produces food on one hand, and is globally the largest user of freshwater resources on the other hand (CAWMA, 2007). Agricultural water management is concerned with issues like drainage, field conservation practices, rain water harvesting, and irrigation with respect to optimal crop production. Various strategies intend to reclaim and sustain cropland, whereas others cover water supply in order to meet plant water requirements when water is scarce (Scanlon et al., 2007). However, efficient use of water is essential from an economical as well as from an ecological point of view. Irrigation, for instance, may be necessary to avoid drought stress and thereby guarantee proper yield and quality of agricultural products (Pereira et al., 2002; Steele et al., 2000). Excessive irrigation, on the other hand, can lead to water logging and unproductive losses of energy, water and nutrients, whereof the latter can be leached and deeply drained to groundwater (Scanlon et al., 2007). A sound irrigation strategy that implicates demand-oriented plant water supply may put things right in these matters (Pereira, 1999). In general, knowledge about the hydrological cycle and its components is crucial for various environmental issues, in particular agricultural water management.

The water cycle is a complex dynamical system that includes hydrological processes in atmosphere, vadose zone, and groundwater environment (Huntington, 2006). The vadose zone plays a key role in the soil-plant-atmosphere continuum with respect to retention and transport of water (and nutrients). Extending from top of the ground surface to the groundwater table it represents that soil layer whose pores are partly or totally filled with air and water, respectively. A current soil water status is described best by the physical quantities soil water content and soil matric potential. Soil water content is defined as volume of water per volume of soil. It commonly expresses how much water is available within a certain soil profile – e.g. the rooting zone of a plant – ranging from zero (completely dry) to soil porosity (saturated). Soil matric potential represents the energy per volume that is needed to withdraw water from the soil matrix. It varies from zero (saturated) to -1.5 MPa or even lower, where plant roots are not able to extract water from the soil anymore. The relationship between both quantities describes one part of the hydraulic properties of a certain soil type, illustrated as typical soil water retention function (van Genuchten, 1980).

In natural conditions soil water status is changing permanently within the vadose zone. Water from precipitation (P) and Irrigation (I) may infiltrate into soil, and inversely be emitted to the

atmosphere through evaporation (E) and transpiration (T). In this context, evaporation describes vaporization from bare soil, whereas transpiration means transport of water through a plant. The common term evapotranspiration (ET) reflects both processes since they usually take place at the same time. While seepage water (SW) can percolate downwards into groundwater with gravitation as main driving force, also upward fluxes due to capillary rise (CR) may occur within a soil layer. Considering changes of water content within a certain soil profile (ΔW), a basic water balance equation can be set up to illustrate the relation between the single components of the hydrological cycle described in this paragraph (Eq. 1).

$$P + I - ET + CR - SW \pm \Delta W = 0 \quad (1)$$

Lysimeters are valuable instruments for water balance studies (Feltrin et al., 2011; Loos et al., 2007). Specific subjects may refer to evapotranspiration (Vaughan et al., 2007), crop water requirements (Marek et al., 2006), transport processes (Knappe et al., 2002), or water balance modeling (Wegehenkel et al., 2008), for instance. The basic component of a lysimeter is a vessel filled with soil (either disturbed or monolithic). Lysimeters with a weighing facility enable continuous measurements of mass changes. The latter equal changes of soil water (ΔW) as the mass of the lysimeter vessel and the solid soil remain the same (increase of biomass is usually negligible in this regard). Hence, also root water uptake and plant available water within the soil profile can be deduced. Precipitation (P) is typically measured with a rain gauge or a pluviograph, irrigation (I) should be known or measured, too. Lysimeters with a free draining outlet at the bottom are usually equipped with a tipping bucket or a storage tank on a scale for measuring seepage water (SW). Some lysimeters utilize devices for full control of the lower boundary condition regarding SW and capillary rise (CR). Modern lysimeters are equipped with high precision load cells and sensors that measure processes inside the lysimeter with high accuracy and temporal resolution (von Unold and Fank, 2008; Xiao et al., 2009).

Soil water sensors offer an option for monitoring soil water status under field conditions (Charlesworth, 2005; Jones, 2007; Leib et al., 2003), at which the investigated soil layer is usually undisturbed and not separated from its surroundings as it is the case for lysimeters. Soil water content sensors can be used to measure water content within a certain soil profile that covers more or less the rooting zone of plants, for instance. In that case, changes of soil water content (ΔW) are positive due to rainfall and capillary rise, and negative due to evapotranspiration and deep percolation. Another type of sensors can be used to measure matric potential in different depths of the soil profile. Hence, water fluxes direction can be deduced from gradients between measurements at two certain points, which is important in particular at the lower boundary of the investigated soil layer. Consequently, ET can be determined using Eq. 1, provided that P is measured independently. Moreover, both sensor types can be used (either alternatively or combined) to deliver information on plant available water with respect to the soil characteristics. Upper and lower thresholds for irrigation scheduling, for instance, are defined via the water content within the effective root zone at field capacity (where usually a matric potential of -33 kPa is supposed to occur) and

permanent wilting point (which is commonly assumed to be the water content at a matric potential of -1.5 MPa) (Doorenbos et al., 1979).

As an alternative to soil water monitoring, evapotranspiration (*ET*) can be approximated by means of well-established calculations with weather data as input parameters. On that basis, a water balance can be compiled and used for estimating changes in soil water content and plant water uptake, respectively (Allen et al., 1998; Doorenbos and Pruitt, 1977).

Generally, measurement systems such as lysimeter facilities, soil water monitoring sites, and weather stations ought to be state-of-the-art regarding instrumentation, configuration, and data management. In this regard, the equipment should be easy to install and maintain; sensor readings should be accurate and precise; and data should be up-to-date, easily available, safe, reliable, and straightforward to be interpreted and processed. These criteria provided the basis for defining the objectives of this thesis.

3 Overall objectives and overview

Primary objectives of this thesis

- (1) Performance assessment of a weighing lysimeter facility and evaluation of adapted interpretation tools with respect to enhanced data management (chapters 4 & 5)
- (2) Performance assessment of approved as well as novel soil water sensors integrated into a remote monitoring network (chapters 6 & 7)

Secondary objectives

- (3) Performance assessment of a field weather station with respect to estimation of evapotranspiration (chapter 8)
- (4) Performance assessment of the serviceability of a sophisticated remote monitoring station for irrigation management (chapter 9)

Both chapters of objective (1) deal with the weighing lysimeter facility at the experimental site of the University of Natural Resources and Life Sciences, Vienna (BOKU) in Groß-Enzersdorf, Austria ($48^{\circ}12'N$, $16^{\circ}34'E$; 157 m). There two weighing lysimeters were established in 1983 aiming for the assessment of water balance components at a site that is representative for the agricultural area "Marchfeld" in the east of Austria (Neuwirth and Mottl, 1983). In order to meet current standards the weighing system and peripheral equipment were partly renewed, and data management was gradually adapted during the past years (Nolz et al., 2011). In this regard it became necessary to assess system performance and enhance data interpretation.

Chapter 6 contains a paper on calibration and performance test of two types of matric potential sensors with respect to objective (2). One sensor was the well-established Watermark by Irrrometer Co., which due to its many advantages is commonly used for soil water monitoring, particularly for irrigation scheduling (Centeno et al., 2010; Shock et al., 2002; Thompson et al., 2006; Thompson et al., 2007b; Vellidis et al., 2008). The other sensor was the relatively new MPS-1 by Decagon Devices Inc., which has a greater measuring range than the Watermark (Decagon Devices, 2009; Malazian et al., 2011). Sensors of both types were integrated into a wireless monitoring network, calibrated and tested regarding sensor performance.

In chapter 7 two multi-sensor capacitance probes for measuring water content in different depths of a soil profile were compared referring to objective (2). The well-known EnviroSCAN by Sentek Pty. Ltd. (Sentek, 1997) served as reference. Such probes are commonly used for soil water monitoring as basis for irrigation management (Cepuder and Nolz, 2007; Fares and Alva, 2000; Thompson et al., 2007a). AquaCheck soil moisture probes operate with an identical principle (AquaCheck, 2008) and are used in the same field of application (Cronje & Mostert, 2010; Murungu et al., 2011). Since little was published about calibration and performance of AquaCheck sensors, a probe was integrated into a remote monitoring network and compared with EnviroSCAN readings.

Chapter 8 is related to objective (3). Data of a remote field weather station (Adcon, 2011) that are used for calculation of reference evapotranspiration were compared to a nearby reference weather station of the Austrian Central Institute for Meteorology and Geodynamics (ZAMG).

Finally, objective (4) in chapter 9 assessed the serviceability of a sophisticated remote monitoring station equipped with weather instruments as well as soil water sensors (Adcon, 2011). Data from the field station served as basis for irrigation management of a subsurface drip irrigation system (Himmelbauer et al., 2011).

4 Interpretation of lysimeter weighing data affected by wind¹

Nolz R., Kammerer G., Cepuder P.

Abstract

Weighing lysimeters are valuable devices for measuring water balance components with high temporal resolution and high accuracy. However, some older lysimeter facilities still operate with lever-arm-counterbalance weighing systems that are sensitive to disturbances, e.g., forces exerted by wind. Filtering and averaging are commonly used for processing noisy raw data. We studied some data of a lever-arm weighing system and performed additional experiments in order to (1) determine the measurement accuracy of the current weighing scheme (facility, and measuring and averaging procedure) regarding wind effects, (2) describe the oscillation behavior, (3) test the mechanical performance of the system, and (4) adapt the averaging procedure with respect to improved interpretation of the weighing data.

The measurement accuracy for a wind velocity $<5 \text{ m}\cdot\text{s}^{-1}$, measured in 10 m height, was about $\pm 0.4 \text{ kg}$ (equivalent to $\pm 0.14 \text{ mm}$); at a higher wind velocity the accuracy was three times lower, but there was no linear relationship. Additional experiments showed that the weighing system is oscillating with more or less irregular amplitudes. A loading-unloading-experiment delivered proper results of the measured loads. The mechanical system reacted immediately, and no directional effects were found. However, small changes of app. $\pm 0.5 \text{ kg}$ could hardly be determined due to the oscillations. A time series of raw data measured every 2 seconds served as basis for improving the averaging method. A moving average from 64 values was computed representing the currently used method, and serving as reference. With this procedure an accuracy of $\pm 0.38 \text{ kg}$ could be reached. Averaging 150 values led to an accuracy of 0.28 kg (0.1 mm) for a wind velocity $<5 \text{ m}\cdot\text{s}^{-1}$.

Keywords: accuracy, averaging, filtering, lysimeter, resolution, water balance

¹ In press as Nolz et al. (2013)

4.1 Introduction

Lysimeters are valuable instruments for measuring water- and solute transport in the soil (Meissner et al., 2000; Zenker, 2003). Equipped with weighing devices, lysimeters allow direct measurements of mass changes in certain time intervals. Since the mass of the lysimeter vessel and the solid soil remains the same (increase of biomass is usually negligible in this regard), registered mass changes equal changes of water ΔW . Hence, real evapotranspiration ET can be determined by means of a simple water balance equation (Eq.1), if precipitation P , irrigation I and seepage water SW amount are measured separately (Aboukhaled et al., 1982).

$$ET = P + I - SW \pm \Delta W \quad (1)$$

Generally, it is a challenge to measure a large mass with high accuracy. In the 1970s and 1980s, lever-arm-counterbalance weighing systems were state-of-the-art in lysimeter construction (Aboukhaled et al., 1982). This technique reduced weighing mass to a fractional amount, which could be measured more easily with desired accuracy. In the beginning, mass changes were determined mechanically, later by means of electronic load cells. Modern lysimeters rest on three load cells for very accurate measurements of mass changes (Meissner et al., 2007; von Unold and Fank, 2008; Xiao et al., 2009). Compared to such systems, lever-arm balances measure less accurate (Marek et al., 1988; Young et al., 1996). Nevertheless, lysimeters with older weighing systems are still useful for current research tasks (Haferkorn, 2000; Knappe et al., 2002; Zenker, 2003; Knoblauch and Swaton, 2007; Wegehenkel et al., 2008). In this regard, the facility may be evaluated and adapted in order to meet up-to-date standards. Lysimeter stations can be upgraded by renewing parts of the facility (e.g. load cell, data logger, or computer system), installing additional lysimeters, expanding the measuring equipment (e.g. soil water sensors), or improving data management (e.g. measuring interval). However, a remaining disadvantage of lever-arm-counterbalance weighing systems is that accuracy can be significantly decreased by forces exerted by wind (Castel, 1997; Howell et al., 1995; Malone et al., 1999; Zenker, 2003). As an approach for solving the measurement inaccuracies, some of these authors mentioned filtering and averaging procedures, respectively.

For assessment of evapotranspiration and drainage water two weighing lysimeters, equipped with lever-arm-counterweight systems, were established 1983 in Groß-Enzersdorf, Austria (Neuwirth and Mottl, 1983; Cepuder and Supersperg, 1991).

In order to advance system performance load cells, peripheral equipment (e.g. converter, amplifier, logging devices), and data management (measurement, conversion, averaging, storage, a.s.o.) were gradually improved during the past years. Consequently, changes in mass could be measured with higher accuracy and higher temporal resolution. However, the weighing became more sensitive to disturbances, mainly forces exerted by wind (Nolz et al., 2009). This is supposed to be triggered by oscillations of the mechanical system.

Following these ideas, the aim of this study was

- (1) to determine the measurement accuracy of the current weighing scheme (facility, and measuring and averaging procedure) regarding wind effects,
- (2) to describe the oscillation behavior,
- (3) to test the mechanical performance of the system, and
- (4) to adapt the averaging procedure with respect to improved interpretation of the weighing data.

4.2 Materials and methods

The construction of the lysimeters in Groß-Enzersdorf was completed according to the standard of knowledge at that time. A concrete basement with shafts for two lysimeter vessels accommodates the weighing system, tipping buckets for measuring seepage water, and several devices for data acquisition. The cylindrical vessels have an inner diameter of 1.9 m (surface area 2.85 m²) and a hemispherical bottom made of glass fiber-reinforced plastic with a maximum depth of 2.5 m. At that position, an outlet for the drainage water is situated. The outflow is measured with a tipping bucket below the lysimeter. Each lysimeter vessel rests on a base frame that transmits the weight through a lever system with a counterweight to an electronic load cell (Figure 4.1). The lever arm reduces the total mass of about 11-13 tons to a small fraction of some hundreds of kilograms that are measured by a load cell. The total mass of the lysimeters is not known exactly. The output signal of the load cell is transmitted via an analog carrier frequency-measuring amplifier (0-10 V) to an Analog-to-Digital-Converter (A/D-Converter). Weighing data are measured every few seconds following a randomized procedure. A moving average is computed from 64 digitalized values (digits) and stored every 10 minutes on a data logger together with the raw counts (digits) from the tipping bucket (Nolz et al., 2011).

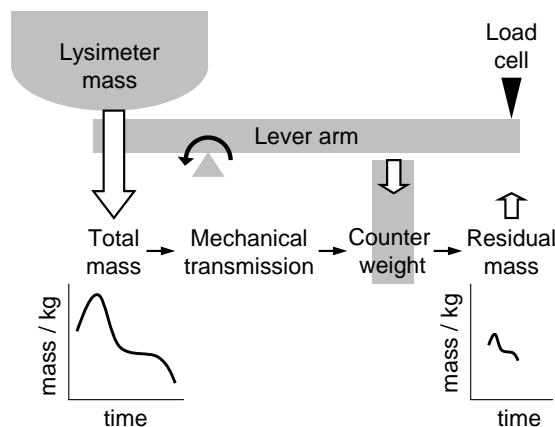


Figure 4.1. Lysimeter weighing facility: a small fraction of the total mass is transmitted to an electronic load cell via a lever-arm mechanism with a counterweight

Weather data are measured every minute at the neighboring meteorological station of the Central Institute for Meteorology and Geodynamics, Austria (ZAMG). Some of the available quantities are air temperature, relative humidity, air pressure, solar radiation, precipitation and wind velocity. The latter is measured in 10 m height.

Raw data (lysimeter mass, amount of seepage water and meteorological quantities) are stored on a local server with a common time stamp.

Calibration is essential in order to convert raw weighing data W_{lys} (digits) into physical quantities. In 2009 new load cells were installed, and the subsequent calibration of the weighing system delivered a conversion factor $c_{lys} = 0.068 \text{ kg}\cdot\text{digit}^{-1}$. Hence, lysimeter mass can be computed as $m_{lys} = W_{lys} \cdot c_{lys}$. Dividing by the lysimeter surface area gives water equivalent in mm (Figure 4.2). In order to exemplify this, some computations are summarized in Table 4.1. Load cell accuracy is $\pm 0.18 \text{ kg}$, which is equivalent to approximately $\pm 0.06 \text{ mm}$ of water. One can see that the resolution of 1 digit is about 2.7 times higher than the load cell accuracy. Consequently, the calibrated weighing data provide the relative lysimeter mass in kg, defined as current mass minus a reference mass. The current mass depends on the soil water content, whereas the reference mass approximates the lysimeter mass with dry soil. As mentioned above, the real mass is not known – only mass changes are determined.

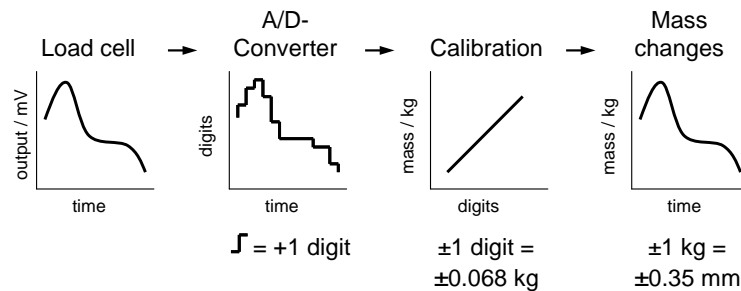


Figure 4.2: Data processing

Table 4.1. Exemplary computations of mass changes from weighing data and calibration factor ($m_{lys} = W_{lys} \cdot c_{lys}$), and conversion into water equivalent ($m_{lys} \cdot A_{lys}^{-1}$)

weighing system output W_{lys} / digits	calibration factor c_{lys} / $\text{kg}\cdot\text{digit}^{-1}$	calibrated mass changes m_{lys} / kg	lysimeter surface area A_{lys} / m^2	changes in water equivalent / mm	Comments
1	0.068	0.07	2.85	0.02	system resolution
2		0.14		0.05	
2.7		0.18		0.06	load cell accuracy
3		0.20		0.07	
4		0.27		0.10	desired accuracy
5		0.38		0.13	

4.2.1 Measurement accuracy regarding wind effects

Preliminary, a straightforward statistical analysis of wind data based on daily and monthly mean values was compiled for the period 1999-2009.

The effects of wind forces on the weighing data were studied on one of the lysimeters that is permanently grown with grass namely the grass lysimeter which is utilized for measuring reference evapotranspiration on different time scales. As basis served weighing and the mean wind velocity measured in 10 m height in the respective 10-minutes-interval.

For estimating the accuracy of the weighing system a period with a high wind velocity, few rainfall events and low outflow at the lysimeter bottom was chosen. Irrigation and rainfall were subtracted from the weighing data in order to get a time series only of evapotranspiration for the entire study period. Since real evapotranspiration without interfering wind effects was not known, a well-defined smoothing function was found for evapotranspiration data series by means of curve fitting. The residuals between evapotranspiration data and the smoothing function were interpreted as wind effects, thus they were plotted against the wind velocity within the respective measuring interval. From this correlation, the accuracy of the current weighing scheme was determined. A simple statistical analysis of the residuals was executed with standard software (SPSS 15.0).

On December 16, 2009, several experiments were carried out at the lysimeter station aiming at additional data for studying oscillation behavior, mechanical performance, and averaging procedures (Table 4.2). Changes in lysimeter mass, standard wind velocity (10 m, 10 minutes) and wind velocity near the surface (0.75 m) were measured with high temporal resolution. A separate logger (Campbell CR23X) stored these raw data from the lysimeter load cell and from a wind sensor (Vaisala WXT510). The logging resolution of 1 mV was equivalent to 6.6 digits, 0.45 kg, or 0.16 mm, respectively.

Table 4.2. Overview on the experiments carried out at the lysimeter station

Experiments		Measuring intervals		
Testing...	By means of...	weighing data	10 m-wind data	
Oscillation behavior	disturbing pulse	0.1 s	-	Figure 4.7
Mechanical performance & Calibration	loading-unloading	2 s	-	Figure 4.8 & Figure 4.9
Averaging procedures	basic oscillation	2 s	10 min	Figure 4.10

4.2.2 Oscillation behavior

A manual disturbing pulse was exerted on the lysimeter. The weighing data were measured and stored in intervals of 0.1 s in order to get the fading signal from the load cells with high resolution. Wind velocity was not taken into account for this experiment.

4.2.3 Mechanical performance of the system

The lysimeter was loaded and unloaded several times. Weighing data were measured and stored in intervals of 2 seconds. The mass changes were referred to an initial measurement (± 0 kg). A calibrated mass of 20.337 kg was put near the edge of the lysimeter in order to verify if there are any directional effects of the weighing mechanism. Firstly, the load was placed at position East (E), and then it was moved 90 degrees counter-clockwise to North (N), West (W) and South (S). After unloading the lysimeter for a reference measurement, 40.645 kg were put on the lysimeter. Then, the mass was removed again, and reloaded stepwise with +5.084 kg, +10.132 kg, +10.174 kg, +10.167 kg, +10.089 kg, +1.000 kg, +0.500 kg, -0.500 kg, and +0.500 kg. The calibration function in use for the weighing facility was evaluated by means of the results from this measuring series.

4.2.4 Averaging procedure

The weighing signal and wind velocity were measured and stored in intervals of 2 seconds, and plotted for more than one hour. Wind velocity from the weather station measured every minute was averaged to 10-minutes-intervals representing the standard wind velocity. During the measuring period no precipitation and no drainage water occurred. Raw data were referred to a datum level of ± 0 kg, and the trend representing evapotranspiration was eliminated. Consequently, the processed data illustrate fluctuations around a mean value of zero, characterizing typical raw weighing data at a certain wind velocity.

According to the currently applied averaging procedure, a moving average $Y_{i,n}$ from 64 values ($n = 64$) was computed (Eq. 2). Additionally, moving averages $Y_{i,n}$ from 150, 300, and 600 values ($n = 150, 300, \text{ and } 600$) and the respective maximum error ϵ_n (difference from zero) were calculated.

$$Y_{i,n} = \frac{1}{n} \sum_{j=1}^n x_{i-j} \quad (2)$$

4.3 Results and discussion

The wind regime at the lysimeter station in Groß-Enzersdorf has no distinctive annual cycle. In the period 1999-2009 the highest monthly mean wind velocity was measured in February and March (Figure 4.3). The mean daily wind velocity in the whole period was $3.6 \text{ m}\cdot\text{s}^{-1}$, the maximum daily wind velocity was $11.1 \text{ m}\cdot\text{s}^{-1}$. Daily peaks occurred typically between 1:00 pm and 2:00 pm local time. Lower values were measured during night time, when atmospheric circulation was low.

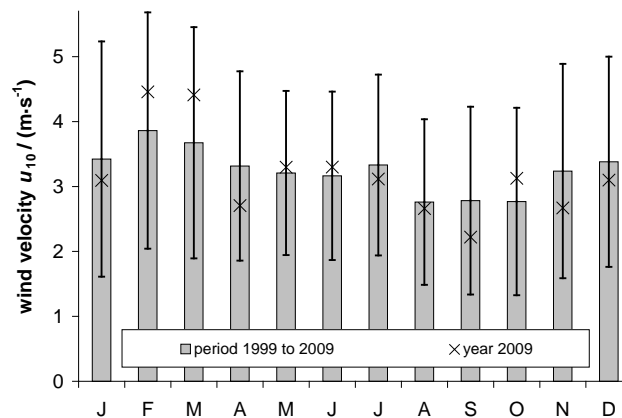


Figure 4.3: Mean daily wind velocity with standard deviation (bars) in the period 1999-2009, and mean daily wind velocity 2009 (crosses), measured at the lysimeter station in Groß-Enzersdorf, Austria

4.3.1 Measurement accuracy regarding wind effects

The period from September 23 to October 22, 2009 fulfilled the criteria mentioned in paragraph 4.2.1. A main focus was set on wind velocity ranging from low to high in terms of representativeness. Little rainfall and no seepage water were desirable in order to reduce sources of possible inaccuracies. The observed period is displayed in Figure 4.4. Substantial positive changes of lysimeter mass came from irrigation (October 1), and from rainfall (October 9, 12, and 15). The 10-minute-wind velocity in 10 m height (u_{10}) ranged from zero to $13 \text{ m}\cdot\text{s}^{-1}$, and the mean wind velocity was $3.2 \text{ m}\cdot\text{s}^{-1}$.

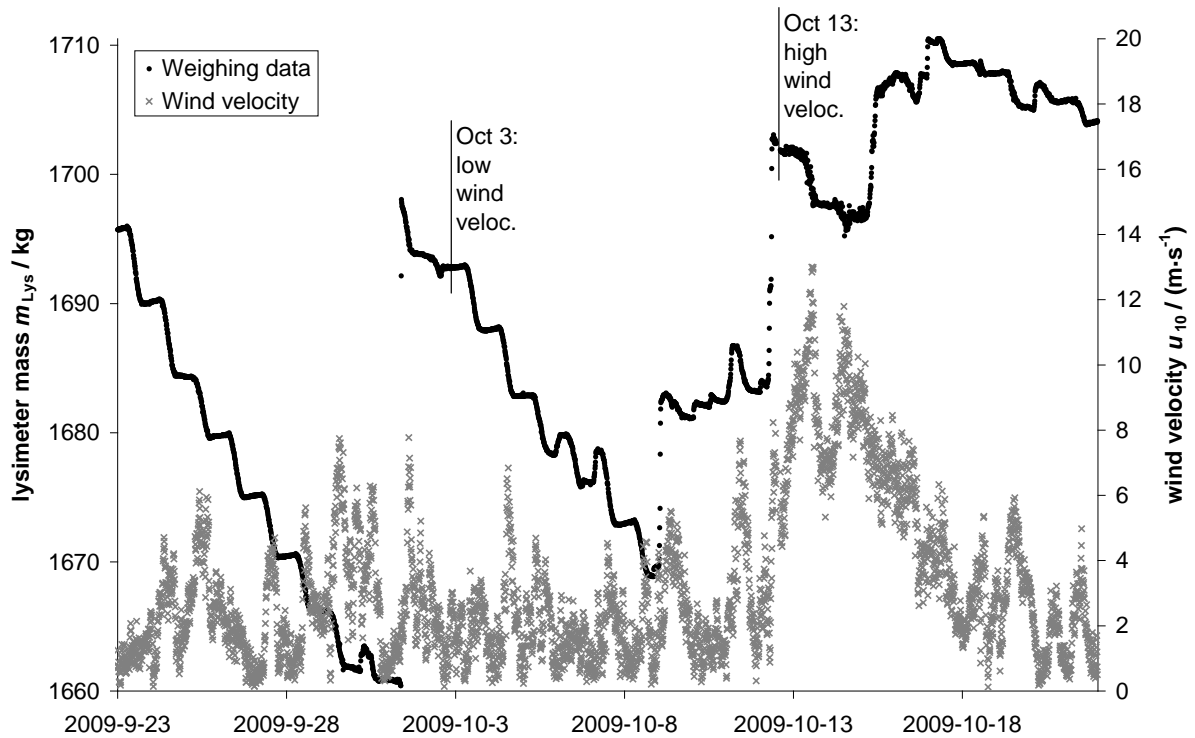


Figure 4.4: Lysimeter weighing data and wind velocity in 10-minute-intervals in the investigated period from September 23 to October 22, 2009

Irrigation and rainfall were subtracted from the weighing data in order to yield pure evapotranspiration data. The measurements from October 16 had to be neglected, because the exact amount of rainfall could be determined neither from the rain gauge nor directly from the weighing data. The best fitting curve for the daily characteristics of evapotranspiration was a sigmoid smoothing function of the form

$$y = a + b / (1 + \exp(-(x - c) / d)). \quad (3)$$

Two days of the study period – one with a low mean wind velocity (October 3) and one with a very high one (October 13) – are shown exemplarily in Figure 4.5. Mean and maximum wind velocity of the respective day is summarized in Table 4.3. The fitting of a sigmoid function worked well in both cases. It is reasonable that the coefficient of determination was higher for the data not affected from wind disturbances. Accordingly, the residuals between smoothing function and measured data were significantly higher for the wind affected data (Table 4.3). These results are comparable to former investigations (Nolz et al., 2009), which emphasizes the representativeness of the selected period.

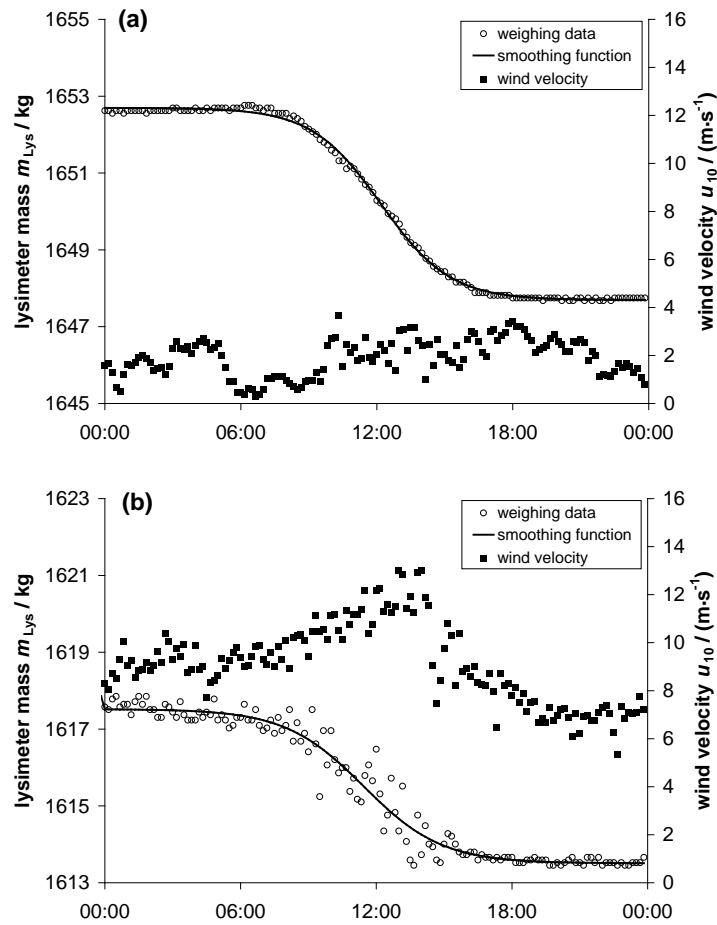


Figure 4.5: Weighing data with smoothing function (a) on a day with low wind velocity, 2009-10-03; (b) on a day with high wind velocity, 2009-10-13

Table 4.3. Statistical characteristics of two selected days with different wind velocities

		2009-10-03	2009-10-13
Wind velocity	Mean / $\text{m}\cdot\text{s}^{-1}$	1.9	9.1
	Maximum / $\text{m}\cdot\text{s}^{-1}$	3.7	13.0
Sigmoid smoothing function	Coefficient of determination / R^2	0.9987	0.9667
Residuals	Standard deviation / mm	0.027	0.110
	Maximum / mm	0.07	0.45
	Minimum / mm	-0.08	-0.45

Curve fitting was done for each day of the study period. Finally, the residuals between weighing data and smoothing function were correlated with wind velocity u_{10} (Figure 4.6). Approximately 10 % of the 10-minute-weighing data exceeded the theoretical accuracy of the

load cell of ± 0.18 kg (equivalent to ± 0.06 mm). Furthermore, one can see that the residuals increased with wind velocity. At a wind velocity higher than $5 \text{ m}\cdot\text{s}^{-1}$ more than one third of the data were out of range. Consequently, an effective accuracy of the weighing scheme of ± 0.4 kg (equivalent to ± 0.14 mm) could be deduced for a wind velocity $< 5 \text{ m}\cdot\text{s}^{-1}$ in the investigated period. At a higher wind velocity the accuracy ranged from zero to ± 1.2 kg (equivalent to ± 0.42 mm). However, no linear relationship could be found between increasing wind velocity and decreasing measuring accuracy. A straightforward statistical analysis of the residuals by means of SPSS software showed that the residuals fluctuate around a mean value, but they are not normally distributed according to Kolmogorov-Smirnov (with Lilliefors Significance Correction) and Shapiro-Wilk. Thus, we assumed an oscillating effect of the weighing system to be the reason.

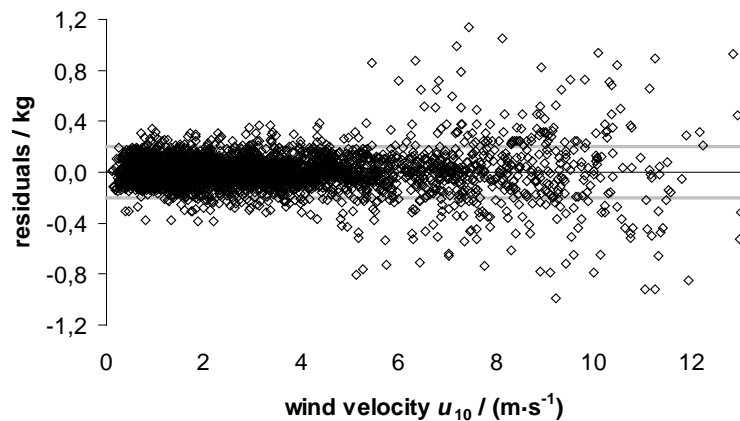


Figure 4.6: Residuals between smoothing function and weighing data in relation to wind velocity; the grey lines indicate the accuracy of the load cell (± 0.2 kg)

4.3.2 Oscillation behavior

The manual disturbing pulse caused a maximum peak of about 30 kg (Figure 4.7). High resolution measurements (0.1 s) demonstrated perfectly the oscillation of the weighing system. Figure 4.7a illustrates the oscillation in the first 6 seconds after the disturbance. The fading signal was measured for 10 minutes representing the current storage interval of the weighing data (Figure 4.7b). It can be described as damped oscillation. We interpreted the last two minutes of the recorded data (Figure 4.7b, small window with enlarged y-axis) as basic oscillation after the disturbing pulse faded completely. This phase demonstrated how wind forces affected the weighing signal in particular, because the amplitudes of the oscillation increased, and decreased again. It can be concluded that depending on the instant of time when the driving force appeared, the fluctuation was either built up or rather decreased. Theoretically, the frequency of an oscillation is related to the swinging mass. The lysimeter mass is changing with water content. Consequently, neither the exact amplitude nor the frequency of the oscillation could be determined. This experiment explained well the reduced measurement accuracy of the weighing system, and it gave an idea how the system

reacts on noticeable wind gusts. Furthermore, it pointed out why no linear relation between measurement error and wind velocity could be found previously.

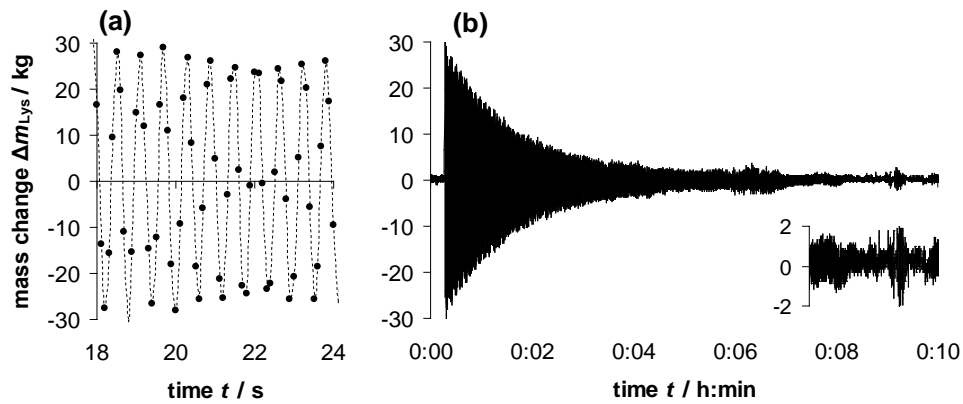


Figure 4.7: Oscillating effect of the weighing system after manual disturbing pulse: 6 seconds in detail (a), and 10 minutes of fading (b) – the small window shows the last 3 minutes with enlarged y-axis

4.3.3 Mechanical performance of the system

Although the loading and unloading sequences were done very carefully, the weighing system responded very sensitive to unintended disturbances (Figure 4.8). Obviously, this lowered the accuracy. Mass changes could only be determined after the oscillation had faded, by averaging 10 to 20 values. However, the changes of $\pm 0.5 \text{ kg}$ could hardly be determined. The weighing mechanism reacted immediately; no mechanical inertia was visible. No eccentric effects could be deduced from the position changes of the loads; however, the oscillations were relatively high during this stage of the experiment.

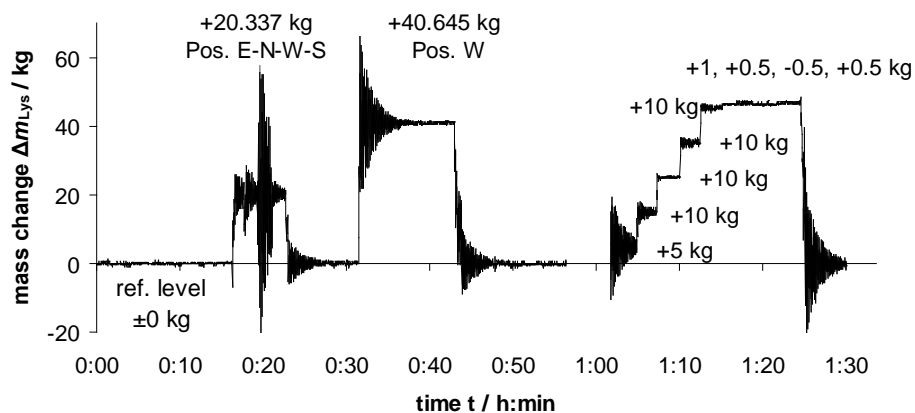


Figure 4.8: Testing the mechanical performance of the weighing facility with a stepwise loading-unloading-experiment

The added loads and the measured mass changes showed a very good linear correlation ($R^2 = 0.998$) and a root mean square error (RMSE) of 0.272 kg (equivalent to 0.1 mm) (Figure 4.9). The latter illustrated the system accuracy during the loading-unloading-experiment.

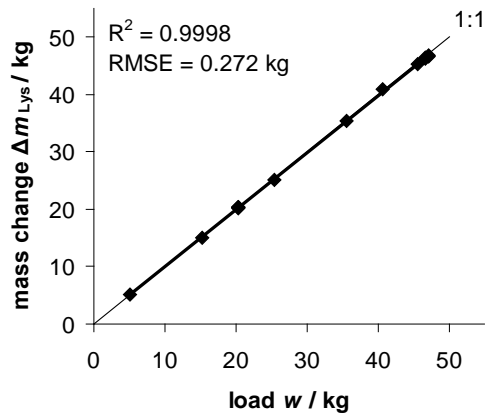


Figure 4.9: Evaluation of calibration and system accuracy during the loading-unloading-experiment: mass changes in kg (squares) with linear trend (thick line) and 1:1 line (thin line)

4.3.4 Averaging procedure

As mentioned above, the accuracy of the weighing system depends on data acquisition and data processing. Common procedures are filtering, which may cause stern data loss, and averaging. The weighing data presented above (Figure 4.4 to Figure 4.6) were computed from a moving average from 64 values. The same procedure was applied to the raw weighing data in Figure 4.10a. Even though the resolution was different, we assumed that this time series (2100 values) represents typical characteristics of a measuring signal at a low wind velocity ($u_{10} < 5 \text{ m}\cdot\text{s}^{-1}$). In fact, the mean standard wind velocity (10-minutes-interval, 10 m height) was $4.7 \text{ m}\cdot\text{s}^{-1}$, and the maximum was $5.1 \text{ m}\cdot\text{s}^{-1}$ during the experiment (Figure 4.10b). However, the fluctuations of 1-minute-measurements were even higher, and wind velocity measured every 2 seconds 0.75 m above ground delivered lower values but highest fluctuations (Figure 4.10b). Once more, this illustrates the complex relationship between wind velocity and oscillation of the weighing system. The current averaging reduced weighing data noise from approximately $\pm 2 \text{ kg}$ to $\pm 0.37 \text{ kg}$. The latter corresponded with the accuracy limits in Figure 4.6.

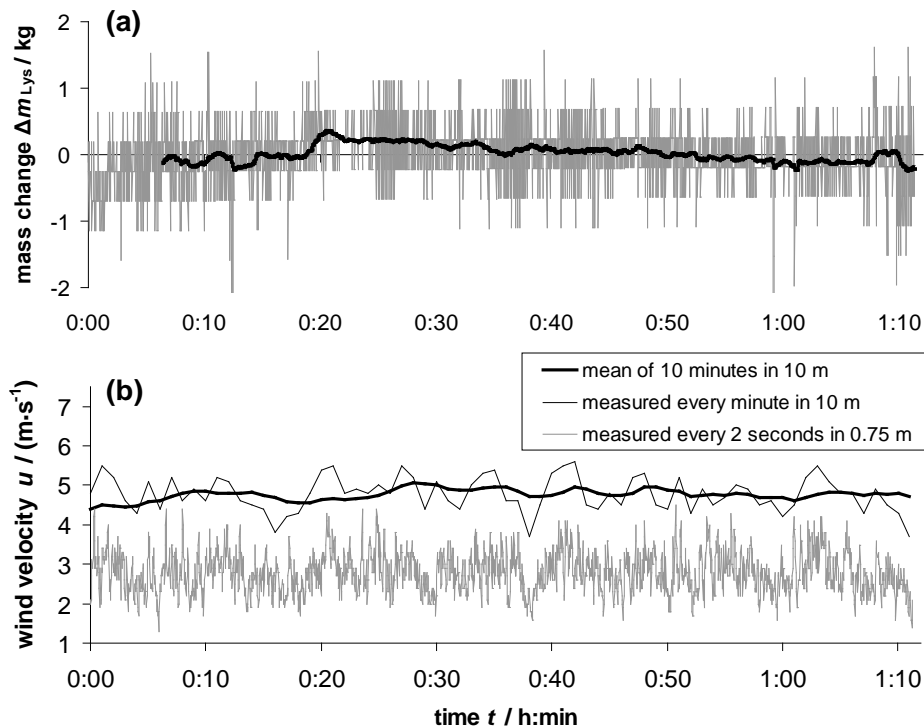


Figure 4.10: (a) Weighing signal: the black line displays the moving average $Y_{i,64}$ (maximum = 0.37 kg); (b) Wind velocity measured every 2 seconds 0.75 m above ground (thin grey line), measured every minute in 10 m (thin black line), and mean of 10 minutes in 10 m (thick black line)

Generally, taking into account more values for averaging reduces the maximum deviation. On the other hand, the measurements are limited through the storage interval. Furthermore, it must be stressed that the stored value does not represent a point measurement, which has to be considered with respect to data interpretation. In Table 4.4 relations between some numbers of averaged values and the respective maximum error are summarized. Using 150 values for the moving average improved the accuracy to a maximum error of 0.28 kg, which is equivalent to <0.1 mm. Averaging over a 10-minute-storage interval (300 values) led to a maximum deviation of 0.27 kg (0.09 mm). In order to reach the accuracy of the load cell of 0.18 kg (0.06 mm), at least 600 values were necessary. For that accuracy, the measuring and storage interval should be set to 30 minutes. Extending the interval, on the other hand, lowers the resolution of the weighing data, thus of the desired water balance components. It is generally questionable if an accuracy of 0.1 mm (150 averaged values) is good enough for 10-minutes-weighing data. Since the maximum deviation was about three times higher at windy conditions (Figure 4.6), an accuracy of 0.29 mm can be estimated if wind velocity exceeds $5 \text{ m}\cdot\text{s}^{-1}$. Averaging 300 values gave a maximum error of 0.28 mm (Table 4.4), which seems to be no substantial improvement. Changing the measuring interval to 30 minutes and averaging 600 values provided an accuracy of less than 0.2 mm.

Table 4.4. Number of values for computing the average from weighing data and the respective maximum error

Number of values for the moving average	Maximum error / kg	Comments
1	App. ± 2	Raw data
64	0.37	Current averaging
150	0.28	Desired accuracy (equivalent to 0.1 mm)
300	0.27	Maximal values in 10 minutes
600	0.18	Accuracy of load cell
2100	0.00	Entire data series (1 h 10 min)

Another option is to fit a sigmoid smoothing function (Eq. 3) in order to improve the interpretation of wind affected weighing data (Figure 4.5). However, this is applicable only on days without rainfall.

4.4 Conclusions

We illustrated the relation between averaging procedure and system performance (resolution, accuracy) of a lever-arm-counterbalance-weighing system. Detailed studies of the weighing data of a selected period in 2009 proved that the weighing procedure was considerably affected from wind. There was no linear relation between wind velocity and measuring accuracy, but rather a stepwise change. The measuring accuracy for a wind velocity $< 5 \text{ m}\cdot\text{s}^{-1}$ was about $\pm 0.4 \text{ kg}$ (equivalent to $\pm 0.14 \text{ mm}$); at a higher wind velocity the accuracy was about three times lower.

Additional experiments showed that the weighing system is oscillating with more or less irregular amplitudes that are affected from disturbances, especially wind gusts. A loading-unloading-experiment delivered proper results of the measured loads. However, small changes (app. $\pm 0.5 \text{ kg}$) could hardly be determined due to the oscillations. A time series of raw data measured every 2 seconds served as basis for improving the averaging method. A moving average from 64 values was computed representing the currently used method, and serving as reference. With this procedure an accuracy of $\pm 0.38 \text{ kg}$ (equivalent to $\pm 0.13 \text{ mm}$) could be reached, which is consistent with the accuracy mentioned above. Taking into account more values improved the accuracy, but was restricted by the desired temporal resolution (measuring interval).

A standard accuracy for lever-arm lysimeters with 1 m^2 surface area seems to be 0.1 mm (Haferkorn, 2000; Zenker, 2003). Modern systems, for comparison, measure with an accuracy of $\leq 0.01 \text{ mm}$ (Meissner et al., 2007; von Unold and Fank, 2008). From our point of view, an accuracy of 0.1 mm and a temporal resolution (storage interval) of 30 minutes would

be an acceptable compromise for the investigated weighing lysimeter with 2.85 m² surface area (at normal wind conditions). This demand would lead to an averaging of 150 values of 2-seconds-measurements.

Generally, it has to be taken into account that the wind affected inaccuracy may be about three times higher. In that case, optional data processing (e.g. curve fitting) would be required.

The main results of this study are transferable to similar lysimeter facilities; however, the oscillation behavior of a lysimeter system depends mainly on lysimeter size and wind conditions. Consequently, it is recommended to adapt averaging procedures to the local situation.

Acknowledgments

We thank Wolfgang Sokol (IHLW) for assistance, our colleagues from the Institute of Meteorology (BOKU-Met) for technical support, and the Central Institute for Meteorology and Geodynamics, Austria (ZAMG) for the weather data.

4.5 References

- Aboukhaled, A., Alfaro, A., Smith, M. (1982): Lysimeters. In: FAO Irrigation and Drainage Paper 39, FAO, Rome (Italy)
- Castel, J. R. (1997): Evapotranspiration of a drip-irrigated Clementine citrus tree in a weighing lysimeter. In Chartzoulakis, K. S. (ed.): Proceedings of the 2nd International Symposium on Irrigation of Horticultural Crops. Acta Hort. 449(1), 91-98.
- Cepuder, P., Supersperg, H. (1991): Erfahrungen mit der Lysimeteranlage Groß-Enzersdorf. In Bundesanstalt für alpenländische Landwirtschaft (ed.): Proceedings of the Lysimeter Conference, Gumpenstein, Austria, 16.-17. April 1991, 25-35.
- Haferkorn, U. (2000): Größen des Wasserhaushaltes verschiedener Böden unter landwirtschaftlicher Nutzung im klimatischen Grenzraum des Mitteldeutschen Trockengebietes: Ergebnisse der Lysimeterstation Brandis. Ph.D. thesis, Universität Göttingen, Germany.
- Howell, T. A., Schneider, A. D., Dusek, D. A., Marek, T. H., Steiner, J. L. (1995): Calibration and Scale Performance of Bushland Weighing Lysimeters. Transact. ASAE 38(4), 1019-1024.
- Knappe, S., Haferkorn, U., Meissner, R. (2002): Influence of different agricultural management systems on nitrogen leaching: results of lysimeter studies. J. Plant Nutr. Soil Sci. 165(1), 73-77.

- Knoblauch, S., Swaton, T. (2007): Erweiterung der Lysimeteranlage Buttelsee für die Bestimmung von standortabhängigen Schwellenwerten für N-Salden. In: In LFZ Raumberg-Gumpenstein (ed.): Proceedings of the 12th Lysimeter Conference, Gumpenstein, Austria, 17.-18. April 2007, 35-41.
- Malone, R. W., Stewardson, D. J., Bonta, J. V., Nelsen, T. (1999): Calibration and Quality Control of the Coshocton Weighing Lysimeters. *Transact. ASAE* 42(3), 701-712.
- Marek, T. H., Schneider, A. D., Howell, T. A., Ebeling, L. L. (1988): Design and construction of large weighing monolithic lysimeters. *Transact. ASAE* 31(2), 477-484.
- Meissner, R., Rupp, H., Schubert, M. (2000): Novel lysimeter techniques – a basis for the improved investigation of water, gas and solute transport in soils. *J. Plant Nutr. Soil Sci.* 163, 603-608.
- Meissner, R., Seeger, J., Rupp, H., Seyfarth, M., Borg, H. (2007): Measurement of dew, fog, and rime with a high-precision gravitation lysimeter. *J. Plant Nutr. Soil Sci.* 170, 335-344.
- Neuwirth, F., Mottl, W. (1983): Errichtung einer Lysimeteranlage an der agrar-meteorologischen Station in Groß-Enzersdorf. *Wetter und Leben* 35, 48-53.
- Nolz, R., Kammerer, G., Cepuder, P. (2009): Windeinfluss auf die Lysimetermessungen in Groß-Enzersdorf. In LFZ Raumberg-Gumpenstein (ed.): Proceedings of the 13th Lysimeter Conference, Gumpenstein, Austria, 21.-22. April 2009, 17-20.
- Nolz, R., Kammerer, G., Cepuder, P. (2011): Datenmanagement der wägbaren Lysimeter in Groß-Enzersdorf. In LFZ Raumberg-Gumpenstein (ed.): Proceedings of the 14th Lysimeter Conference, Gumpenstein, Austria, 3.-4. May 2011, 33-38.
- von Unold, G., Fank, J., (2008): Modular design of field lysimeters for specific application needs. *Water, Air, & Soil Pollution, Focus* 8, 233-242.
- Wegehenkel, M., Zhang, Y., Zenker, T., Diestel, H. (2008): The use of lysimeter data for the test of two soil-water balance models: A case study. *J. Plant Nutr. Soil Sci.* 171, 762-776.
- Xiao, H., Meissner, R., Seeger, J., Rupp, H., Borg, H. (2009): Testing the precision of a weighable gravitation lysimeter. *J. Plant Nutr. Soil Sci.* 172, 194-200.
- Young, M., Wierenga, P., Mancino, C. (1996): Large weighing lysimeters for water use and deep percolation studies. *Soil Sci.* 161, 491-501.
- Zenker, T. (2003): Verdunstungswiderstände und Gras-Referenzverdunstung. Lysimeter-untersuchungen zum Penman-Monteith-Ansatz im Berliner Raum. Ph.D. thesis, Berlin University of Technology, Germany.

5 Improving interpretation of lysimeter weighing data²

Nolz R., Kammerer G., Cepuder P.

Abstract

Weighing lysimeters are valuable devices for measuring soil water balance components. Older lysimeter facilities are usually equipped with lever-arm-counterbalance weighing systems. A disadvantage of such systems is their sensitivity to external disturbances, mainly forces exerted by wind, which can significantly decrease measuring accuracy. Two types of smoothing functions were tested on a set of noisy lysimeter weighing data with respect to improved data interpretation. A basic piecewise sigmoid function was easy to fit and gave proper results of typical diurnal variation of evapotranspiration on single days without rainfall. However, on a longer time period with rainfall events, a polynomial spline function performed better.

Keywords: data management, measurement resolution, accuracy, sigmoid, spline smoothing

² Accepted as Nolz et al. (2013)

5.1 Introduction

Understanding of the water cycle and its components is crucial for various environmental issues such as drinking water supply, water resources management, groundwater protection, or agricultural water management. The latter, for instance, is concerned with drainage and irrigation with respect to optimal crop production. In this regard, it would be helpful to observe processes in the soil-plant-atmosphere-system. Furthermore, long-term monitoring of water balance components may provide a database for climate change studies.

Lysimeters proved to be valuable instruments for various water balance studies (Feltrin et al., 2011; Loos et al., 2007; Meissner et al., 2007; von Unold and Fank, 2008). Two large weighing lysimeters were established in Groß-Enzersdorf, Austria (48°12'N, 16°34'E; 157 m) in 1983. The purpose was to determine evapotranspiration and seepage water at a location that was assumed to be representative for the nearby agricultural area "Marchfeld" (Neuwirth and Mottl, 1983). According to the state-of-the-art at that time (Aboukhaled et al., 1982), each lysimeter was equipped with a lever-arm-counterbalance weighing system. While the structural facilities of the lysimeter station in Groß-Enzersdorf remained substantially unchanged since initial operation, data management was adapted to contemporary standards over the years (Nolz et al., 2011). The main focus was set on assessment of soil water balance components with high accuracy and high temporal resolution. Improvements concerned data acquisition (measurement, conversion, averaging, and storage), transmission, backup, and processing (calibration, filtering, and plausibility check). Consequently, also data interpretation had to be adapted. A particular problem was a reduced measuring accuracy induced by wind forces (Nolz et al., 2009). This oversensitivity to external disturbances is a general disadvantage of lever-arm-counterbalance systems (Howell et al., 1995; Malone et al., 1999). Experiments at the lysimeter station in Groß-Enzersdorf have shown that the weighing system itself is subject to mechanical oscillations, and that disturbances such as wind gusts significantly decrease measuring accuracy (Nolz et al., 2013). The measuring accuracy for a wind velocity $<5 \text{ m}\cdot\text{s}^{-1}$ (measured in 10 m height) was approximately $\pm 0.4 \text{ kg}$ (equivalent to $\pm 0.14 \text{ mm}$ water ponding), at higher wind velocities the accuracy was about three times lower. Severely noisy weighing data make it almost impossible to determine water balance components in certain (short) time intervals (as demonstrated later on in Figure 5.7 and Figure 5.8). According to Vaughan and Ayars (2009) well-adjusted averaging procedures provide an option for noise reduction arising from mechanical oscillation of the weighing system. A straightforward method is to compute a moving average; however, this procedure is limited by the temporal resolution (storage interval), and may not work proper with severely noisy data (Nolz et al., 2013).

The main objective of this study was to enhance data interpretation of noisy lysimeter weighing data by means of smoothing functions.

5.2 Materials and methods

5.2.1 Data acquisition and water balance

The basic parts of the lysimeters in Groß-Enzersdorf are cylindrical vessels with an inner diameter of 1.9 m (surface area 2.85 m²) and a hemispherical bottom made of glass fiber-reinforced plastic with a maximum depth of 2.5 m. At the time of construction the vessels were packed with sandy loam soil (0-140 cm) over gravel (140-250 cm). Each vessel rests on a base frame that transmits the weight through a lever system with a counterweight to an electronic load cell. This mechanical system reduces the total mass of about 11-13 tons (the total mass of the lysimeters is not known exactly) to a fractional mass of some hundreds of kilograms, which is measured by the load cell with an accuracy of ± 0.2 kg (Figure 5.1). The weighing system registers mass changes in a certain time interval that equal changes of soil water ΔW , because the mass of the lysimeter vessel and the solid soil remain the same.

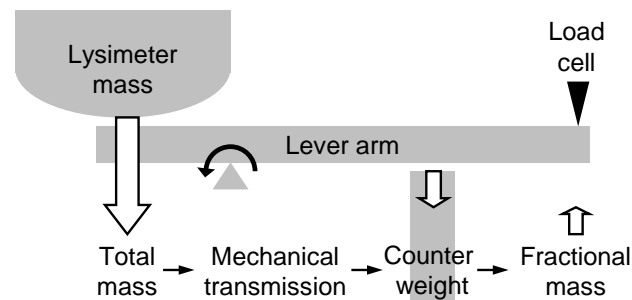


Figure 5.1: Lysimeter weighing facility: via a lever-arm mechanism with a counterweight a proportional fraction of the total mass is transmitted to an electronic load cell

Outlets for seepage water SW are situated at the deepest point of each vessel where outflow is measured by means of tipping buckets. A concrete basement with two shafts for the lysimeter vessels accommodates the weighing- and seepage water facilities, and devices for data acquisition.

Precipitation P_{ZAMG} is measured in a few meters distance with a standard pluviograph from the Central Institute for Meteorology and Geodynamics, Austria (ZAMG). Alternatively, precipitation P_{LYS} is determined directly from the lysimeter weighing data, based on the approach that either P (positive mass change) or ET (negative mass change) occurs during a certain (short) time interval (von Unold and Fank, 2008). On one hand, this method can provide only an estimation of P , because during rainfall events evaporation and transpiration are often not negligible; on the other hand, measurements from standardized pluviographs often show deviations to the increase of soil water ΔW in the lysimeter, and the solution of the water balance equation (Eq. 1) gives more plausible results for evapotranspiration ET when using P_{LYS} .

Eq.1 symbolizes a basic water balance with the components measured at the lysimeter station: precipitation P , irrigation I , seepage water SW , and change of soil water ΔW . Hence, it can be used to calculate evapotranspiration ET .

$$P + I - ET - SW \pm \Delta W = 0 \quad (1)$$

5.2.2 Data management

Figure 5.2 shows the scheme of data transmission and storage. The output signal of the load cell is transmitted via an analog carrier frequency-measuring amplifier (AMP) (0-10 V) to an Analog-to-Digital-Converter (A/D-Converter) that converts the analog signal to digital units (digits). Lysimeter weighing data (W_{raw}) are measured every few seconds. A moving average is computed from 64 values and stored every 10 minutes on a data logger and on a local server (LYS-server) together with the cumulated raw counts (digits) from the tipping bucket (SW_{raw}).

Meteorological data (MET) in 1-minute-intervals are transmitted directly from the near ZAMG-station, and stored on the LYS-server with a common time stamp. Some of the available quantities are air temperature, relative humidity, air pressure, solar radiation, precipitation and wind velocity in 10 m height.

Stored data are frequently transmitted to a server at the Institute of Hydraulics and Rural Water Management (IHLW) that operates the lysimeters.

Additional information on cultivation actions (tillage operations, sowing, irrigation, fertilization, and harvest) is necessary for proper data interpretation. Such metadata are recorded in a protocol that is sent via e-mail on demand. In this regard, also pictures from a webcam that monitors activity on the lysimeters are used to facilitate data interpretation. The pictures are taken every minute and stored at IHLW-server, where they are available for data processing and interpretation.

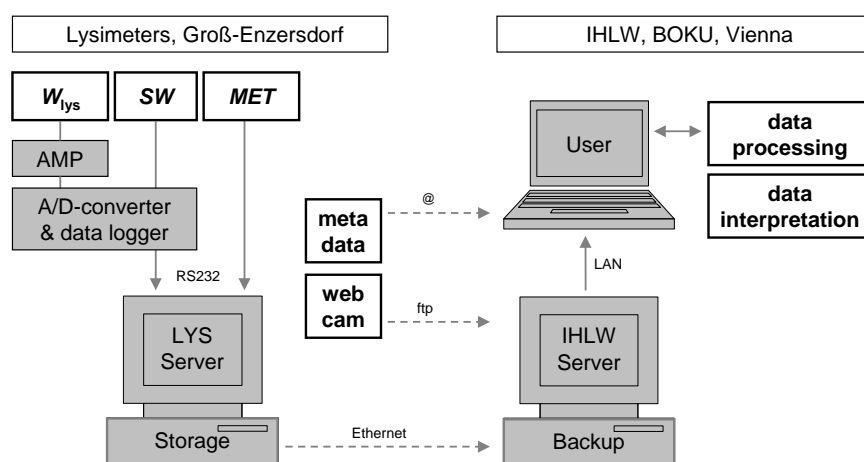


Figure 5.2: Scheme of data transmission and storage

First step of data processing is the conversion of stored weighing data and seepage water data into physical quantities by means of calibration factors.

The actual conversion factor for the weighing data $c_{lys} = 0.068 \text{ kg}\cdot\text{digit}^{-1}$ was determined subsequently to a general overhaul of the lysimeter facilities in 2007. Several loads (m_G) with a total mass of 106 kg were added to both lysimeters. Referring to this Figure 5.3 illustrates data from the grass reference lysimeter. The amount of seepage water during the measuring period was taken into account. Evapotranspiration was determined from the difference between the lysimeter mass without additional load at the beginning and at the end of the calibration procedure, and distributed to the respective intervals. The calibration factor was verified and confirmed by simplified calibration procedures in 2009 and 2011.

Multiplication of raw weighing data W_{raw} (digits) with the calibration factor c_{lys} ($\text{kg}\cdot\text{digit}^{-1}$) gives the relative lysimeter mass m_{lys} (kg), which is defined as current mass minus a reference mass. The current mass depends on the soil water content, whereas the reference mass approximates the lysimeter mass with dry soil. As mentioned above, the real mass is not known exactly – only mass changes are determined. Dividing $m_{lys} = W_{raw} \cdot c_{lys}$ by the lysimeter surface area ($A_{lys} = 2.85 \text{ m}^2$) and the density of water ρ_w delivers water equivalent of W with the dimension of a length (Eq. 2).

$$W = W_{raw} \cdot c_{lys} \cdot \rho_w^{-1} \cdot A_{lys}^{-1} \tag{2}$$

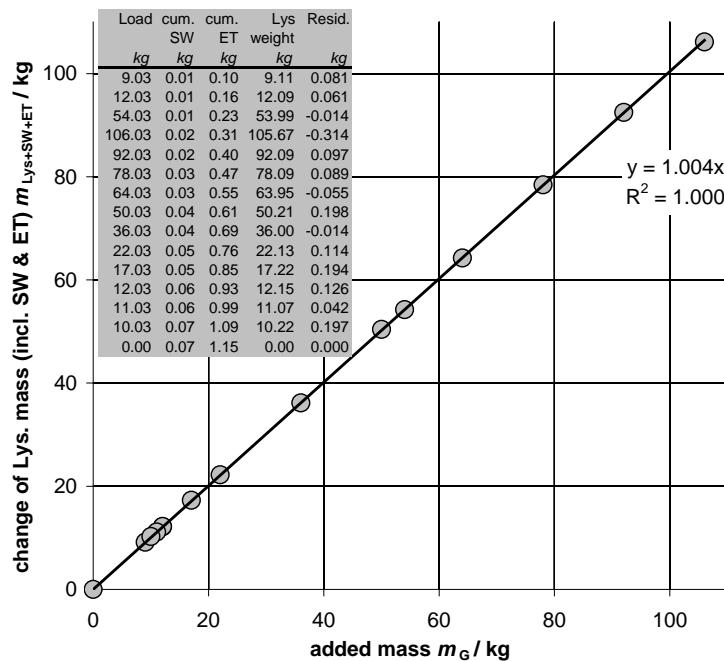


Figure 5.3: Calibration of the weighing system

One overturn of a tipping bucket for seepage water acquisition gives an impulse (one digit) that represents the volumetric content of a bucket. The factor $c_{tip} = 4.878 \text{ ml}\cdot\text{digit}^{-1}$ for converting raw seepage water SW_{raw} (digits) into outflow data SW was validated in 2010.

Dividing by the lysimeter surface area (A_{lys}) gives water equivalent of SW with the dimension of a length (Eq. 3).

$$SW = SW_{raw} \cdot c_{tip} \cdot A_{lys}^{-1} \quad (3)$$

5.2.3 Fitting smoothing functions

Weighing data from the grass reference lysimeter and weather data (wind and rain) from September 23rd to October 21st, 2009 were utilized for detailed interpretation. This period was selected mainly because of its wide range of wind velocity – 10-minute-wind velocity in 10 m height (u_{10}) ranged from zero to $13 \text{ m}\cdot\text{s}^{-1}$. Hence, rather smooth as well as severely noisy weighing data were found within the selected period. Furthermore, no drainage water and several days without rainfall occurred in the selected period, which reduced sources of possible inaccuracies.

Two types of smoothing functions were tested: a natural cubic approximation spline with discontinuities (for considering rainfall an irrigation), and a basic piecewise (daily) sigmoid function of the form

$$y(x) = a + b / (1 + \exp(-(x - c) / d)). \quad (4)$$

In contrast to the sigmoid function, spline smoothing could be applied to longer than daily datasets. However, a sound smoothing factor was determined manually for the respective dataset depending on wind velocity and precipitation. The standard factor was 0.001, a higher smoothing factor (0.01) giving less curvature had to be chosen for days with highly wind-affected data (Table 5.1).

Evaluation criteria were applicability, and quality of fitting between observed (W_i) and predicted data ($W_{i,p}$) expressed as root mean squared error ($RMSE$) (Eq. 5).

$$RMSE(W_{i,p}, W_i) = \sqrt{\frac{\sum_{i=1}^n (W_{i,p} - W_i)^2}{n}} \quad (5)$$

An example demonstrates the advantage of smoothing when evapotranspiration is determined on a shorter than daily time interval (e.g. hourly).

5.3 Results and discussion

As mentioned in section 5.2.3, no drainage water occurred during the studied period. Figure 5.4 illustrates (a) weighing data in equivalent water head (mm) and cumulated daily precipitation (mm), and (b) wind velocity in 10 m height. Raw data intervals were 10 minutes. Weighing data increased due to irrigation (on 2009-10-01) and precipitation, and decreased due to evapotranspiration from the grass surface.

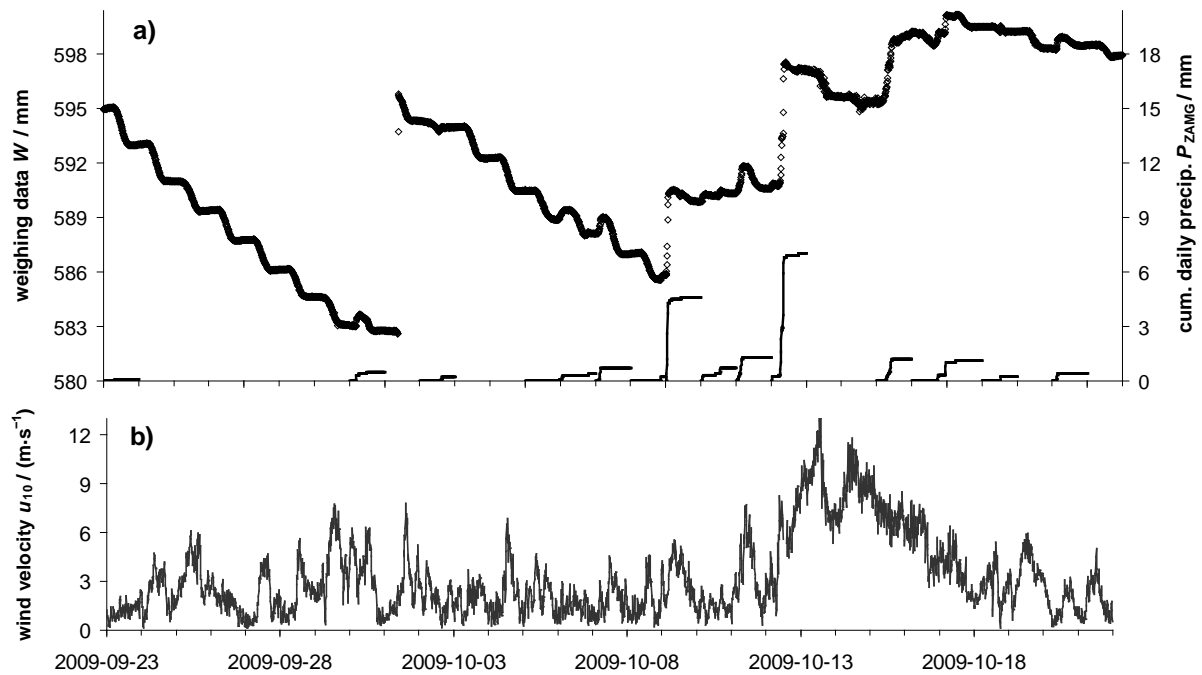


Figure 5.4: (a) Lysimeter weighing data, cumulated daily precipitation, and (b) wind velocity during the entire investigated period

Irrigation and daily precipitation (from 0:00 to 24:00) from ZAMG-weather data (P_{ZAMG}) and from changes in weighing data (P_{LYS}) are summarized in Table 5.1. Noticeable differences were identified only between October 14th and 16th due to snowfall that was detected by the lysimeter, but not by the pluviograph. Both smoothing functions worked well on data of days without precipitation. Individual factors for spline smoothing are also given in Table 5.1. *RMSE* was generally lower for spline smoothing, except for the drastically noisy data on October 13th. Since sigmoid functions are limited by their shape, sigmoid smoothing could not be applied on days with precipitation.

Table 5.1: Daily data of precipitation (irrigation), wind velocity, and performance of smoothing functions for the entire investigated period

	P_{ZAMG} (mm)	P_{LYS} (mm)	Mean wind vel. $u_{10,mean}$ ($m \cdot s^{-1}$)	Max. wind vel. $u_{10,max}$ ($m \cdot s^{-1}$)	Sigmoid smoothing <i>RMSE</i> (mm)	Spline smoothing <i>RMSE</i> (mm)	Spline smoothing factor	Example
2009-09-23	0.1	0.0	1.2	2.4	no fitting	0.025	0.001	
2009-09-24	none	none	2.3	4.7	0.040	0.028	0.001	
2009-09-25	none	none	3.5	6.1	0.035	0.024	0.001	
2009-09-26	none	none	1.7	3.5	0.033	0.021	0.001	
2009-09-27	none	none	1.9	4.7	0.033	0.021	0.001	
2009-09-28	none	none	2.2	5.6	0.028	0.022	0.001	
2009-09-29	none	none	4.0	7.7	0.033	0.033	0.001	Fig. 5.6
2009-09-30	0.6	0.6	3.4	6.3	no fitting	0.061	0.001	
2009-10-01		13.4 (irrigation)	2.5	7.8	no fitting	0.026	0.001	
2009-10-02	0.2	0.2	2.0	4.2	no fitting	0.019	0.001	Fig. 5.9
2009-10-03	none	none	1.9	3.7	0.027	0.012	0.001	Fig. 5.5
2009-10-04	none	none	2.3	6.8	0.032	0.015	0.001	
2009-10-05	0.2	0.2	2.2	4.7	no fitting	0.021	0.001	
2009-10-06	0.4	0.4	1.4	2.9	no fitting	0.021	0.001	
2009-10-07	0.8	0.8	2.0	4.5	no fitting	0.029	0.001	
2009-10-08	0.2	0.2	1.6	4.6	no fitting	0.024	0.001	
2009-10-09	4.8	4.7	3.2	5.5	no fitting	0.074	0.001	
2009-10-10	0.9	0.9	1.4	2.8	no fitting	0.017	0.001	
2009-10-11	1.3	1.3	3.4	7.7	no fitting	0.015	0.001	Fig. 5.10
2009-10-12	7.0	6.9	5.0	8.8	no fitting	0.049	0.001	
2009-10-13	none	none	9.1	13.0	0.111	0.115	0.01	Fig. 5.7
2009-10-14	none	0.3	8.7	11.8	no fitting	0.085	0.005	
2009-10-15	1.2	4.0	7.2	10.0	no fitting	0.086	0.005	
2009-10-16	1.3	1.7	5.5	7.9	no fitting	0.055	0.005 / 0.001	Fig. 5.11
2009-10-17	0.1	0.1	3.6	6.3	no fitting	0.017	0.005	
2009-10-18	0.4	0.4	2.6	5.4	no fitting	0.025	0.001	
2009-10-19	none	none	3.6	5.9	0.043	0.035	0.001	
2009-10-20	0.7	0.6	1.6	3.2	no fitting	0.028	0.005	
2009-10-21	none	none	1.8	5.0	0.029	0.020	0.001	

Six days with different weather conditions concerning precipitation and wind velocity were selected to illustrate exemplarily the performance of the smoothing functions (Figure 5.5 to Figure 5.11). Each figure shows (a) lysimeter weighing data with smoothing functions, and (b) wind velocity and eventually rainfall for a certain day.

Figure 5.5 to Figure 5.7 represent days without precipitation. In this case both smoothing functions were applicable. *RMSE* was low when weighing data were rather smooth. Figure 5.5 provides a characteristic illustration of decreasing profile water content due to plant water uptake and evaporation. In this example smoothing would not have been necessary; the original data allow a proper determination of *ET* (1.7 mm).

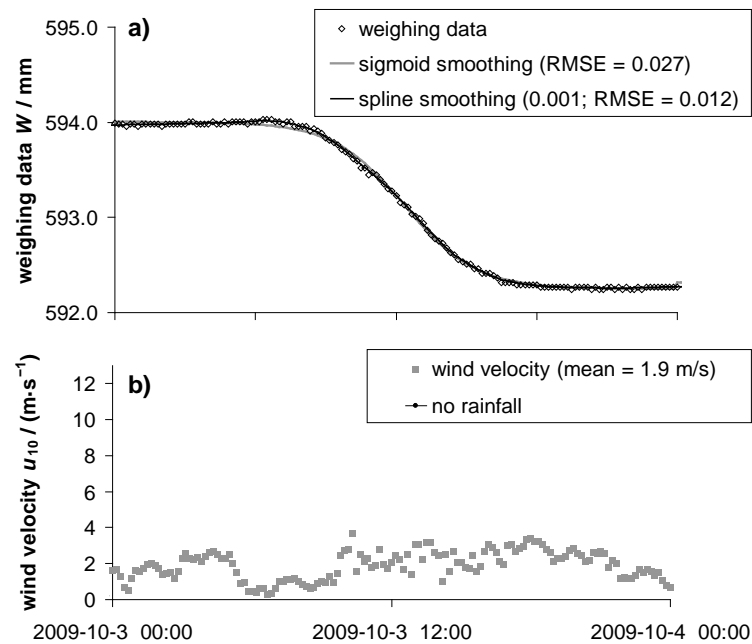


Figure 5.5: Sigmoid and spline smoothing on a day without rainfall and low wind velocity

Figure 5.6 shows a day with changing wind conditions. *RMSE* between original weighing data and smoothed data was equally low for both functions. Outliers were properly smoothed. Such outliers in the weighing data may complicate determination of mass changes in shorter time intervals.

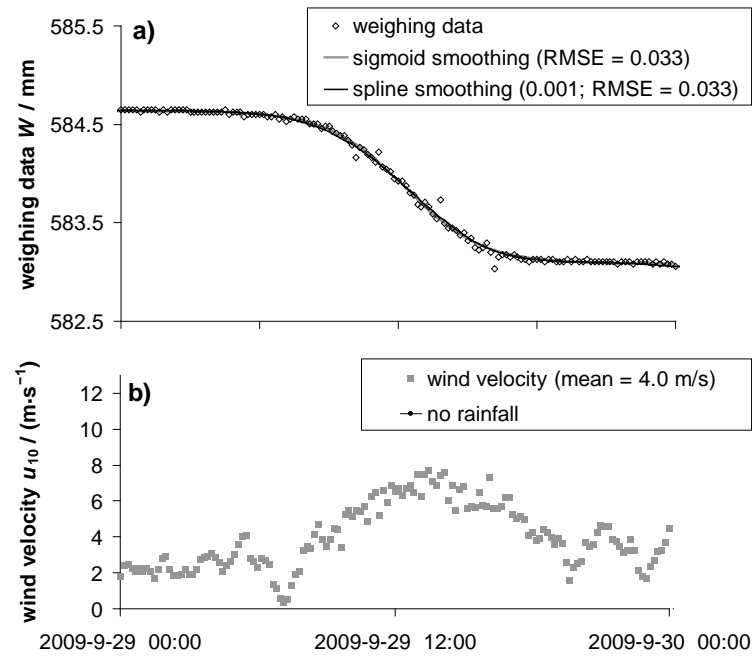


Figure 5.6: Sigmoid and spline smoothing on a day without rainfall and varying wind conditions that caused outliers in weighing data

High wind velocity on October 13th significantly affected weighing accuracy (Figure 5.7). In that case both smoothing functions offered a major improvement with respect to data interpretation, especially for short time intervals. Figure 5.8 illustrates evidently the advantage of smoothing functions when evapotranspiration is determined, for example, on hourly base (see Eq. 1: $SW = 0, P = 0 \rightarrow ET = -\Delta W$).

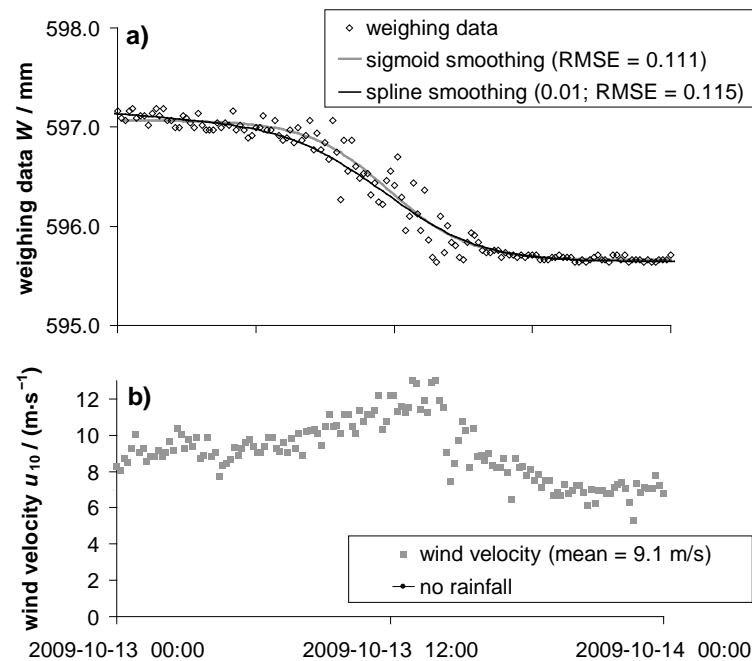


Figure 5.7: Sigmoid and spline smoothing of significantly noisy weighing data

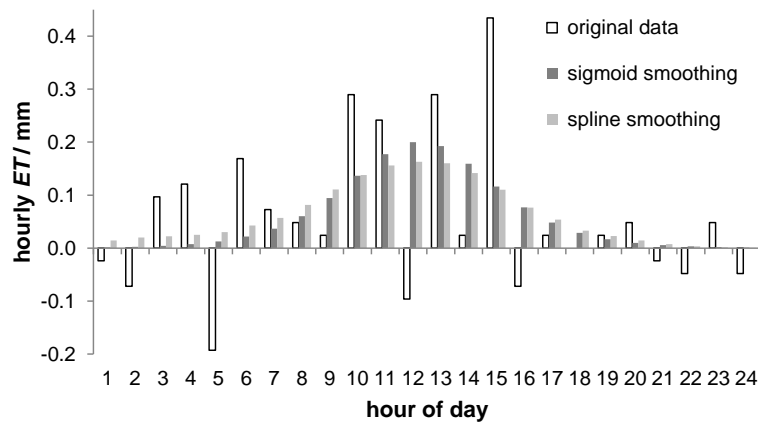


Figure 5.8: Hourly evapotranspiration ET on day 2009-10-13, calculated based on original data and both smoothing functions

Spline smoothing behavior and data interpretation for days with precipitation is illustrated in Figure 5.9 to Figure 5.11. Smoothing with distinct factors delivered proper results applied on a day with low wind velocity (Figure 5.9) as well as on a day with changing wind conditions (Figure 5.10). $RMSE$ was low in both cases, but smoothing factor had to be adjusted manually in order that slight variations were not flattened. P_{LYS} determined from weighing data corresponded well with P_{ZAMG} at these days (Table 5.1).

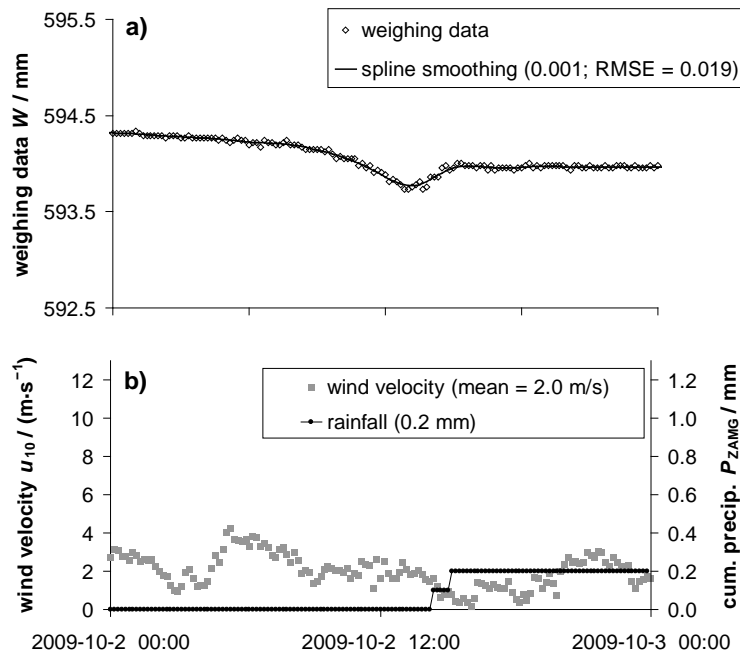


Figure 5.9: Spline smoothing on a day with low rainfall and low wind velocity

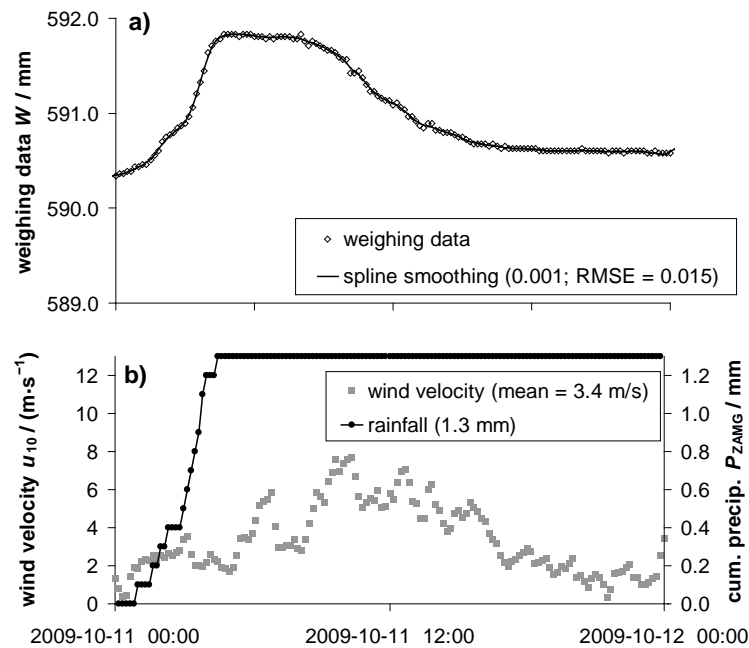


Figure 5.10: Spline smoothing on a day with rainfall and varying wind conditions

Unintended flattening of small changes in weighing data is a general disadvantage of smoothing and filtering procedures, respectively. For weighing data from October 16th, for example (Figure 5.11), it was necessary to adjust the smoothing factor within the daily dataset to get a proper compensation of the noisy data (0:00-15:00) on the one hand, but still indicate changes due to precipitation (snowfall) on the other hand. This example illustrates challenges with respect to automatic data processing. The latter is recommended only if a final personal check is executed.

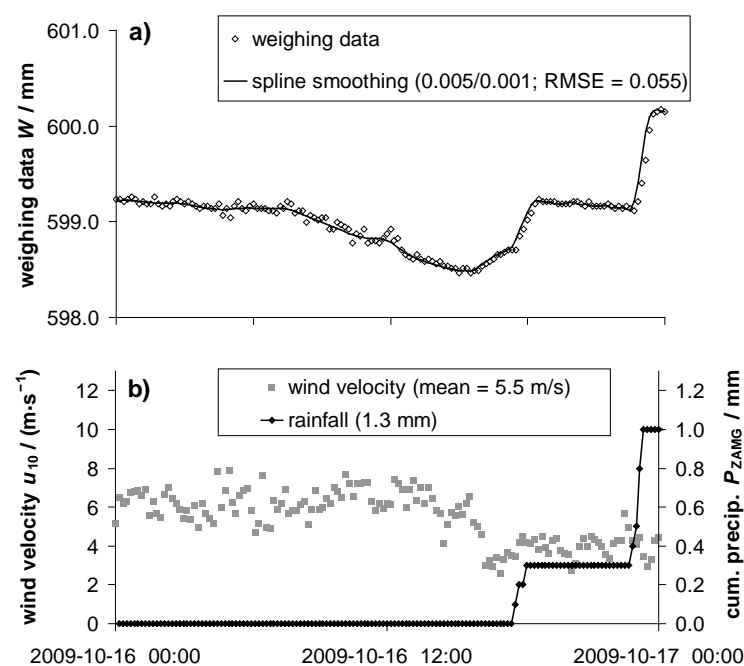


Figure 5.11: Spline smoothing on a day with high wind velocity and snowfall

5.4 Conclusions

A natural cubic approximation spline and a basic piecewise sigmoid function were tested on a dataset of partly noisy data from a weighing lysimeter with respect to simplified data interpretation. The sigmoid function was straightforward to fit, and it gave sound results of the typical diurnal variation of evapotranspiration. However, its applicability was restricted to datasets of single days without rainfall. The spline function performed generally better, except for one day (out of 28) with severely noisy data. Application was user-friendly, because it was calculated for the whole dataset in one work process. On the other hand, in several cases it was necessary to adjust the smoothing factor, which was rather time-consuming.

Generally, both smoothing methods provided an option for enhancing interpretation of noisy lysimeter weighing data. A main advantage was seen in investigations focusing on shorter than daily time intervals.

Acknowledgements

We thank our co-workers from IHLW and the staff from BOKU experimental station in Groß-Enzersdorf for maintaining the lysimeter facilities. We also thank the Central Institute for Meteorology and Geodynamics, Austria for providing weather data, and our colleagues from the Institute of Meteorology (BOKU-Met) for preparing them.

5.5 References

- Aboukhaled, A., Alfaro, A., Smith, M. (1982): Lysimeters. In: FAO Irrigation and Drainage Paper 39, FAO, Rome (Italy)
- Feltrin R.M., de Paiva J.B.D., de Paiva E.M.C.D., Beling F. A. (2011): Lysimeter soil water balance evaluation for an experiment developed in the Southern Brazilian Atlantic Forest region. *Hydrol. Process.* 25, 2321-2328.
- Howell, T.A., Schneider, A.D., Dusek, D.A., Marek, T.H., Steiner, J.L. (1995): Calibration and scale performance of Bushland weighing lysimeters. *Transact. ASAE*, 38(4), 1019-1024.
- Loos C., Gayler S., Priesack E. (2007): Assessment of water balance simulations for large-scale weighing lysimeters. *J. Hydrol.* 335, 259-270.
- Malone, R.W., Stewardson, D.J., Bonta, J.V., Nelsen, T. (1999): Calibration and quality control of the Coshocton weighing lysimeters. *Transact. ASAE*, 42(3), 701-712.
- Meissner, R., Seeger, J., Rupp, H., Seyfarth, M., Borg, H. (2007): Measurement of dew, fog, and rime with a high-precision gravitation lysimeter. *J. Plant Nutr. Soil Sci.*, 170, 335-344.

- Neuwirth, F., Mottl, W. (1983): Errichtung einer Lysimeteranlage an der agrar-meteorologischen Station in Groß-Enzersdorf. *Wetter und Leben*, 35, 48-53.
- Nolz, R., Kammerer, G., Cepuder, P. (2009): Windeinfluss auf die Lysimetermessungen in Groß-Enzersdorf. In: LFZ Raumberg-Gumpenstein (ed.): Proc. 13th Lysimeter Conf., Gumpenstein, Austria, 21.-22. April 2009, 17-20.
- Nolz, R., Kammerer, G., Cepuder, P. (2011): Datenmanagement der wägbaren Lysimeter in Groß-Enzersdorf. In: LFZ Raumberg-Gumpenstein (ed.): Proc. 14th Lysimeter Conf., Gumpenstein, Austria, 3.-4. May 2011, 33-38.
- Nolz R., Kammerer G., Cepuder P., 2013. Interpretation of lysimeter weighing data affected by wind. *Journal of Plant Nutrition and Soil Science*. doi 10.1002/jpln.201200342 (in press)
- Vaughan, P.J., Ayars, J.E. (2009): Noise reduction methods for weighing lysimeters. *J. Irrig. Drain. Eng.* 135(2), 235-240.
- von Unold, G., Fank, J., (2008): Modular design of field lysimeters for specific application needs. *Water, Air, & Soil Pollution, Focus* 8, 233-242.

6 Calibrating soil water potential sensors integrated into a wireless monitoring network³

Nolz R., Kammerer G., Cepuder P.

Abstract

Monitoring of the soil water status is a proper method for optimizing agricultural irrigation. Wireless sensor networks enhance data availability, thus, they can be used as decision support systems. In this study two types of soil water potential sensors were tested. One was the well-established Watermark sensor by Irrrometer Co., the other was the relatively new MPS-1 by Decagon Devices, Inc. The goal was to (1) integrate the sensors into a wireless monitoring network, (2) determine and evaluate calibration functions for the integrated sensors, and (3) compare the measuring range and the reaction time of both sensor types in a soil layer during drying. The integration of the sensors into the telemetry network worked well. Data were transmitted over several kilometers and made available via Internet access. Calibration was done for several sensors in a pressure pot. A general calibration function was found for the combination of Watermark sensors with the required interface. Sensor specific calibrations became essential for the MPS-1 due to the very large sensor-to-sensor variation. Four approaches were applied and evaluated: Fitting of a standard power function, fitting of a retention function, using so-called one-point calibrations, and using the factory calibration. The latter was not useful at all. The first two methods performed best. The one-point calibrations turned out to be a sound alternative, because the method is less time consuming. A set of sensors was installed in a thin soil layer in the laboratory in order to compare the water potential measurements during drying. Both sensor types delivered water potential measurements in a range from -10 kPa to -600 kPa. For values < -130 kPa the Watermark sensors reacted significantly more slowly than the MPS-1.

Keywords: Watermark; MPS-1; calibration; telemetry; irrigation management

³ Published as Nolz et al. (2013)

6.1 Introduction

In agriculture, the availability of sunlight, water and nutrients throughout the vegetation period is crucial for the development of plants, and consequently for the yield and quality. In agricultural areas where water is a limiting factor, irrigation is necessary in order to guarantee an optimal plant growth. Lack of water causes drought stress; over-irrigation, on the other hand, can lead to water logging and unproductive losses of energy, water and nutrients, since the latter can be leached and deeply drained to groundwater. A sound irrigation strategy implicates a demand-oriented plant water supply. Monitoring the soil water status provides an option to reach this goal.

The actual soil water content and the soil water matric potential are those physical quantities that describe the soil water status of a highly dynamic system at best. The soil profile water content expresses the available water within the rooting zone of a plant, ranging from zero (completely dry) to soil porosity (saturated). The soil water matric potential represents the energy per volume that is needed to withdraw water from the soil matrix. It varies from zero (saturated) to -1.5 MPa or even lower, where plant roots are not able to extract water from the soil anymore. The relation between both quantities describes one part of the hydraulic properties of a certain soil type, illustrated as typical soil water retention function. The soil profile water content can be calculated by way of soil water balance models, or measured by sensors of different types (Fares and Alva, 2000; Loiskandl et al., 1999; Thompson et al., 2007a; Tuller et al., 1997). Upper and lower thresholds for irrigation scheduling, for instance, are defined via the water content within the effective root zone at field capacity (where usually a matric potential of -33 kPa is supposed to occur) and permanent wilting point (which is commonly assumed to be the water content at a matric potential of -1.5 MPa). However, the respective soil water contents strongly depend on the pore size distribution (Thompson et al., 2007b). Thus, measuring soil water matric potential seems to be the straighter option as basis for irrigation management, because it is directly correlated to the water holding force and drought stress, respectively.

A traditional method for determining the matric potential of the pore water is to measure the pressure head in a water reservoir that is hydraulically connected to the soil by a porous medium. Water-filled tensiometers are based upon this principle. Their measuring range is theoretically restricted by the saturation vapor pressure; usually its limits are zero to about -80 kPa (Young and Sisson, 2002). Modern tensiometers measure matric potential with pressure transducers, which are very robust and an industrial standard since decades. However, conventional tensiometers require regular maintenance, mainly to keep the reservoir saturated throughout the monitoring period (Young and Sisson, 2002). Regarding irrigation management, tensiometers are proper tools in the wet range of the soil water status; this holds for example for vegetables (Thompson et al., 2007b).

An alternative strategy is to measure the electrical properties within a porous medium whose water matric potential is in equilibrium with the surrounding soil (Campbell and Gee, 1986). Watermark® sensors (Irrometer Co., Riverside, CA, USA) use this principle (Scanlon et al., 2002). They can measure matric potential over a wider range than tensiometers, namely

from approx. -10 kPa to -200 kPa (Centeno et al., 2010). Watermark sensors are inexpensive, easy to install, deliver reliable results, require little maintenance, and can be integrated into wireless sensor systems (Terzis et al., 2010; Thompson et al., 2006; Thompson et al., 2007b; Vellidis et al., 2008). Thus, they are commonly used for soil water status monitoring, particularly for irrigation scheduling (Centeno et al., 2010; Loiskandl et al., 1999; Shock et al., 2002).

Especially in horticulture and viticulture, Deficit Irrigation (DI) or Partial Rootzone Drying (PRD) may be applied in order to improve fruit quality (Leib et al. 2006; McCarthy et al., 2002). Such irrigation strategies allow soil water matric potentials to -200 kPa or even lower (Centeno et al., 2010; Goodwin, 2002; Kriedemann et al., 2003). In that case, the measuring range of Watermark sensors may reach their limits.

Recent developments brought sensors that are able to measure lower matric potentials. Novel resistance sensors have an extended measuring range with a lower limit of -1000 kPa or even less (Xin et al., 2007). Alternative improvements for measuring matric potential are porous matrix sensors with measurement of the relative permittivity and its relationship to water content of a porous block (Noborio et al., 1999; Or and Wraith, 1999). The porous medium is in equilibrium with the matric potential of the surrounding soil. After laboratory calibration the water retention function of the porous material is known, thus, the matric potential can be deduced from the sensor readings. Whalley et al. (2007) reported the development of a porous matrix sensor with a measuring range from -50 kPa to -300 kPa. Another relatively new sensor, the MPS-1 soil water potential sensor (Decagon Devices, Pullman, WA, USA) consists of a dielectric probe to measure the water content of two ceramic discs with known water retention characteristics. It can measure soil water matric potential from about -10 kPa to -500 kPa with an accuracy of 40 % (Decagon Devices, 2009). Malazian et al. (2011) recently reported a highly nonlinear sensitivity of the MPS-1, a relatively large sensor-to-sensor variation, and relatively small temperature- and hysteresis effects. Since the factory calibration turned out to deliver inaccurate results, they developed optimized common calibrations, and recommended to determine sensor-specific calibrations for detailed studies.

Beyond sensor principles and calibration, data management is an important issue regarding soil water monitoring. Electrical sensors can be operated with handheld logger devices or with stand-alone logger systems. During the past decade, wireless sensor networks for environment monitoring became more popular (Terzis et al., 2010; Vellidis et al., 2008). Sophisticated telemetry systems are available for data logging and data transmission. Adcon Telemetry GmbH (Klosterneuburg, Austria) developed a wireless sensor network that uses Remote Terminal Units (RTUs) to collect and transmit data from different sensors (Adcon, 2011), measuring e. g. weather data or soil water status (water content, matric potential). The readings are temporarily stored in an RTU, and transmitted via UHF or via GSM/GPRS to a central logger. Then, data are transferred to a server, processed automatically (i.e. conversion of raw data by means of calibration functions) and made available for registered users via the Internet.

The aim of this work was to (1) integrate Watermark and MPS-1 sensors into a wireless monitoring network, (2) determine and evaluate calibration functions for the integrated sensors, and (3) compare the measuring range and the reaction time of both sensor types in a soil layer during drying.

6.2 Materials and methods

6.2.1 Sensor setup

Six Watermark sensors and six MPS-1 sensors were tested and calibrated in the laboratory.

The Watermark® sensor (Irrometer Co., Riverside, CA, USA) is a granular matrix sensor (GMS) with internal electrodes measuring the electrical resistance of the reference material (Irrometer, 2010). Generally, the sensor output has to be converted to sensor- and soil water matric potential via a sensor-specific calibration function. Several calibration functions have been published in the past (Scanlon et al., 2002). Thomson and Armstrong (1987) determined the relation between matric potential from -10 kPa to -100 kPa and sensor resistance (k Ω) for the Watermark 200, a prior sensor model. Furthermore, they showed that sensor readings were significantly affected by temperature (1.8 % per $^{\circ}\text{C}$ related to temperature of 18.3°C) and considered that for their calibration. Spaans and Baker (1992) determined sensor-specific non-linear calibrations, and concluded that measurements were not accurate and not reproducible. Shock et al. (1998) developed a calibration function for the Watermark Model 200SS in the range between -10 kPa and -75 kPa and at 15°C and 25°C , and compared it to previously published equations. Several authors used these calibration functions or evaluated them (Eldredge et al., 1993; Intrigliolo and Castel, 2004; Leib et al., 2003; Thomson et al., 1996).

The MPS-1 is a dielectric water potential sensor with a measuring range of -10 kPa to -500 kPa (pF 2 to pF 3.71). Its main parts are two circular ceramic discs assembled on both sides of a circuit board that measures the water content of the ceramics with a frequency domain principle (Decagon Devices, 2009). When a sensor is installed in the soil with constant matric potential, the matric potential of the water inside the ceramics reaches equilibrium after some time by water uptake or release, thus, a relationship between the sensor signal and the matric potential of the surrounding soil can be found.

Both sensor types require special interfaces for their linkage to the telemetry system. The Adcon Watermark-interface is an amplifier, to which up to three standard Watermark sensors (Model 200SS) can be connected. The interface transforms the Watermark signal into an analog output signal. Since the Watermarks' common calibration relationship between the electrical resistance and the water potential largely depends on the measuring device, and the internal signal transformation processes of the Adcon Watermark-interface are unknown, sensors and interface have to be treated as one device. The default calibration relationship for this system is a linear function between the matric potential ψ_m (0 kPa to -200 kPa) and the analog output signal (0 V to 2.5 V).

MPS-1 sensors require a stabilized excitation voltage of 2 to 5 V DC, returning an output voltage from approx. 0.5 V (dry) to 0.8 V (wet). A standard interface from Decagon Devices, Inc. supplies up to three sensors with the required voltage and delivers the sensor output (maximal range from 0 V to 2.5 V) to a logger.

A Remote Terminal Unit (RTU) with analog inputs served as data logger. The analog signal (0-2.5 V) is converted into a digital format with a resolution of 12 bit (zero to 4095 digital units). Due to the above-mentioned reasons the Watermark readings are displayed in digits, hence the results are very system specific. In contrast, the MPS-1 readings are expressed in mV in order to make the data comparable and the results of the calibration more general.

6.2.2 Sensor calibration

Establishing the relationship between the matric potential ψ_m in the soil and the sensor signal requires a laboratory-apparatus in which a certain value for ψ_m can be set (Campbell and Gee, 1986). In the low range ($\psi_m < -0.1$ MPa) only pressure plate apparatuses are convenient (Klute, 1986). The Watermark and MPS-1 soil water potential sensors were calibrated in separate pots (Fig. 6.1).

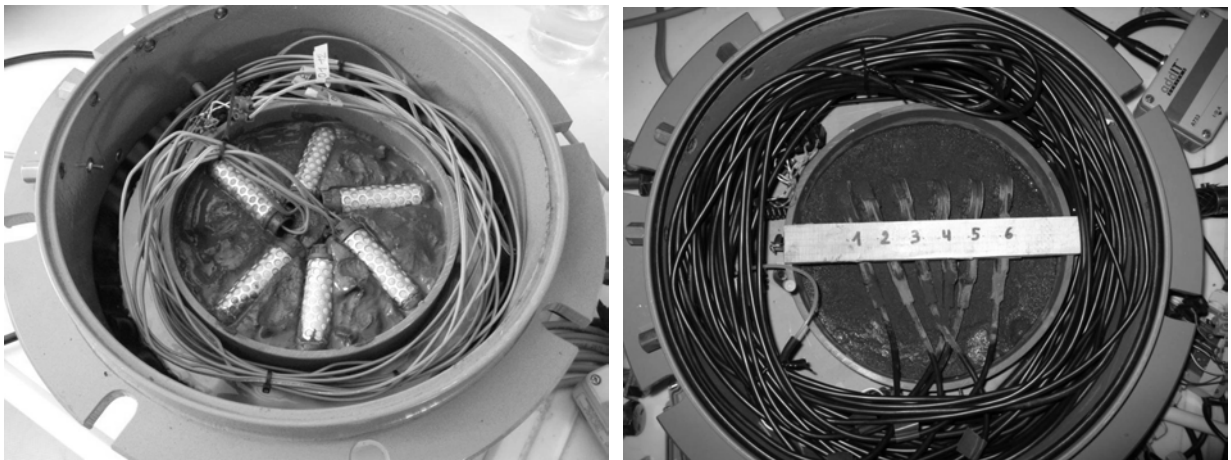


Fig. 6.1. Pressure plate apparatus with Watermark sensors (left) and MPS-1 (right)

According to Scanlon et al. (2002), dynamic response of the sensor and poor contact between sensor and soil are the main sources of error. The sensor response should be improved by using a 2 mm-sieved material with a corresponding higher unsaturated hydraulic conductivity. A mixed soil sample with a texture of 40 % sand ($2 \text{ mm} > d > 0.063 \text{ mm}$), 40 % silt and 20 % clay was taken for contact material between the sensor surface and the ceramic plate of the pot. Slurry was made and filled with a height of approx. 2 cm into a PVC-ring that was positioned centrally on a saturated pressure plate. The sensors were slightly pressed into the slurry in order to guarantee a good contact between the soil and the sensor material. For the same reason this procedure is also recommended for field installation. Since the matric potentials (not the water contents) of sensor and soil are in equilibrium, the results

from the disturbed installation should be transferable to field conditions. However, in very coarse soil and in clay soil large differences between the pore size of the sensor matrix and the surrounding soil may cause hydraulic decoupling of the two materials (Scanlon et al., 2002).

The sensor cables were connected to a lead-through. The lid of the pot was closed and the desired air pressure applied. The sensors and the surrounding soil layer started to drain. After reaching equilibrium between air pressure in the pot and matric potential inside the sensor and the contact material, each sensor reading at a respective equilibrium pressure gave a certain point of the calibration curve.

As mentioned above, the default calibration relationship for the Adcon Watermark sensors is a linear function between the converted output (0-4095 digits) and the soil water potential ψ_m (0 kPa to -200 kPa). In order to validate this relation and sensor-to-sensor variation, six sensors were tested in the pressure plate apparatus with a 3 bar pressure-plate at an equilibrium pressure of 150 kPa. Equilibrium status was reached, when no water outflow from the soil was measured. Then, three Watermarks were selected for repeated measurements at equilibrium pressures of 50, 100, 150, 200, 250, and 290 kPa. A standard curve was fitted to the data pairs as calibration function.

Preliminary MPS-1 sensor readings were done in air and water in order to verify the measuring range and sensor-to-sensor variations. Afterwards the sensors were put into a prepared pressure pot with a 3 bar-pressure plate. Applied air pressures were 50, 100, 150, 200, 250, and 300 kPa. A second measuring series was carried out at 20, 50, 100, 200, 300, and 400 kPa on a 15 bar pressure-plate. Equilibrium status again was reached, when no more water outflow was observed.

Four calibration methods were tested in this study from the dataset of the second measuring series of the MPS-1 pressure plate experiment. They were applied to the five sensors No. 1, 2, 4, 5, and 6 (sensor No. 3 showed implausible results for the second measuring series, very likely due to a poor soil contact).

Firstly, the general factory calibration (Decagon Devices, 2009) was applied, yielding the matric potential ψ_m as a function of the respective amplified sensor reading U :

$$\psi_m / \text{kPa} = -\exp [4.80 \times 10^{-5} (U/\text{mV})^2 - 8.46 \times 10^{-2} U/\text{mV} + 39.45] \quad (1)$$

The second method was a sensor-specific fit of a power function of the form

$$\psi_m (U) / \text{kPa} = a \cdot (U/\text{mV})^b \quad (2)$$

to the data pairs. This method was chosen as an example of a traditional approach, where measured data pairs serve as basis for fitting a calibration function. The latter was calculated easily by means of a standard spreadsheet.

As basic approach for the methods three and four it was assumed that the hydraulic behavior of the sensor ceramic can be modeled equally to soils, and a typical soil water retention function is suitable for the relationship between the water content and the matric potential of the ceramic disc. Most of these models describe the relationship between ψ_m and the effective saturation S_e

$$S_e(\theta) = (\theta - \theta_r) / (\theta_s - \theta_r), \quad (3)$$

where the parameters θ_r and θ_s represent the residual and saturated water content. The relationship between S_e and the matric potential ψ_m in equilibrium with the applied pressure was calculated by means of the soil water retention function after van Genuchten (1980)

$$S_e(\psi_m) = (1 + (\alpha \cdot \psi_m)^n)^{1/n-1}. \quad (4)$$

α ($\dim \alpha = (\dim \psi_m)^{-1}$) and n are shape parameters of the model, ψ_m is positive. Combining Eq. (3) and (4) gives a set of 4 parameters for the function $\theta(\psi_m)$.

The third method applied was a so-called one-point calibration (*OP*) developed by Malazian et al. (2011). The *OP*-method is based on three single functions of a normalized voltage $f(U/U_{ref})$, where U_{ref} is the sensor reading at one of the three reference potentials ψ_{ref} 50, 100 or 200 kPa. The curves are supposed to fit best for the entire pool of MPS-1 sensors near the respective ψ_{ref} . The normalization became necessary because of the relatively large sensor-to-sensor variation. The advantage of this method is that only one reading U_{ref} is required, which simplifies the calibration procedure.

U_i are the sensor readings at the respective equilibrium pressure ψ_i , and U_{ref} are the readings at ψ_{ref} 50, 100, and 100 kPa, respectively. Combining and rearranging Eqs. (3) and (4) yields the water potential (ψ_m) as a function of the normalized sensor output (U/U_{ref})

$$\psi_m = \alpha^{-1} \left(\left(\frac{(U/U_{ref}) - \theta_r}{\theta_s - \theta_r} \right)^{n/(1-n)} - 1 \right)^{1/n}, \quad (5)$$

with the calibration parameters θ_r , θ_s , α , and n after Malazian et al. (2011).

For the fourth method the sensor readings U_i in mV and the unknown water content of the sensor ceramic expressed as effective saturation S_e were linearly correlated.

$$S_e(U) = U \cdot a + b. \quad (6)$$

Equations 3, 4 and 6 establish the relation $\theta(U)$ with six model parameters, but θ_r and θ_s are not independent from the coefficients a and b , so the latter could be chosen randomly. In order to yield typical values for the van Genuchten parameters, the linear coefficients a , and b were specified more or less arbitrarily leading to an effective saturation (S_e) ranging approx. from zero to 0.5. Thus, for each of the five tested sensors, a specific calibration function was determined by optimizing θ_r , θ_s , α and n . Combining and rearranging Eqs. (3) and (4) yields the matric potential (ψ_m) as a function of the sensor output (U) in mV

$$\psi_m = \alpha^{-1} \left(\left(\frac{(U \cdot a + b) - \theta_r}{\theta_s - \theta_r} \right)^{n/(1-n)} - 1 \right)^{1/n} \quad (7)$$

6.2.3 Evaluation of calibrations

In order to evaluate the calibration results, the Root Mean Square Error (RMSE / kPa) was calculated for the calibrated values $\psi_{i,c}$ of sensors 1, 2, 4, 5, and 6, at six equilibrium pressures ψ_i (20, 50, 100, 200, 300, and 400 kPa).

$$\text{RMSE} (\psi_{i,c}, \psi_i) = \sqrt{\frac{\sum_{i=1}^n (\psi_{i,c} - \psi_i)^2}{n}} \quad (8)$$

The Mean Relative Error (MRE / %) expresses the ratio of the mean residuals of all sensor readings to the equilibrium pressures.

$$\text{MRE} (\psi_{i,c}, \psi_i) = \frac{\sum_{i=1}^n \left[\sqrt{(\psi_{i,c} - \psi_i)^2} / \psi_i \right]}{n} \quad (9)$$

6.2.4 Comparison of sensors

Three Watermark sensors and three MPS-1 sensors (S2, S3, and S6) were installed in a 6 cm soil layer bedded in a small box (16 x 26 cm). The soil was initially wetted, then soil water was evaporated in an environmental chamber (air temperature: 25°C, relative humidity: 50 %) for four days. Since it turned out that the soil in the box dried very fast at these conditions, the rest of the experiment was conducted under laboratory conditions (air temperature: 18-22°C, relative humidity: approx. 60-70 %). Two more wetting-drying-cycles were initiated at which matric potential was measured continuously.

The sensors were connected to an RTU that was integrated into an existing telemetry network. Raw data were transmitted via other RTUs to an external server from where they were available via an Internet connection.

6.3 Results and discussion

In this section the calibrated matric potentials $\psi_{m,c}$ from sensor readings are expressed in absolute values (kPa).

6.3.1 Watermark calibration

The default calibrated measurements of six sensors delivered 92, 89, 87, 92, 87, and 86 kPa (average $\mu = 89$ kPa, standard deviation $\sigma = 3$ kPa). The applied pressure of 150 kPa was significantly underestimated. Since it was a single measurement at a constant temperature, the differences were mainly caused by sensor-to-sensor variation. We decided to determine a general calibration for the interfaces and the sensor set we used. The main reason was to keep the monitoring network user-friendly, because the calibration function could be implemented into the automatic processing of the system, and single sensors were exchangeable, i.e. when damaged. The three measuring series for calibration purposes delivered several sensor readings for each equilibrium pressure. In this experiment, the differences may have been referred not only to sensor-to-sensor variations, but also to measuring errors, poor reproducibility, or temperature effects (Spaans and Baker, 1992). We decided to interpret the deviation as uncertainty, and expressed the results as average μ (kPa) and $2\text{-}\sigma$ -error (%), representing about 95 % of the measurements ($\mu \pm 2\cdot\sigma$).

The sensor readings of the calibration series were summarized in a single graph (Fig. 6.2). The box plots express the range of all sensor readings ($\mu \pm 2\cdot\sigma$). The data pairs show nonlinear characteristics. In order to yield a calibration function $\psi_m(U)$, the axis were switched and basic curve was fitted by means of a standard spreadsheet. A power function of the form

$$\psi_m(U) = a \cdot U^b \tag{10}$$

with the coefficients $a=0.00021$ and $b=1.79390$ turned out to give the best correlation (coefficient of determination $R^2 = 0.99910$) (Fig. 6.3). The $2\text{-}\sigma$ -errors were transformed to the output-axis of the calibrated sensor readings as matric potential $\psi_{m,c}$ in kPa (Fig. 6.3). The mean error was 14 %. We assumed that this uncertainty included sensor-to-sensor variations and temperature effects: The $2\text{-}\sigma$ -error of sensor-to-sensor variation (see above) was approx. 6 %. The air temperature in the laboratory was 21°C to 26°C during the calibration series. The sensors reacted on a 5°C higher temperature with approx. 5 % lower readings at the 100 kPa pressure step (data not shown). Estimating a temperature effect of 1.8 % per °C (Thomson and Armstrong, 1987) would result in an error of approx. 9 % for a 5°C

temperature difference. Working with a temperature corrected calibration function would improve the measuring accuracy. On the other hand, a separate temperature sensor would be necessary, because a Watermark sensor cannot measure temperature itself. We consider the installation of additional soil temperature sensors unpractical with respect to irrigation management.

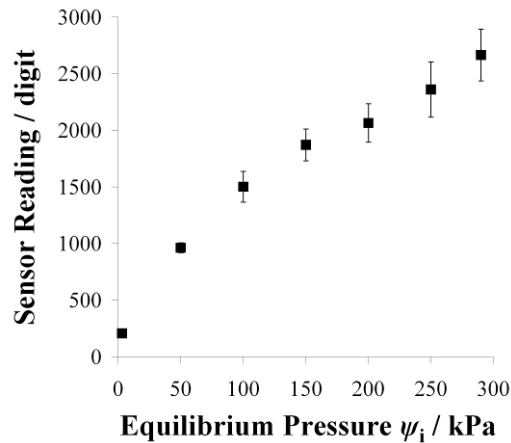


Fig. 6.2. Readings of three Watermark sensors and two repetitions at several equilibrium pressures in the pressure pot (boxes = mean, bars = 2- σ -error)

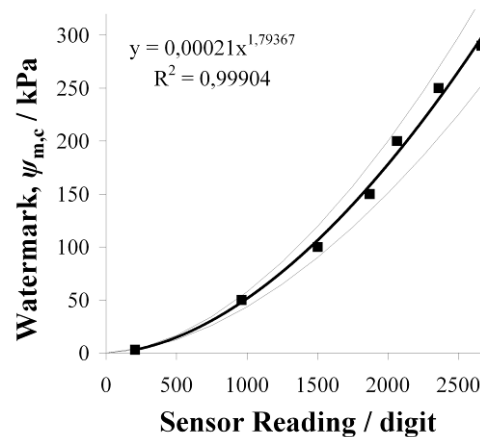


Fig. 6.3. Watermark calibration function (line) with transformed mean 2- σ -error (thin lines) and measured data pairs (boxes)

However, the mentioned uncertainty (14 %) has to be taken into account regarding data interpretation, especially if soil water movement is to be investigated via gradients in matric potential.

6.3.2 MPS-1 test

Since it was the very first time that MPS-1 sensors were used with the Decagon interface and the Adcon RTU, preliminary tests were essential. Manual multimeter measurements showed that the sensors required a stable excitation voltage for about 4 seconds (the default setting was 2 seconds) in order to deliver a stable output signal. Thus, the RTU was programmed to measure every minute for 5 seconds, and store the mean value once per hour. Nevertheless, the MPS-1 readings in air showed an unusual random noise with measured values in a range of approx. ± 20 mV (Fig. 6.4a). The noise could be reduced to approx. ± 2 mV by adding an inductance of 100 mH in series to the excitation cable (Fig. 6.4a). After the modification, the air dry sensors gave an output signal of 540-570 mV, at the wet end the readings were 750-790 mV (Fig. 6.4b). One can see considerable sensor-to-sensor variations.

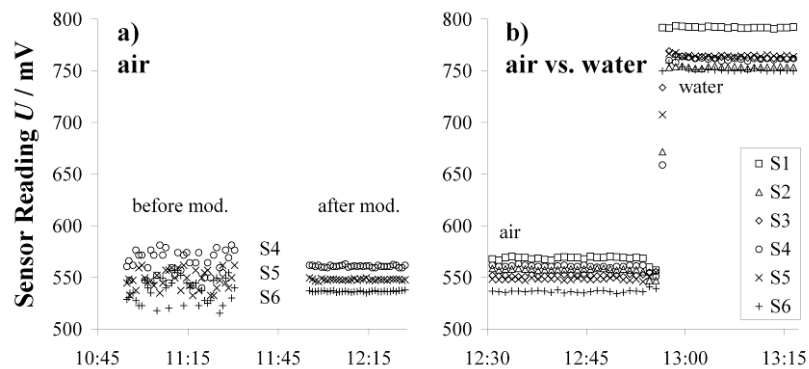


Fig. 6.4. (a) MPS-1 readings in air: Noisy output signal before modification and stable values after modification; (b) MPS-1 readings in air and water (after modification)

6.3.3 MPS-1 calibration

The first MPS-1 measurement series gave sensor readings at equilibrium pressures of 50, 100, 150, 200, 250, and 300 kPa (Fig. 6.5a). Sensor number 2 (S2) had a cable failure. The second series with pressure steps at 20, 50, 100, 200, 300, and 400 kPa (Fig. 6.5b) lasted about nine months, because the soil needed much more time to drain through the 15 bar-pressure plate. The longest time intervals occurred at the pressures of 300 kPa (approx. 50 days) and 400 kPa (approx. 100 days), respectively. Readings of Sensor 3 (S3) were not reliable, likely due to a poor contact between sensor and soil.

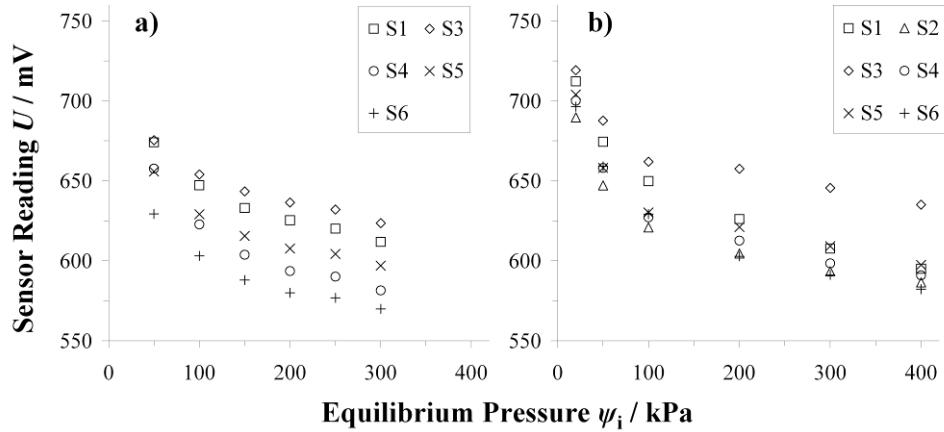


Fig. 6.5. MPS-1 readings in the pressure plate apparatus: (a) series 1 (equilibrium pressures: 50, 100, 150, 200, 250, and 300 kPa), (b) series 2 (equilibrium pressures: 20, 50, 100, 200, 300, and 400 kPa)

The common pressure steps of both series (50, 100, 200, and 300 kPa) were analyzed regarding the consistency of the sensor readings (sensors number 1, 4, 5, and 6) (Fig. 6.6). Sensor 1 (S1) delivered almost the same output values for the respective pressures at series 1 and 2. S1 was already tested in the field (unpublished data) and had therefore already gone through several wetting and drying cycles. The other sensors were just initially wetted; the second measurement series produced higher sensor outputs at higher pressures compared to the previous series (Fig. 6.6). It could have happened that the soil was not perfectly drained, despite the long drainage interval mentioned above, and despite the controlling of the amount of water outflow. The latter is very low at dry soil conditions, and the determination of the volume (weight) difference is affected by evaporation losses from the storage cup. Nevertheless, we decided to use the second measurement series (except for sensor 3) as basis for the calibration procedure, mainly because of the slightly lower sensor-to-sensor variation (Fig. 6.6) and the readings at the equilibrium pressure of 400 kPa.

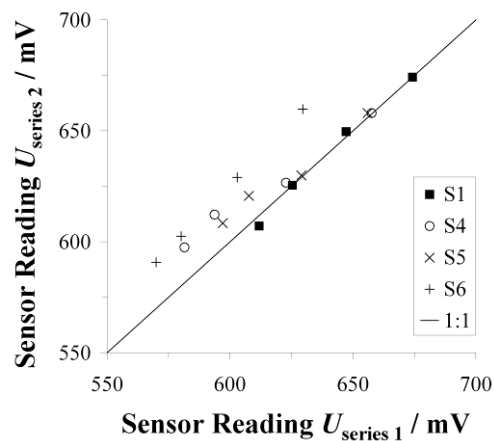


Fig. 6.6. Consistency test of MPS-1 readings: measuring series 1 (x-axis) versus series 2 (y-axis)

The factory calibration establishes the default relationship between sensor reading and pressure (Eq. 1). The resulting coefficients a and b for sensor-specific power function (Eq. 2, second method) as well as the respective coefficient of determination R^2 are summarized in Tab. 6.1. One-point calibration functions, representing method three, were calculated by means of Eq. 5 and the fitted parameters θ_r , θ_s , α , and n after Malazian et al. (2011). The results of method four (retention function) required for Eq. 7 – the optimized parameters θ_r , θ_s , α , and n and the fixed values for a , and b – are given in Tab. 6.2. Hence, a specific calibration for each of the tested sensors (1, 2, 4, 5, and 6) was calculated. All sensor-specific calibration functions are demonstrated in Fig. 6.7. Differences between the curves seem to be lower for S1 and S6 compared to S2, S4, and S5, respectively. Calibrated matric potential $\psi_{m,c}$ was calculated from each sensor reading and related to the respective equilibrium pressure ψ_i (Fig. 6.8). Factory calibration delivered diverging results for ψ_i at increasing pressures. It generally overestimated $\psi_{m,c}$ clearly (Fig. 6.8a). However, factory calibration was suitable for sensor S1 (Fig. 6.8a, boxes). Approximating the sensor readings to the applied pressures by means of a standard function delivered a better adjustment of the sensor readings with more or less evenly distributed deviations at the equilibrium pressures (Fig. 6.8b). The sensor-specific calibration based on the retention function showed the best fit (Fig. 6.8c). However, noticeable deviations were found for the readings at 200 kPa, and the readings of S5 at 300 and 400 kPa. A reason may be a sensor-soil-non-equilibrium. By definition, the OP-calibrations suited best near the optimized pressures of 50, 100, and 200 kPa, respectively (Fig. 6.8d-f). The OP₅₀-calibration generally underestimated pressures higher than 100 kPa (Fig. 6.8d). The OP₁₀₀-calibration gave a good fit with S1 and S6, but underestimated the other sensors at pressures exceeding 100 kPa (Fig. 6.8e). Among the OP-calibrations, OP₂₀₀ showed the best fit, except for the outlier of S1 at 400 kPa (Fig. 6.8f).

Tab. 6.1: Coefficients a , and b of a standard calibration function $\psi_m = a \cdot U^b$, and coefficients of determination (R^2) for the five tested MPS-1

	S1	S2	S4	S5	S6
$a =$	4E+49	9E+53	5E+51	8E+54	2E+48
$b =$	-16.94	-18.57	-17.73	-18.85	-16.53
$R^2 =$	0.9974	0.9856	0.9872	0.9701	0.9983

Tab. 6.2: Optimized parameters for the sensor calibration (θ_r , θ_s , α , and n) based on the retention function of the MPS-1 ($a = 0.002$ and $b = -0.833$)

	S1	S2	S4	S5	S6
$\theta_r =$	0.000	0.058	0.033	0.101	0.035
$\theta_s =$	0.407	0.564	0.683	0.779	0.385
$\alpha =$	0.043	0.296	0.600	0.594	0.044
$n =$	1.319	1.366	1.307	1.419	1.427

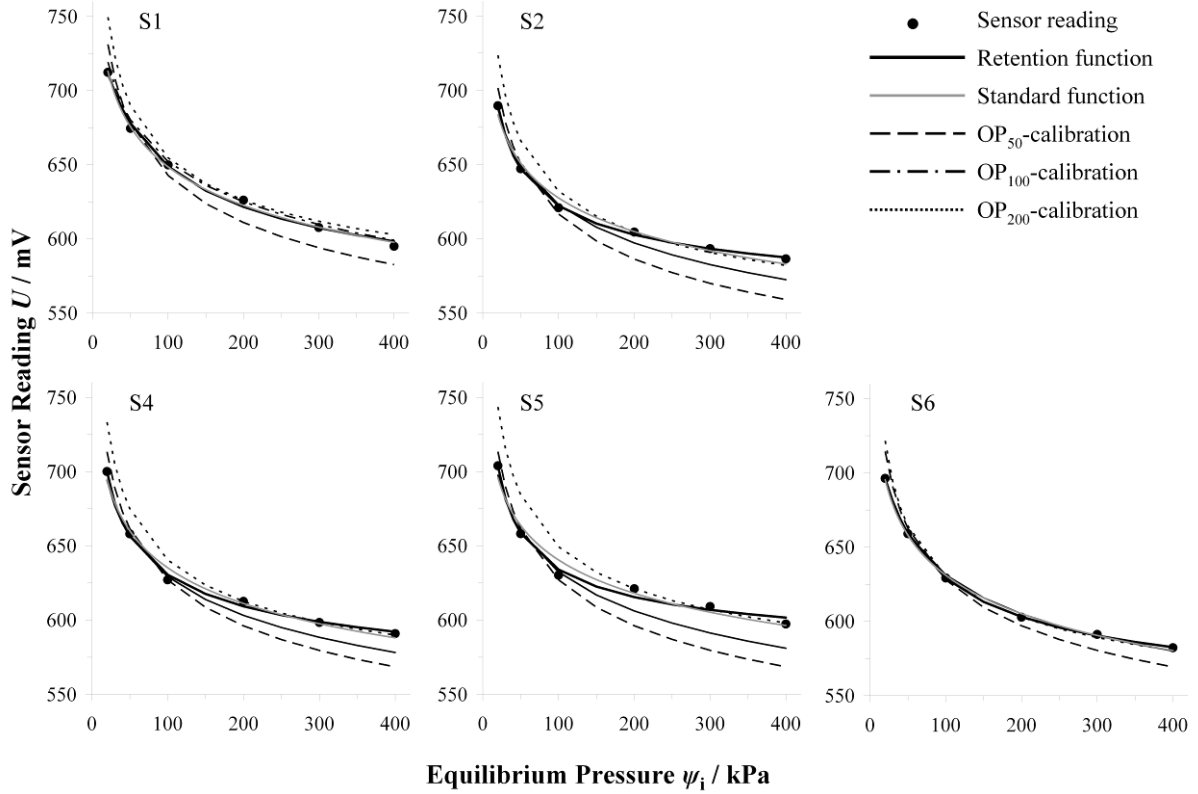


Fig. 6.7. Sensor-specific calibration functions (fitted standard function, fitted retention function and one-point calibrations) and sensor readings of five sensors at six equilibrium pressures

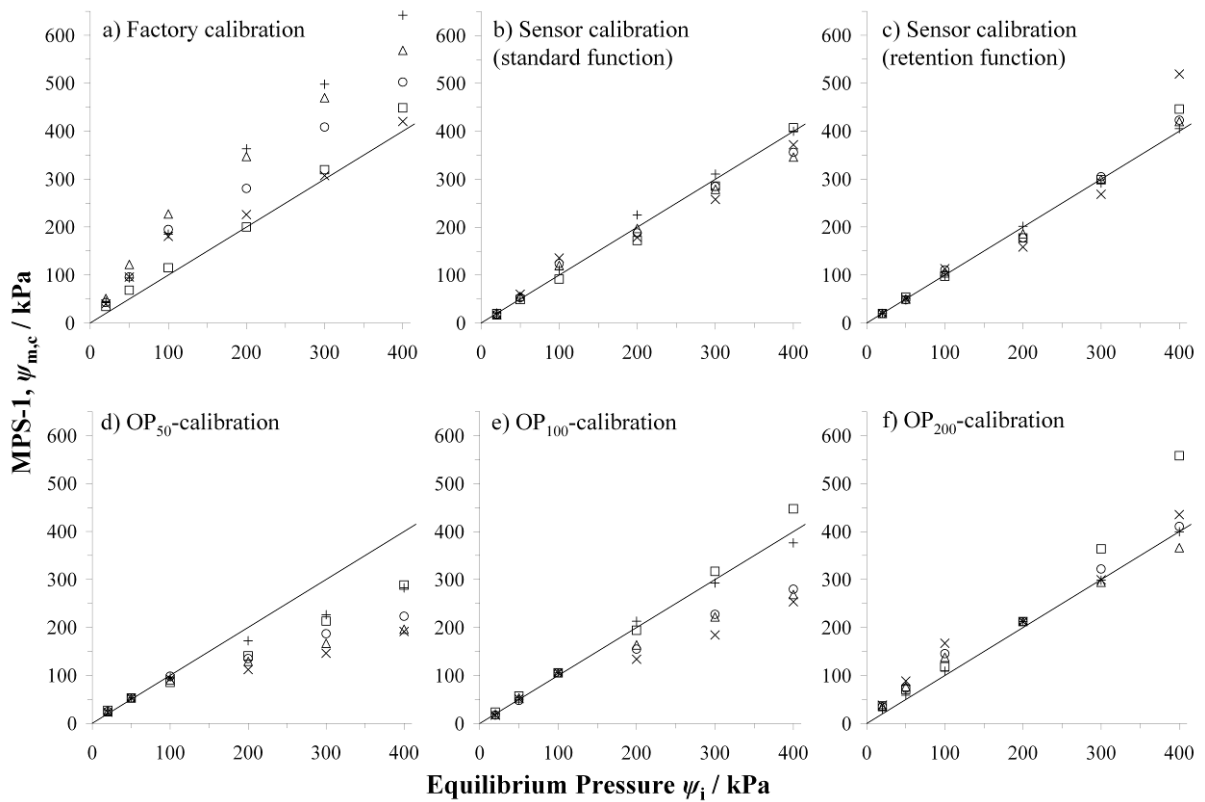


Fig. 6.8. Calibrated matric potentials (factory calibration, standard function, retention function, and one-point calibrations) of five sensors at six equilibrium pressures

6.3.4 Evaluation of the calibrations

Root mean square errors (RMSE) (Eq. 8) and mean relative errors (MRE) (Eq. 9) for the calibrated matric potential in relation to the applied pressures are summarized in Tab. 6.3. Generally, the factory calibration had the worst performance with the highest RMSE (85 kPa) and MRE (65 %), respectively. Comparing the one-point calibrations in general, the OP₂₀₀-calibration delivered the best RMSE (36 kPa). On the other hand, it had a very high MRE (33 %) because of the relatively large deviations in the wet range. In summary, sensor calibration based on the standard function and on the retention function performed best, with slight advantages for the latter due to the lowest MRE of 6 %. Regarding a single sensor, however, another calibration function may fit best, as it was stated above referring, e.g., to Fig. 6.8.

Tab. 6.3: Root Mean Square Error (RMSE / kPa) and Mean Relative Error (MRE / %) of five MPS-1 sensors (S1, 2, 4, 5, and 6) at six equilibrium pressures (20, 50, 100, 200, 300 and 400 kPa), for each calibration method

Calibration	RMSE (kPa)	MRE (%)
Factory calibration	85	65
Sensor calibration (standard function)	21	6
One-point calibrations		
OP ₅₀	76	25
OP ₁₀₀	48	14
OP ₂₀₀	36	33
Sensor calibration (retention function)	20	10

6.3.5 Comparison of sensors

The common calibration function (Fig. 6.3) was applied to the Watermark sensors, for the MPS-1 the sensor specific calibration parameters from Tab. 6.2 were used. In the wet range both sensor types started at 3-9 kPa. According to the sensor specifications the measuring range was confirmed starting at approx. 10 kPa. In the dry state both sensor types exceeded their defined measuring ranges of 200 kPa and 500 kPa, respectively. The Watermark readings were cut at 620 kPa from the system (the interface). The MPS-1 delivered readings up to 1.2 MPa, but the values decreased after reaching a maximum (Fig. 6.9). At this point it must be restated that the calibration was done only up to 300 kPa. However, it seems that both sensor types delivered reliable results up to a water potential of 600 kPa. On the other

hand, the MPS-1 reacted faster than the Watermarks (Fig. 6.9). It is noticeable that the trends were similar until a value of approx. 130 kPa, and then the Watermark readings diverged. The mean time shift between MPS-1 and Watermarks at water potentials >200 kPa was four days during the first wetting-drying-cycle, five days during the second, and six days during the third cycle. Due to this time lag the Watermark measurements seemed to underestimate the water potential in the soil (Fig. 6.10).

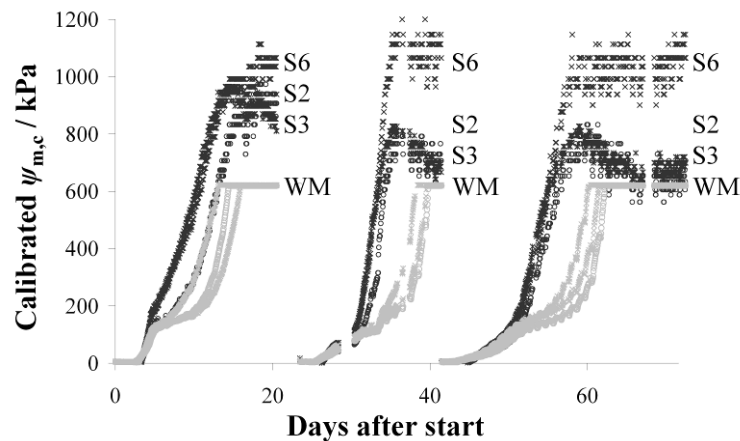


Fig. 6.9. Comparison of both sensor types during three wetting-drying-cycles; Three Watermarks (WM) and three MPS-1 (S2, S3, and S6) were installed in a 6 cm soil layer.

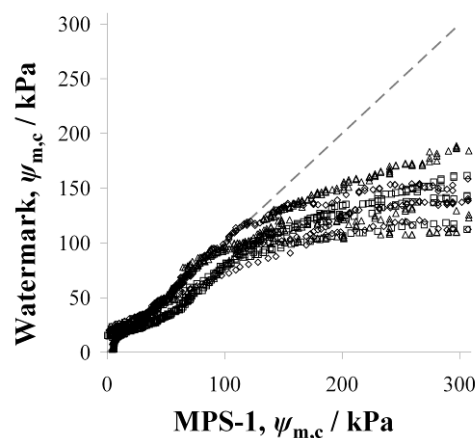


Fig. 6.10. Calibrated matric potentials: Watermark versus MPS-1

6.4 Conclusions

The integration of the Watermark sensors and the MPS-1 into a wireless monitoring network worked well. Three sensors of a type were connected to one analog-to-digital-interface. Data were logged by means of a Remote Terminal Unit, transmitted over several kilometers and made available via an Internet connection.

Six Watermark sensors were calibrated in a pressure pot in order to determine a common calibration for the sensors in combination with the interface. A function was fitted to pairs of sensor readings and equilibrium pressures. The mean $2\text{-}\sigma$ -error of the sensor measurements was 14 % in the calibration range from 10 kPa to 300 kPa. We assess this accuracy to be sufficient for several purposes, especially for irrigation management. The advantage is that single sensors can be exchanged without an additional time consuming calibration procedure. For more accurate measurements, however, sensor specific calibrations are recommended. The MPS-1 showed very high sensor-to-sensor variations. Thus, sensor specific calibrations became essential. Six MPS-1 were calibrated in a pressure pot. A standard power function was fitted to the data pairs as a basic approach. Furthermore, a retention function was fitted representing a more soil physical approach. Both methods delivered proper calibrations with high accuracies. A sound alternative was found in so-called one-point calibrations after Malazian et al. (2011). Although the results were less accurate, this approach seems to be very valuable, because only one data pair (equilibrium pressure/sensor reading) is needed for calibration, which makes the method less time consuming. The factory calibration was not useful at all.

After one and a half year in the laboratory, one set of sensors (three Watermarks and three MPS-1) were installed in the field. Unfortunately, two of the MPS-1 broke down during this test. Another set with three Watermark sensors and three MPS-1 was installed in a thin soil layer in the laboratory in order to compare the water potential measurements during drying. Both sensor types delivered water potential measurements in a range from 10 kPa to 600 kPa. At pressures >130 kPa the Watermark sensors responded significantly more slowly than the MPS-1, most likely because equilibrium status is reached faster with the thin ceramic disk of the MPS-1. A proper contact of the sensor material and the soil is a crucial pre-condition in any case.

In the meantime an improved version – the MPS-2 – is available (Decagon Devices, 2011). It delivers a digital output of matric potential (kPa) according to a factory calibration, and temperature ($^{\circ}\text{C}$). Since sensor ceramics and measuring principle are still the same, the calibration functions from this study may also be interesting for calibrating the MPS-2.

Acknowledgements

This work was supported by „Universitätsfonds der Wirtschaftskammer Wien“ in the frame of the „Wirtschaftskammerpreis 2010“. Special thanks to the staff members of Adcon Telemetry GmbH, Klosterneuburg.

6.5 References

Adcon, 2011. Information on Adcon wireless sensor networks. Adcon Telemetry GmbH, Klosterneuburg, Austria, <http://www.adcon.at>

- Campbell, G.S., Gee, G.W., 1986. Water potential: miscellaneous methods. In: Klute, A. (Ed.), *Methods of Soil Analysis. Part 1*, second ed. American Society of Agronomy, Madison, WI, pp. 619-633.
- Centeno, A., Baeza, P., Lissarrague, J.R., 2010. Relationship between soil and plant water status in wine grapes under various water deficit regimes. *Horttechnology* 20, 585-593.
- Decagon Devices, 2009. Dielectric Water Potential Sensor MPS-1. Operator's Manual Version 3.0. Decagon Devices, Inc. 2350 NE Hopkins Court, Pullman, WA 99163.
- Decagon Devices, 2011. Dielectric Water Potential Sensor MPS-2. Operator's Manual Version 1.0. Decagon Devices, Inc. 2350 NE Hopkins Court, Pullman, WA 99163.
- Eldredge, E., Shock, C., Stieber, T., 1993. Calibration of granular matrix sensors for irrigation management. *Agronomy Journal* 85, 1228-1232.
- Fares, A., Alva, A.K., 2000. Evaluation of capacitance probe for monitoring soil moisture content in a sandy Entisol profile with citrus trees. *Irrigation Science* 20(1): 1-8.
- Goodwin, I., 2002. Managing water stress in grape vines in Greater Victoria. Agriculture notes of the Victoria Department of Primary Industries, AG1074, November 2002, Victoria, Australia, pp. 1-2.
- Intrigliolo, D., Castel, J., 2004. Continuous measurement of plant and soil water status for irrigation scheduling in plum. *Irrigation Science* 23, 93-102. DOI: 10.1007/s00271-004-0097-7|10.1007/s00271-004-0097-7.
- Irrrometer, 2010. Watermark Soil Moisture Sensor – Model 200SS. Specification Document. Irrrometer company, Inc. P.O. Box 2424, Riverside, CA 92516. <http://www.irrometer.com>
- Klute, A., 1986. Water retention: laboratory methods. In: Klute, A. (Ed.), *Methods of Soil Analysis. Part 1*, second ed. American Society of Agronomy, Madison, WI, pp. 635-662.
- Kriedemann, P.E., Sturt, C., Goodwin, I., 2003. Regulated deficit irrigation and partial rootzone drying - an information package on two new irrigation methods for high-input horticulture. *Irrigation Insights* No. 4, Land & Water Australia, Canberra, Australia
- Leib, B., Jabro, J., Matthews, G., 2003. Field evaluation and performance comparison of soil moisture sensors. *Soil Science* 168, 396-408. DOI: DOI 10.1097/01.ss.0000075285.87447.86.
- Leib, B.G., Caspari, H., Redulla, C., Andrews, P., Jabro, J.D., 2006. Partial rootzone drying and deficit irrigation of 'Fuji' apples in a semi-arid climate. *Irrigation Science* 24, 85-99. DOI: DOI 10.1007/s00271-005-0013-9.
- Loiskandl, W., Kammerer, G., Zartl, A., Kastanek, F., 1999. Comments on new and traditional methods for soil and water behavior measurements. In: Slovak National Committee of ICID (Ed.): *Proceedings of International ICID-Symposium. New Approaches in Irrigation, Drainage and Flood Control Management*, Bratislava, Slovakia (CD-ROM), ISBN 80-85755-05-X

- Malazian, A., Hartsough, P., Kamai, T., Campbell, G., Cobos, D., Hopmans, J., 2011. Evaluation of MPS-1 soil water potential sensor. *Journal of Hydrology* 402, 126-134. DOI: DOI 10.1016/j.jhydrol.2011.03.006.
- McCarthy, M.G., Loveys, B.R., Dry, P.R., Stoll, M., 2002. Regulated deficit irrigation and partial rootzone drying as irrigation management techniques for grapevines. In: *Deficit irrigation practices*. FAO Water Reports 22, Rome, Italy, pp. 79-87.
- Noborio, K., Horton, R., Tan, C.S., 1999. Time domain reflectometry probe for simultaneous measurement of soil matric potential and water content. *Soil Science Society of America Journal* 63, 1500-1505.
- Or, D., Wraith, J., 1999. A new soil matric potential sensor based on time domain reflectometry. *Water Resources Research* 35, 3399-3407.
- Scanlon, B.R., Andraski, B.J., Bilskie, J., 2002. Miscellaneous methods for measuring matric or water potential. In: Dane, J.H., Topp, G.C. (Eds.), *Methods of Soil Analysis. Part 4 – Physical Methods*. Soil Sci. Soc. Am., Inc., Madison, Wisconsin, USA, pp. 643-669.
- Shock, C.C., Barnum, J.M., Seddigh, M., 1998. Calibration of Watermark soil moisture sensors for irrigation management, *Proceedings of the International Irrigation Show*. Irrigation Association, San Diego, CA, USA, pp. 139-146.
- Shock, C.C., Feibert, E.B.G., 2002. Deficit irrigation of potato. In: *Food and Agricultural Organization of the United Nations (FAO) (Ed.), Deficit Irrigation Practices*. Rome, Italy, 47-56.
- Spaans, E.J.A., Baker, J.M., 1992. Calibration of Watermark soil moisture sensors for soil matric potential and temperature. *Plant Soil* 143, 213-217.
- Terzis, A., Musaloiu-E, R., Cogan, J., Szlavecz, K., Szalay, A., Gray, J., Ozer, S., Liang, C.J.M., Gupchup, J., Burns, R., 2010. Wireless sensor networks for soil science. *International Journal of Sensor Networks* 7, 53-70.
- Thompson, R.B., Gallardo, M., Aguera, T., Valdez, L.C., Fernandez, M.D., 2006. Evaluation of the Watermark sensor for use with drip irrigated vegetable crops. *Irrigation Science* 24, 185-202. DOI: DOI 10.1007/s00271-005-0009-5.
- Thompson, R.B., Gallardo, M., Valdez, L.C., Fernandez, M.D. 2007a. Determination of lower limits for irrigation management using in situ assessments of apparent crop water uptake made with volumetric soil water content sensors. *Agricultural Water Management* 92, 13-28.
- Thompson, R.B., Gallardo, M., Valdez, L.C., Fernandez, M.D., 2007b. Using plant water status to define threshold values for irrigation management of vegetable crops using soil moisture sensors. *Agricultural Water Management* 88, 147-158.
- Thomson, S.J., Armstrong, C.F., 1987. Calibration of the Watermark Model 200 soil moisture sensor. *Applied Engineering in Agriculture* 3, 186-186.

- Thomson, S.J., Youmos, T., Wood, K., 1996. Evaluation of calibration equations and application methods for the Watermark granular matrix soil moisture sensor. *Applied Engineering in Agriculture* 12, 99-103.
- Tuller, M., Shukla, M.K., Loiskandl, W., 1997. Wasseranteilsbestimmung unter Feldbedingungen mittels Time Domain Reflectometry und Gipsblöcken. *Österr. Wasserwirtschaft* 3/4, 64-69.
- van Genuchten, M.Th., 1980. A closed-form equation for predicting the hydraulic conductivity of unsaturated soils. *Soil Science Society of America Journal* 44, 892-898.
- Vellidis, G., Tucker, M., Perry, C., Wen, C., Bednarz, C., 2008. A real-time wireless smart sensor array for scheduling irrigation. *Computers and Electronics in Agriculture* 61, 44-50.
- Whalley, W.R., Clark, L.J., Take, W.A., Bird, N.R.A., Leech, P.K., Cope, R.E., Watts, C., 2007. A porous-matrix sensor to measure the matric potential of soil water in the field. *European Journal of Soil Science* 58, 18-25. DOI: DOI 10.1111/j.1365-2389.00790.x.
- Xin, X.L., Xu, F.A., Zhang, J.B., Xu, M.X., 2007. A new resistance sensor for monitoring soil matric potential. *Soil Science Society of America Journal* 71, 866-871.
- Young, M.H., Sisson, J.B., 2002. Tensiometry. In: Dane, J.H., Topp, G.C. (Eds.), Part 4 – Physical Methods. *Soil Sci. Soc. Am., Inc., Madison, Wisconsin, USA*, pp. 575-606.

7 Comparison of EnviroSCAN and AquaCheck capacitance probe for multi-depth soil water monitoring⁴

Nolz R.

Abstract

Soil water content was measured over three years with an EnviroSCAN and an AquaCheck capacitance probe in sandy loam Chernozem at the experimental site of University of Natural Resources and Life Sciences, Vienna (BOKU) in Groß-Enzersdorf, Austria (48°12'N, 16°34'E; 157 m; app. 550 mm mean annual rainfall, and 10°C average temperature). Each probe consisted of several sensors installed in different depths of a soil profile. Converted AC readings correlated well with ES measurements in 10, 20, 30, 50, 70, and 100 cm in a calibration period, but diverged subsequently during evaluation period. Despite factory normalization AC measurements showed considerable sensor-to-sensor variations and they reacted oversensitive to irrigation and rainfall.

Keywords: soil water content, soil water dynamics, calibration, normalization, FDR

⁴ Published as Nolz (2012)

In: A. Celkova, Institute of Hydrology SAS (Ed.): 20th Int. Poster Day: Transport of Water, Chemicals and Energy in the Soil-Plant-Atmosphere System, Nov. 2012, Bratislava, Slovakia, 496-503.

7.1 Introduction and objectives

Monitoring water content within a soil profile corresponding more or less with the rooting zone gives information about plant available water and water uptake, respectively. Such measurements provide a basis for irrigation management, for instance (Thompson et al., 2007). Capacitance probes are widely used for scientific as well as for agronomic purposes. Consequently, several alternatives are commercially available. EnviroSCAN® probes represent a standard device for monitoring soil water content (Cepuder and Nolz 2007; Fares and Alva, 2000; Thompson et al., 2007). Its sensors consist of two brass rings that act as capacitor with the surrounding soil. Water content is then related to the frequency of an electrical field (Sentek, 1997). AquaCheck® soil moisture probes operate with an identical principle, and they are employed in the same field of application (Cronje and Mostert, 2010; Murungu et al., 2011). However, little is known about calibration and performance of AquaCheck sensors.

In this regard, readings from an AquaCheck (AC) probe were compared to EnviroSCAN (ES) water content measurements as reference.

7.2 Materials and methods

EnviroSCAN (ES) (Sentek Pty Ltd, Stepney, Australia) is a multi-sensor capacitance probe measuring water content in different depths of a soil profile (Sentek, 1997). A support rod is fitted with several sensors, and inserted into a PVC access tube installed in the soil. Each sensor consists of two conductive rings acting as capacitor with the surrounding medium (solid soil, air, and water) as dielectric. Variations of capacitance are due to variations in the dielectric of the surrounding medium, in which the dielectric constant of water (app. 80) is dominating compared to soil (4-8) and air (1). The frequency of oscillation is proportional to the ratio of air and water in the soil (Paltineanu and Starr, 1997). This principle is also known as Frequency Domain Resonance (FDR). Sensor readings were normalized to a so-called Scaled Frequency $SF = (F_a - F_s)/(F_a - F_w)$, where F_a is the sensor-specific reading in air, F_w is the reading in water, and F_s is the frequency reading in moist soil. F_a and F_w were determined for each sensor in the laboratory. Soil water content θ_{ES} was calculated from SF by means of a standard default calibration relationship (Eq. 1), which generally delivers adequate results for common soil types (Evelt et al., 2002; Sentek, 2001). Data were measured, processed, and stored in a standard RT6-logger from Sentek Company, from which the actual database was downloaded frequently on a Notebook.

$$SF = 0.1957 \theta_{ES}^{0.4040} + 0.0285 \quad (1)$$

Similar to ES, AquaCheck (AC) (AquaCheck Soil Moisture Management, Durbanville, South Africa) is a multi-sensor capacitance probe, but the metal rings are fixed at certain distances

inside a PVC tube and sealed with a water resistant resin, thus, they cannot be adapted individually. After assembly, the sensors are individually normalized from the manufacturer to set the default counts for air (app. 32000) and water (app. 1000) for each sensor (AquaCheck, 2008). Furthermore, the probe has an internal temperature variation compensation factor that corrects automatically possible inherent electronic temperature variations. So, the digital SDI-12 interface of the probe delivers Scaled Frequency values from app. 0 to 100. In the standard software these output values are named “soil moisture” (AquaCheck, 2008). In this article, AC readings are referred to as “ACU” (AquaCheck unit) for better readability. A well-established telemetry system from Adcon Telemetry GmbH, Klosterneuburg (Austria) was used for logging and transmitting data. So-called Remote Terminal Units (RTUs) collected and transmitted data from AC. The readings were temporarily stored in another RTU, and transmitted via UHF to a central logger. Data were transferred to a server several times per day and made available via Internet access (Adcon, 2011).

Both probes were installed in the grass reference lysimeter at the experimental site of University of Natural Resources and Life Sciences, Vienna (BOKU) in Groß-Enzersdorf, Austria (48°12'N, 16°34'E; 157 m; app. 550 mm mean annual rainfall, and 10°C average temperature) (Cepuder and Supersperg, 1991). Soil was a sandy loam Chernozem. The access tube for the ES probe was installed following the manufacturers recommendations in order to achieve good contact between tube and soil (Sentek, 2003). The PVC tube with a metal cutting edge at the bottom was hammered into the soil stepwise, while soil material was removed from inside the tube by means of a special auger. The ES rod was equipped with sensors in 10 cm-intervals from 10 to 160 cm. For the AC probe an auger with a slightly larger diameter than the probe itself was used to drill a hole. According to the installation manual (AquaCheck, 2008), the hole was filled with slurry made from fine soil material before the probe was inserted. The AC sensors measured in 10, 20, 30, 50, 70, and 100 cm.

The lysimeter was irrigated additionally to natural rainfall. The measuring period was from January 2009 to December 2011. Half a year was interpreted as start-up phase, where freezing effects were observed, and soil had time to consolidate after probe installation, especially with respect to the AC slurry method. These data were not taken into account for further interpretation. Data from July 2009 to December 2010 (calibration period) were used for relating dimensionless AC readings to water content measurements from ES by means of standard spreadsheet functions. These functions were applied to AC data from January to December 2011 (evaluation period) and compared to ES data. In order to evaluate the results, the Root Mean Square Error (RMSE / %) was calculated for AC measurements θ_{AC} versus ES measurements θ_{ES} (Eq. 2).

$$RMSE (\theta_{AC}, \theta_{ES}) = \sqrt{\frac{\sum_{i=1}^n (\theta_{AC,i} - \theta_{ES,i})^2}{n}} \quad (2)$$

7.3 Results and discussion

Figure 7.1 to Figure 7.6 show sensor readings from AquaCheck (ACU) and EnviroSCAN (θ_{ES}) in 10, 20, 30, 50, 70, and 100 cm depth during calibration period from July 2009 to December 2010 with a data gap of about 4 months in ES-data. AC-data showed considerable peaks after irrigation events (marked with arrows in Figure 7.1 to Figure 7.4). Likely reasons were poor contact between probe and soil, and other hydraulic properties due to the finer slurry-material in the interspaces, respectively.

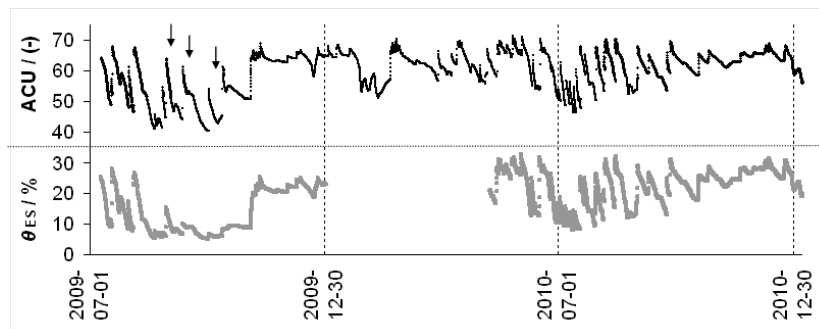


Figure 7.1: Sensor readings from AquaCheck (ACU) and EnviroSCAN (θ_{ES}) in 10 cm

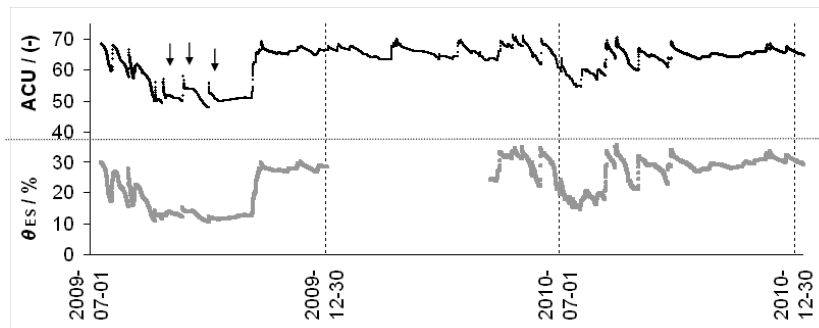


Figure 7.2: Sensor readings from AquaCheck (ACU) and EnviroSCAN (θ_{ES}) in 20 cm

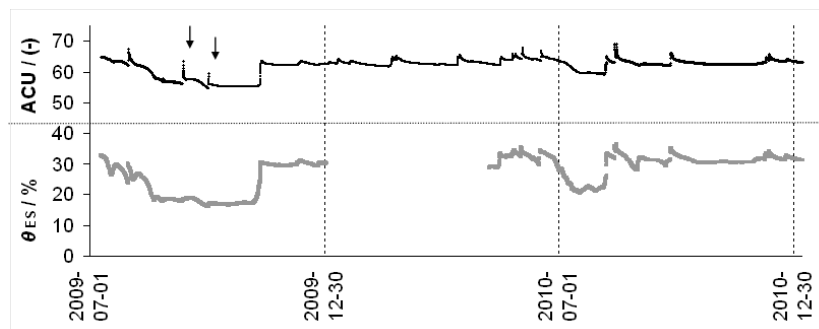


Figure 7.3: Sensor readings from AquaCheck (ACU) and EnviroSCAN (θ_{ES}) in 30 cm

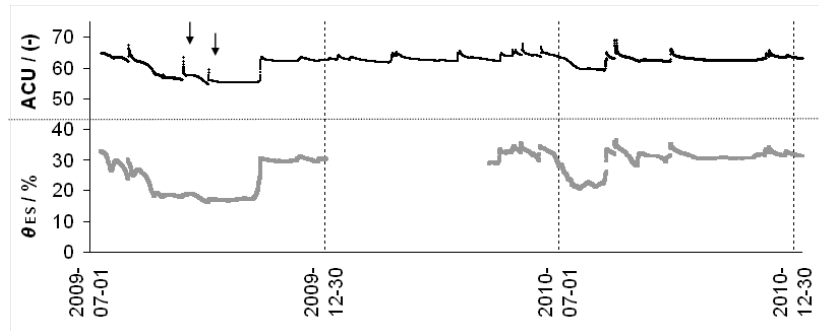


Figure 7.4: Sensor readings from AquaCheck (ACU) and EnviroSCAN (θ_{ES}) in 50 cm

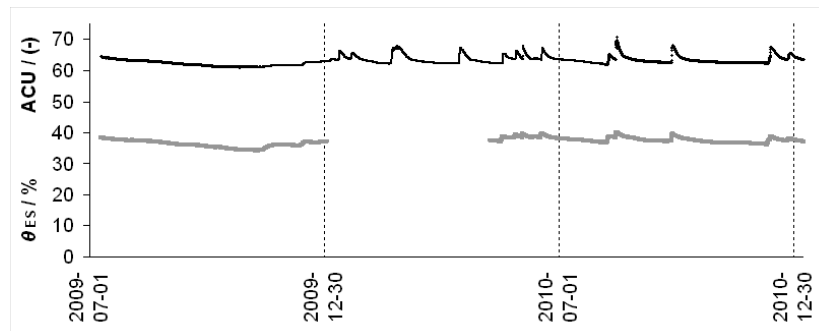


Figure 7.5: Sensor readings from AquaCheck (ACU) and EnviroSCAN (θ_{ES}) in 70 cm

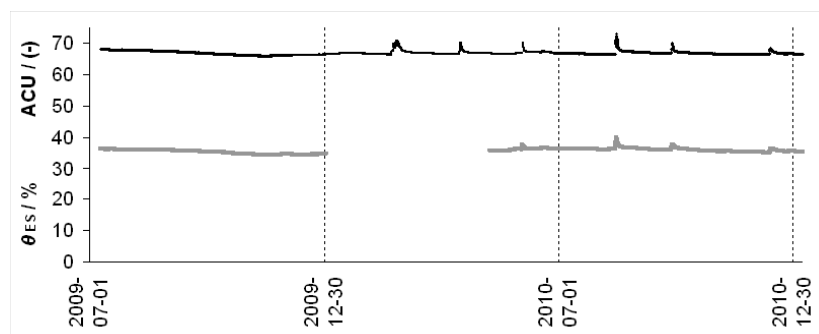


Figure 7.6: Sensor readings from AquaCheck (ACU) and EnviroSCAN (θ_{ES}) in 100 cm

AC and ES readings in 10, 20, and 30 cm depth from July 2009 to December 2010 were correlated via 2nd order polynomial functions (Figure 7.7a-c). Noticeable deviations were especially the reaction after irrigation (marked with horizontal arrows in Figure 7.7a-d), and a delayed reaction of AC in 30 and 50 cm after a rainfall event (marked with vertical arrows in

Figure 7.7c-d). The respective data (marked grey in Figure 7.7c-d) were neglected for the correlation functions. Generally, soil water dynamics driven by temperature changes, evaporation, transpiration, and rainfall are higher near the soil surface. Consequently, soil water content typically fluctuates less in deeper horizons. The latter can be seen in Figure 7.5, Figure 7.6, and Figure 7.7d-f. For the 50, 70, and 100 cm-data linear correlations were chosen. Due to narrow range of data the quality of the correlation functions was rather poor in that case. Furthermore, it looked like the characteristic of relationship changed in the wet range.

Correlations between single sensors were considerably different (Figure 7.8), thus, a general correlation function for all sensors within one probe may not be suitable. Since soil type was the same in all depths, it is recommended to improve sensor normalization, or to perform sensor-specific calibrations.

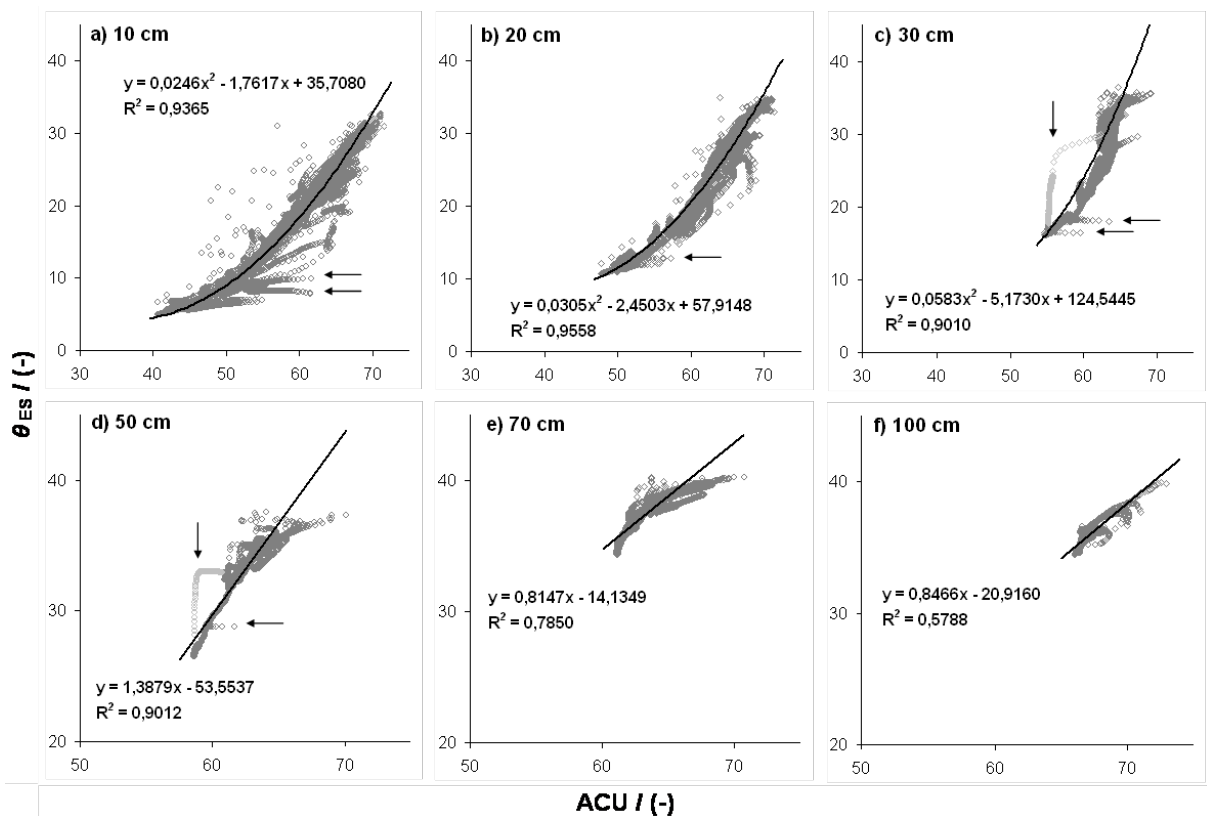


Figure 7.7: Correlation between AC sensor readings and water content measured with ES in six depths (10, 20, 30, 50, 70, and 100 cm)

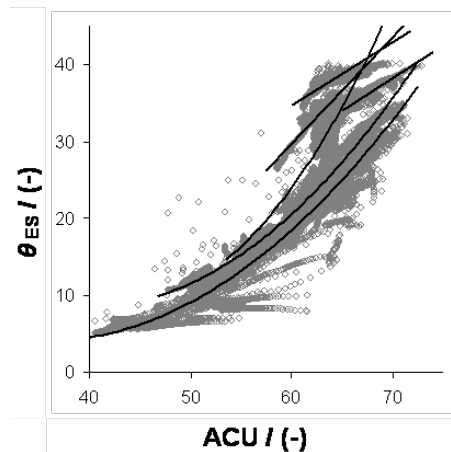


Figure 7.8: Correlation between AC and ES in all depths

AC readings of each sensor-depth were then converted to soil water content (θ_{AS}) by means of the respective correlation function (Figure 7.9 to Figure 7.12). Accordance of soil water dynamics expressed as RMSE was better in calibration period, and it was better in deeper soil layers (Table 7.1). Especially after wetting due to rainfall or irrigation soil water distribution differed (Figure 7.9 to Figure 7.11). Furthermore, it seemed that the graphs diverged with time. Water content characteristics in 70 and 100 cm (data not shown) were similar to that in 50 cm (Figure 7.12).

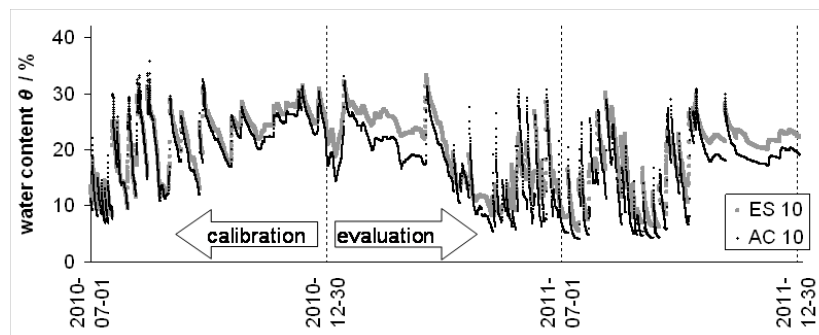


Figure 7.9: Water content measured with AC and ES sensors in 10 cm

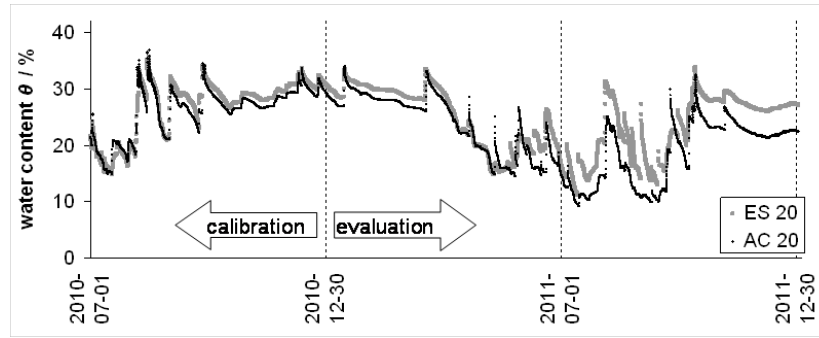


Figure 7.10: Water content measured with AC and ES sensors in 20 cm

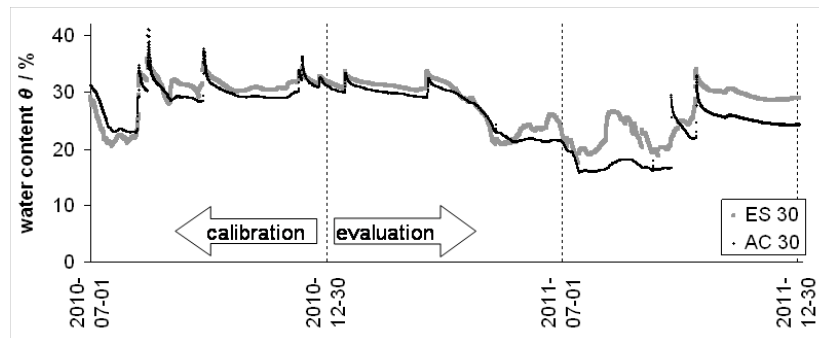


Figure 7.11: Water content measured with AC and ES sensors in 30 cm

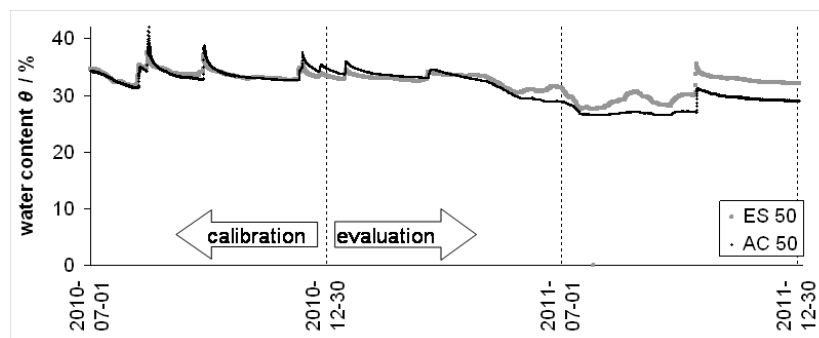


Figure 7.12: Water content measured with AC and ES sensors in 50 cm

Table 7.1: Root mean squared error (RMSE / %) of AC versus ES for sensors in six depths in calibration period (July 2009 to December 2010), and evaluation period (January to December 2011)

	10 cm	20 cm	30 cm	50 cm	70 cm	100 cm
Calibration period	1.9	1.5	1.7	0.8	0.6	0.5
Evaluation period	3.6	3.7	3.4	2.0	0.9	0.9

7.4 Conclusions

EnviroSCAN (ES) probes are standard devices for measuring soil water content, thus, ES measurements served as reference for this study. However, it has to be kept in mind that also ES measurements may not be accurate. Generally, readings of capacitance sensors have to be related to soil water content via calibration functions. Little is known about standard calibration functions of AquaCheck (AC) probes. Direct comparison of ES and AC data showed considerably different performances of single sensors of the AC probe. Since soil type was the same in all depths, sensor normalization should be improved for AC, or sensor-specific calibrations should be performed. Reactions on irrigation and rainfall were oversensitive, likely due to the installation method of AC and preferential flow, respectively. AC readings were correlated to ES water content data via specific functions. The graphs from both probes fitted well in the period for calibration, but they diverged during the evaluation period. Further studies are recommended to explain these time-dependent variations. Additional probes should be used to test consistency of AC measurements.

Acknowledgements

I want to thank the staff of Adcon Telemetry for support, and my colleagues P. Cepuder and G. Kammerer for helpful advice.

7.5 References

- Adcon (2011): Information on Adcon wireless sensor networks. Adcon Telemetry GmbH, Klosterneuburg, Austria, <http://www.adcon.at>. online on Nov. 1, 2011
- AquaCheck (2008): AquaCheck probe Instruction manual, version 1.5, AquaCheck Pty. Ltd., 2008

- Cronje R.B., Mostert P.G. (2010): A Holistic Approach to Improve Litchi Orchard Management in South Africa. In: Proc. 3rd IS on Longan, Lychee & Other Fruit Trees in Sapindaceae Family, Eds.: Qiu Dongliang et al., ISHS 2010, Acta Hort. 863: 433-436
- Cepuder P., Supersperg H. (1991): Erfahrungen mit der Lysimeteranlage Groß-Enzersdorf. In Bundesanstalt für alpenländische Landwirtschaft (ed.): Proceedings of the Lysimeter Conference, Gumpenstein, Austria, 16.-17. April 1991: 25-35
- Cepuder P., Nolz R. (2007): Irrigation management by means of soil moisture sensor technologies. In: Polish Academy of Science, Committee for Land Reclamation and Environmental Engineering in Agriculture, Journal of Water and Land Development 11: 79-90
- Evelt S.R., Ruthardt B.B., Kottkamp S.T., Howell T.A., Schneider A.D., Tolk J.A. (2002): Accuracy and precision of soil water measurements by neutron, capacitance, and TDR methods. In: Transactions of the 17th World Congress of Soil Science, Bangkok, Thailand. 14-21 August 2002. 318-1-318-8
- Fares A., Alva A.K. (2000): Evaluation of capacitance probe for monitoring soil moisture content in a sandy Entisol profile with citrus trees. Irrigation Science 20(1): 1-8
- Murungu F.S., Chiduzza C., Muchaonyerwa P., Mnkeni P.N.S. (2011): Mulch effects on soil moisture and nitrogen, weed growth and irrigated maize productivity in a warm-temperate climate of South Africa. Soil and Tillage Res., 112: 58-65
- Paltineanu I.C., Starr J.L. (1997): Real-time soil water dynamics using multisensor capacitance probes: Laboratory calibration. Soil Sci. Soc. Am. J. 61: 1576-85
- Sentek (1997): EnviroSCAN hardware manual, version 3.0 July 1997
- Sentek (2001): Calibration of Sentek Pty. Ltd. Soil Moisture Sensors
- Sentek (2003): Access tube installation guide for EnviroSCAN, EnviroSMART, and Diviner2000, version 1.0, Sentek Pty Ltd, 2003
- Thompson R.B., Gallardo M., Valdez L.C., Fernandez M.D. (2007): Determination of lower limits for irrigation management using in situ assessments of apparent crop water uptake made with volumetric soil water content sensors. Agricultural Water Management 92: 13-28

8 Weather data as basis for calculating reference evapotranspiration on an irrigation trial plot within a vineyard⁵

Nolz R., Cepuder P.

Abstract

A study plot in the eastern part of Austria was equipped with a remote monitoring station composed of soil water sensors and weather instruments in order to deliver basic data for irrigation management. The weather instrument readings include air temperature, relative humidity, wind velocity, solar radiation and precipitation in 15-minute-intervals. Additionally, weather data from a nearby weather station of the Austrian Central Institute for Meteorology and Geodynamics (ZAMG) were utilized. Both datasets served for calculating reference evapotranspiration (ET_{ref}). A comparison indicated similar characteristics of the measured parameters as well as ET_{ref} . Differences could be interpreted as microclimate effects on the study plot. Generally, 2010 was a wet year; rainfall was above average, exceeding ET_{ref} most of the time.

Keywords: weather station, remote monitoring, microclimate, ET, FAO-Penman-Monteith

⁵ Published as Nolz and Cepuder (2011)

In: Stredova H., Roznovsky J., Litschmann T. (Eds.): Int. Conference on microclimate and mesoclimate of landscape structures and anthropogenic environment. Feb. 2011, Skalní mlýn, Czech Republic

8.1 Introduction

In spring 2010, an irrigation trial was started in a vineyard in the eastern part of Austria, close to the Hungarian border (47°48'16" N, 17°01'57" E; 118 m). The agricultural area is characterized by a long-term mean annual temperature of 10.6°C and an annual precipitation of about 570 mm. Irrigation may be necessary in order to guarantee high-quality grapes as basis for high-quality winemaking. Investigating the soil water status is an appropriate method for irrigation management. This aim can be achieved directly by means of soil water measurements, or indirectly by compiling a water balance. Therefore, the study plot was equipped with a remote monitoring station composed of soil water sensors and weather instruments (Adcon, 2011) in order to deliver basic data for managing a sophisticated subsurface drip irrigation system (hydrip®). Beside the measurements from the field plot, weather data from a nearby weather station (47°46'20" N, 17°01'59" E; 122 m) of the Austrian Central Institute for Meteorology and Geodynamics (ZAMG) were utilized. Evapotranspiration is the main component of the water balance. In this regard, the weather data were used for calculating reference evapotranspiration (ET_{ref}) according to the recommendation of the Food and Agriculture Organization of the United Nations FAO (Allen et al., 1998).

While the measurements from the study plot primarily characterized the vineyards' microclimate, the ZAMG-data provided a more general view – especially due to long-term time series. The goal of this work was to compare both datasets in order to gain a better understanding as basis for future data interpretation.

8.2 Materials and methods

The distance between the vineyard and ZAMG-station was 3.6 km. The weather instrument readings on the field plot included air temperature T in °C, relative humidity RH in %, air pressure p in hPa, wind velocity at 2 m height u_2 in $\text{m}\cdot\text{s}^{-1}$, solar radiation R_s in $\text{W}\cdot\text{m}^{-2}$ and rainfall R in mm (measuring interval: 15 minutes). The measurement station was connected to a telemetry network from Adcon Telemetry GmbH, Klosterneuburg. A Remote Terminal Unit (RTU) collected data from weather sensors (Fig. 8.1), stored them for a short term and then delivered data packages via GSM technology to a server. Processed data – including automatically calculated daily ET_{ref} – were provided via internet for further data interpretation.



Fig. 8.1: Measuring station with RTU, solar panel and weather instruments (photo: R. Nolz)

The ZAMG dataset contained T , RH , p , u_2 , R_s and R in 1-hour-intervals as input parameters for ET_{ref} . Daily ET for both datasets was calculated according to FAO-Penman-Monteith (Allen et al., 1998):

$$ET_{ref} = \frac{0.408\Delta(R_n - G) + \gamma \frac{900}{T + 273} u_2 (e_s - e_a)}{\Delta + \gamma(1 + 0.34u_2)} \quad (1)$$

ET_{ref} ...reference evapotranspiration / $\text{mm}\cdot\text{d}^{-1}$

R_n ...net radiation at the crop surface / $\text{MJ}\cdot\text{m}^{-2}\cdot\text{day}^{-1}$

G ...soil heat flux density / $\text{MJ}\cdot\text{m}^{-2}\cdot\text{day}^{-1}$, (neglected for daily time steps)

T ...air temperature at 2 m height / $^{\circ}\text{C}$

u_2 ...wind speed at 2 m height / $\text{m}\cdot\text{s}^{-1}$

e_s ...saturation vapor pressure / kPa

e_a ...actual vapor pressure / kPa

$e_s - e_a$...saturation vapor pressure deficit / kPa

Δ ...slope vapor pressure curve / $\text{kPa}\cdot^{\circ}\text{C}^{-1}$

γ ...psychrometric constant / $\text{kPa}\cdot^{\circ}\text{C}^{-1}$

8.3 Results and discussion

Fig. 8.2 shows the annual rainfall and the mean annual temperature of the past 15 years. Compared to the long-term averages, this period – particularly 2010 – was relatively wet and cold.

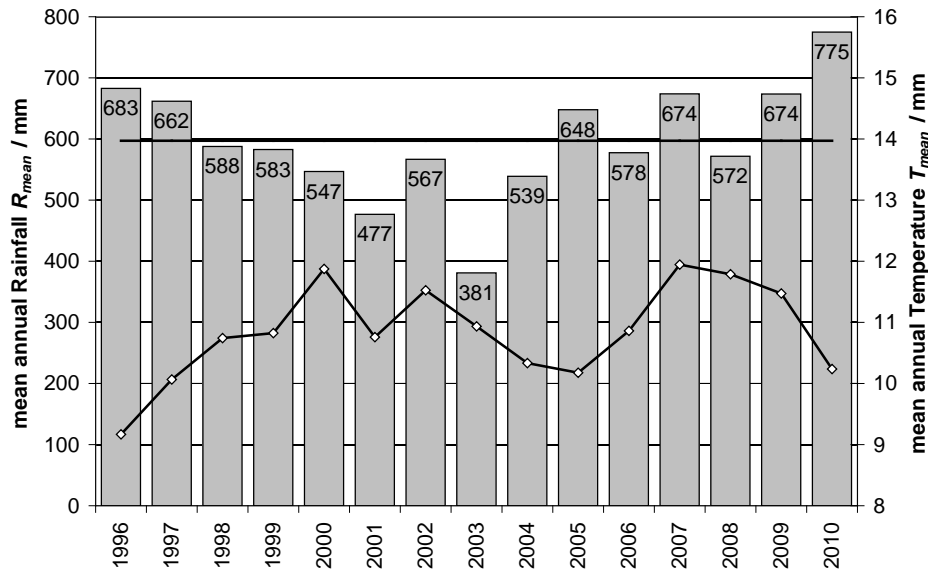


Fig. 8.2: Annual rainfall and mean annual temperature of the past 15 years

The investigation period of the current study started after installation of the remote weather station on July 22nd and lasted until the end of the year. The weather data of the first week of this period (23.7.-31.7.) were analyzed in detail. Tab. 8.1 contains the mean values of the parameters measured on the field plot (Adcon) and at the weather station of the ZAMG, respectively. ET_{ref} was calculated based on each dataset for the short- and the entire period, too.

Tab. 8.1: Mean of the respective parameters from both measuring sites for the entire period (23.7.-31.12.2010) and the first week (23.7.-31.7.2010), respectively

		T	RH	p	u_2	R_s	R	ET_{ref}
		°C	%	hPa	$m \cdot s^{-2}$	$MJ \cdot m^{-2} \cdot d^{-1}$	mm	mm
23.7.-31.12.	Adcon	10.1	77	999.0	2.3	1489	335	280
	ZAMG	10.1	81	999.2	1.9	1471	375	250
23.7.-31.7.	Adcon	19.3	69	998.1	3.1	119	29	32
	ZAMG	19.5	71	998.2	3.0	137	36	35

The following figures show the field plot-data versus ZAMG-data. Both time series are based on hourly values (the ZAMG-values are displayed as a continuous line just for easier reading). The temperature curves in Fig. 8.3 show a good correlation ($R^2 = 0.9769$); nevertheless, some peaks seemed to be lower on the field plot. The mean values were identical in the first week, but taking into account the entire period, T was slightly lower in the vineyard (Tab. 8.1).

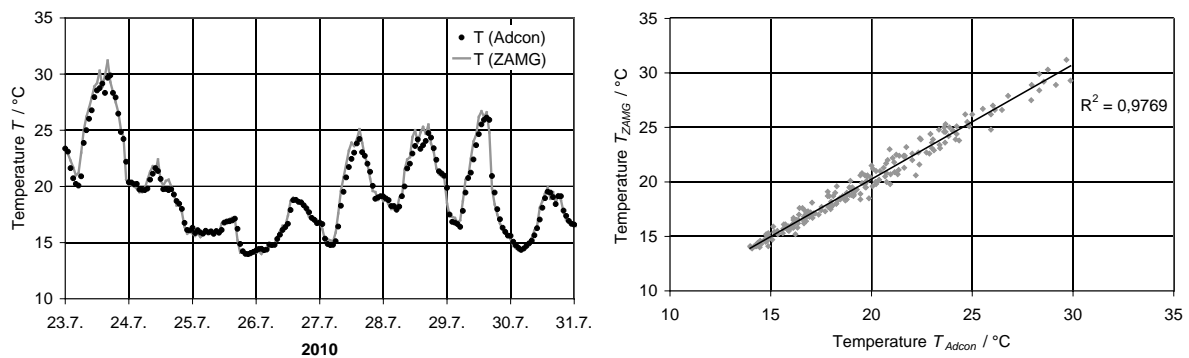


Fig. 8.3: Air temperature T – characteristics and correlation of both measuring sites

Relative humidity measurements expressed a large variability. Fig. 8.4 illustrates a similar trend, but lower values at the field plot. The mean values in Tab. 8.1 confirm this statement. Due to a mechanical malfunction, ZAMG-data did not exceed 90 %.

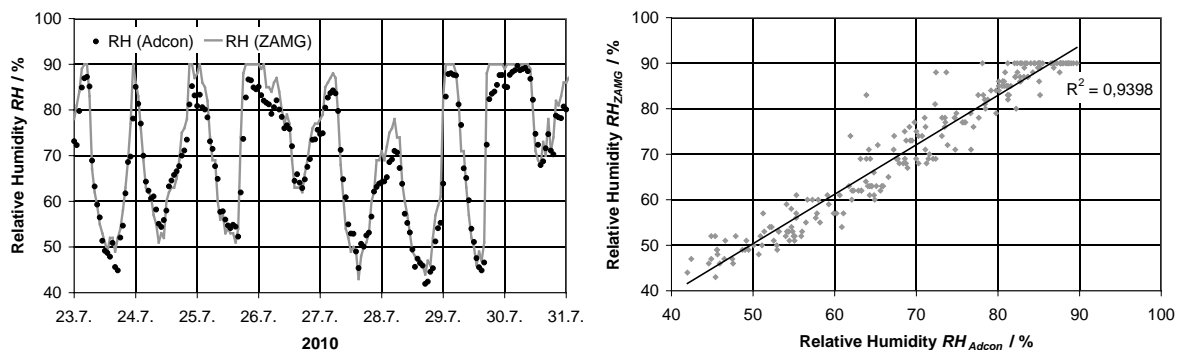


Fig. 8.4: Relative Humidity RH – characteristics and correlation of both measuring sites

Air pressure was almost the same at both sites (Fig. 8.5), this holds also for the entire investigation period (Tab. 8.1).

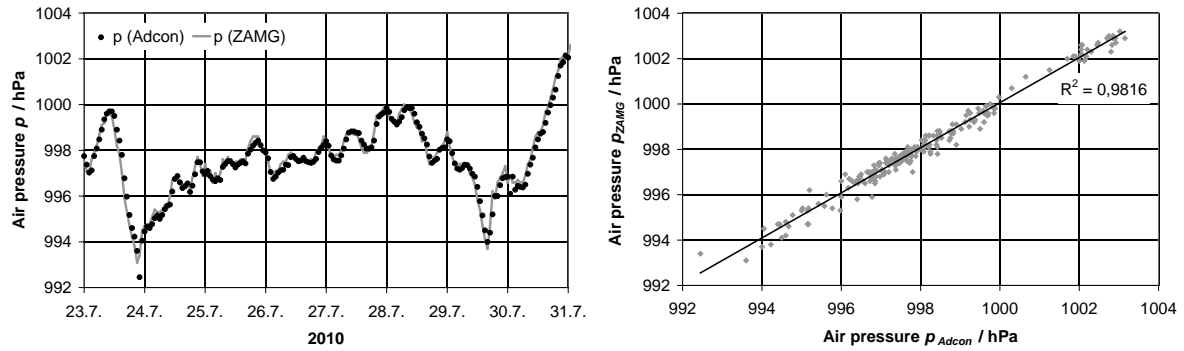


Fig. 8.5: Air pressure p – characteristics and correlation of both measuring sites

As expected, wind velocity fluctuations were appreciable (Fig. 8.6). The mean velocity was lower at the ZAMG-station (Tab. 8.1) – a reason may be that the weather station is situated within a village.

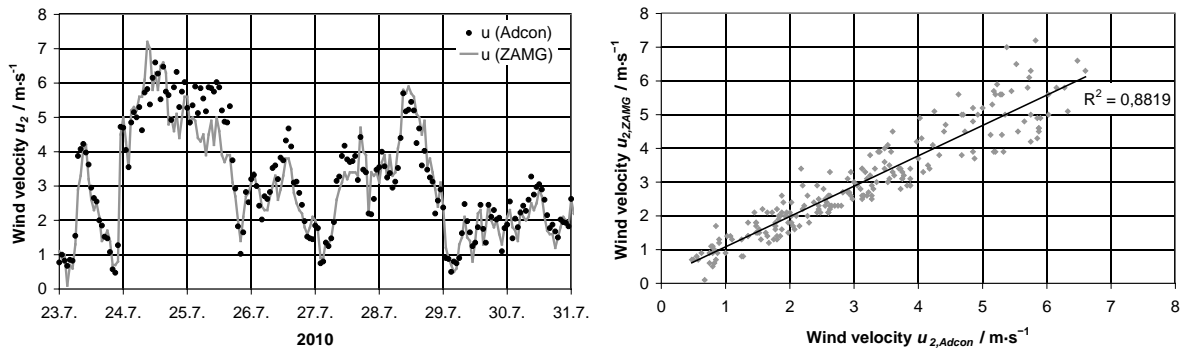


Fig. 8.6: Wind velocity u_2 – characteristics and correlation of both measuring sites

Local differences of solar radiation measurements generally depend on the cloudiness. The radiation sum from 23.7.-31.7.2010 was a little bit lower at the field plot, especially the peak values were lower (Fig. 8.7). Regarding the entire period it was the other way around (Tab. 8.1).

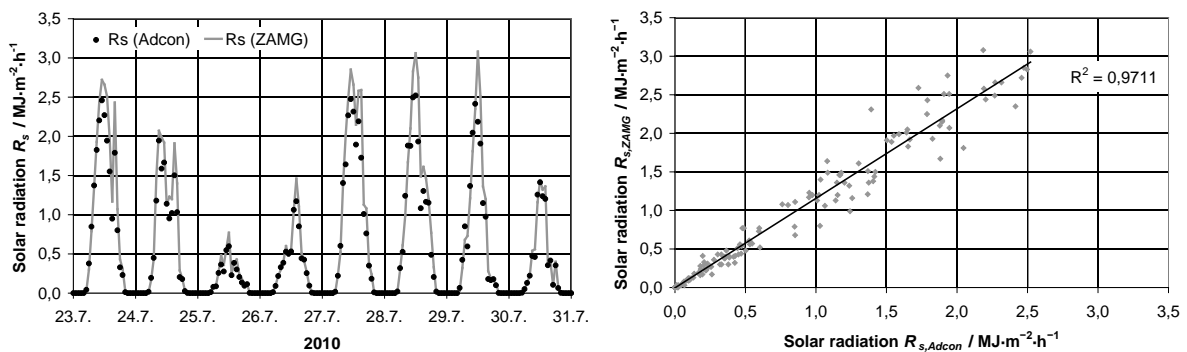


Fig. 8.7: Solar radiation R_s – characteristics and correlation of both measuring sites

The rainfall sum measured at the ZAMG-station exceeded the amount at the field plot by 5 mm (Fig. 8.8 & Tab. 8.1). Fig. 8.9 shows the cumulated rainfall in the entire period. Although the cumulated curves display differences, they equalize at beginning of November. From the end of November until the end of the year snow was falling, causing a difference of about 50 mm (snow was not measured at the field station).

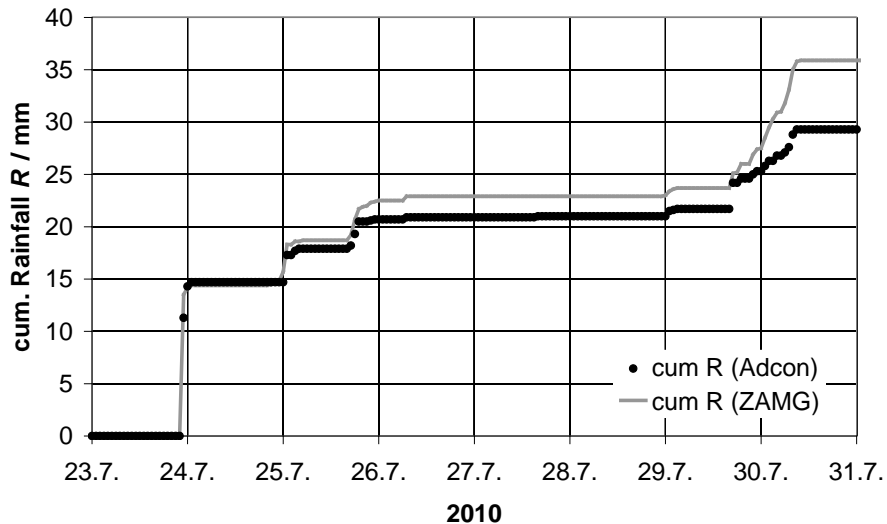


Fig. 8.8: Cumulated rainfall R of both measuring sites at the end of July

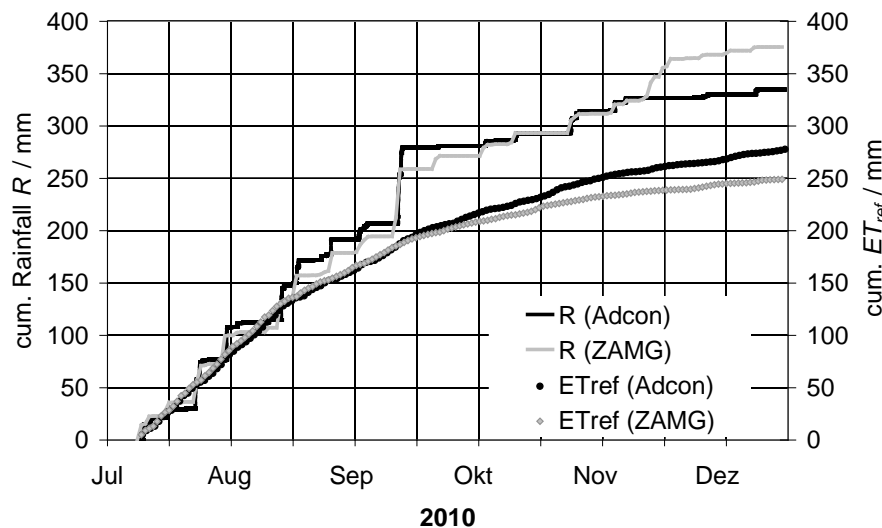


Fig. 8.9: Cumulated rainfall and ET_{ref} for the entire study period (23.7.-31.12.2010)

In the period from 23.7.-31.7.2010 air temperature, relative humidity and solar radiation were lower, and wind velocity was slightly higher at the study plot (Fig. 8.9 & Tab. 8.1). Comparing both datasets for the entire study period, relative humidity was lower at the study plot, but wind velocity and solar radiation were higher than ZAMG-data. Thus, calculated ET_{ref} for the whole period was higher at the vineyard, and it was exceeded by rainfall from end of August to the end of the year (Fig. 8.9).

8.4 Conclusions

Both datasets provided a proper basis for calculating ET_{ref} on hourly basis. Additionally, time series from the weather station of the ZAMG gave an overview about the past years. The remote station on the field plot delivered continuous data, anytime available via internet. Several characteristics of the measured parameters were similar; on the other hand, differences could be detected through detailed study. ET_{ref} based on both datasets delivered feasible results. Nevertheless, the calculation procedures should be compared in detail in order to verify if different results occurred only due to different input data. Since the vineyard was recently planted, the grape-vines and the leaves were rather small. However, adult plants will influence the microclimate within the vineyard. The results of this study should serve as reference for future data interpretation.

Acknowledgements

This work was supported by the “Wirtschaftskammer Wien” in the frame of the „Wirtschaftskammerpreis 2010”. Special thanks also to the Austrian Central Institute for Meteorology and Geodynamics (ZAMG), our colleagues from the Institute of Meteorology (BOKU-Met) and the staff of Adcon Telemetry GmbH, Klosterneuburg.

8.5 References

Adcon, 2011. Information on Adcon wireless sensor networks. Adcon Telemetry GmbH, Klosterneuburg, Austria, <http://www.adcon.at>.

Allen R. G., Pereira L. S., Raes D., Smith M., 1998. Crop Evapotranspiration: Guidelines for computing crop water requirements. Irrig. and Drain. Paper 56, Food and Agriculture Organization of the United Nations, Rome.

9 Remote monitoring of a novel irrigation system in a vineyard⁶

Nolz R., Himmelbauer M., Cepuder P., Loiskandl W.

Abstract

Effective irrigation systems and optimal irrigation management are prerequisites in modern agriculture. A sophisticated remote monitoring station was installed in a vineyard in the eastern part of Austria. The station was equipped with weather- and soil water sensors. Data, available via Internet, served as basis for decisions support regarding the management of a novel irrigation system.

Keywords: soil water content, matric potential, FDR, Watermark, subsurface drip irrigation

⁶ Published in slightly modified form as Nolz et al. (2010)

In: A. Celkova, Institute of Hydrology SAS (Ed.), 18th Int. Poster Day: Transport of Water, Chemicals and Energy in the Soil-Plant-Atmosphere System, Nov. 2010, Bratislava, Slovakia, 393-398.

9.1 Introduction

Irrigation becomes obligatory if rainfall does not satisfy plant water requirements. At a time of increasing drought and water shortage worldwide, efficient irrigation systems are becoming more and more important for sustainable water use (Scanlon et al., 2007). Due to its low evaporation losses, subsurface drip irrigation is assumed to be the most economical irrigation principle (Camp et al., 2000). Besides efficient irrigation systems, optimal irrigation management is necessary in order to ensure sufficient supply of water and nutrients to plants along with minimal water applications (Pereira et al., 2002). Drought stress usually causes loss of yield and decrease of quality, especially regarding grapes for high quality wine production. On the other hand, excessive irrigation, may waste water and energy resources, and put groundwater at risk because of leached nutrients and pollutants. By means of observations of the soil water status, irrigation can be precisely adapted to the current needs of the plant. For these purposes, various sensors are applicable. An advanced irrigation system is currently tested by the Institute for Hydraulics and Rural Water Management, University of Natural Resources and Life Sciences, Vienna (BOKU) in close cooperation with Hydrip GmbH, Vienna. The patented Hydrip® system combines subsurface drip irrigation tubes and a water-holding soil amendment on a clay mineral basis. In April 2010, the laboratory examined system was installed in a newly planted vineyard in East Austria.

The main goal of this project was to develop and implement a remote system for monitoring plant-available soil water as basis for decision support for irrigation strategies, optimized for vineyards, and taking into account special demands arising from the Hydrip® irrigation system.

9.2 Materials and methods

Soil water content and matric potential were measured within the rooting zone of grapes. Both parameters were used to evaluate plant water uptake as well as water flux through the soil profile. Weather data were measured at the field plot for evaluation irrigation needs from a climatic point of view. The entire measuring station was equipped with the less possible number of sensors with respect to user-friendliness. In addition, data should be made available via Internet to offer farmers a simple and objective information basis for their operations. For this purpose an existing well-established radio network from Adcon Telemetry GmbH, Klosterneuburg, was used (Adcon, 2010). The main modules are radio sets for data transmission on the basis of GSM / GPRS technology, corresponding base stations, sensors for data collection, and a comprehensive software solution. The field station with a Remote Terminal Unit (RTU) and several weather- and soil water sensors is shown in Figure 9.1.



Figure 9.1: Measuring station with RTU, solar panel, weather sensors, FDR-probe (white cap) and three watermark sensors in 10, 30 and 50 cm depth.

The RTU stored data for a short term and frequently delivered the data packages via GSM technology to a server. Data were provided via internet, for what adequate software and access authorization were obligatory. The weather sensors measured air temperature, relative humidity, wind velocity and solar radiation according to FAO recommendations for calculating grass reference evapotranspiration (Allen et al. 1998), and precipitation. These data were the basis for balancing soil water content and plant water requirement.

Two types of soil water sensors were installed within the rooting zone of the grapevines in order to measure soil water content and matric potential, respectively. Sentek's EnviroSCAN® sensors (Paltineanu and Starr, 1997) operate based on the Frequency Domain Resonance-principle (FDR). By means of capacitor a high-frequency electric field is applied to a certain volume of soil. The oscillation frequency is then related to the soil water content via a calibration function. Several sensors mounted on a rod measured soil water content in different depths of the soil profile. An access tube that was vertically drilled into the soil with a special technique housed the FDR-probe. Changes of the water content within the soil profile indicated plant water uptake. The sensors had been already used for irrigation monitoring of different crops during the past years (Cepuder and Nolz 2007). Another type of sensors measured matric potential, which is equivalent to the energy that is needed to withdraw water from the point of observation. Hence, drought stress can be identified immediately. Installation of several sensors in different depths gave an impression about the water movement in the soil. At this measurement site, Watermark® granular matrix sensors by Irrrometer Company (Riverside, CA, USA) were used. A sensor consists of two electrodes that are embedded in a reference material. The sensor matrix is in hydraulic equilibrium with the surrounding soil; hence, changes in electrical resistance between sensor-electrodes can

be converted to soil matric potential. Both types of sensors were selected in order to use the advantages of each particular principle.

9.3 Results and discussion

The research site in the eastern part of Austria, close to the Hungarian border, is characterized by a mean annual temperature of 10.6°C and an annual precipitation of about 570 mm. The study period started in July 2010. Rainfall and air temperature, measured in 15-minute-intervals, are shown in Figure 7.1. With a total rainfall sum of 291 mm, the period was identified as a rather wet. Calculation of the reference evapotranspiration on an hourly basis according to Allen et al. (1998) delivered a sum of 230 mm. Since weeds akin to grass emerged at the bare soil between the rows and the juvenile grapevines had not yet a fully developed rooting system it was assumed that the real evapotranspiration was very similar to the calculated one. Consequently, the climatic water balance (rainfall minus evapotranspiration) was positive, and irrigation not necessary.

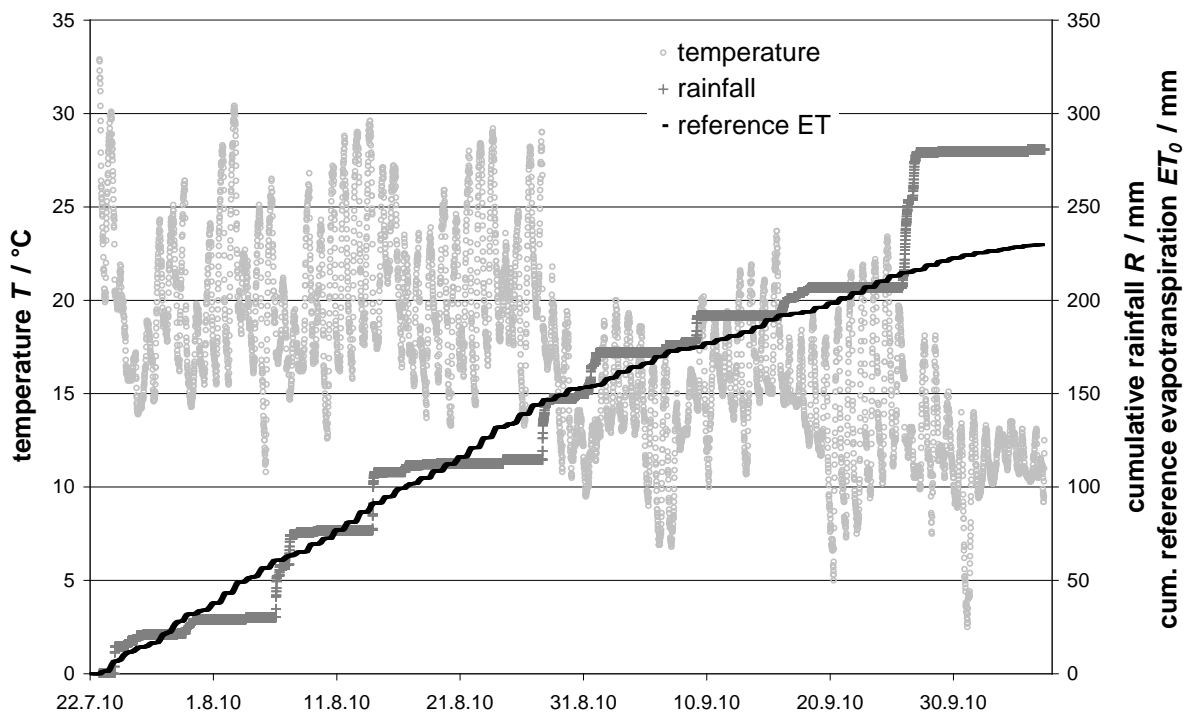


Figure 9.2: Air temperature and cumulative rainfall and reference evapotranspiration

Table 9.1 shows soil texture and hydraulic properties of the soil. Field capacity (FC) and wilting point (WP) were estimated by means of pedotransfer functions after Baumer (1989) and referred to a soil profile of 70 cm depth. The thresholds for irrigation management were defined as follows: onset of stress (OS) at 50 % of available water according to Doorenbos et

al. (1979); full point (FP) at 80 % of available water in order to spare some storage capacity for a possible rainfall event.

Table 9.1: Soil texture, hydraulic properties and thresholds for irrigation management

Sand	42 %	Field Capacity	app. 160 mm
Silt	38 %	Full Point	app. 150 mm
Clay	20 %	Onset of Stress	app. 130 mm
		Wilting Point	app. 100 mm

The FDR-probe measured soil water content in seven depths (10, 20, 30, 40, 50, 60 and 70 cm). Each sensor had a vertical range of about 10 cm. Hence, the sum of the readings represents the cumulative water storage in a soil profile from 5 to 75 cm depth (Figure 9.3).

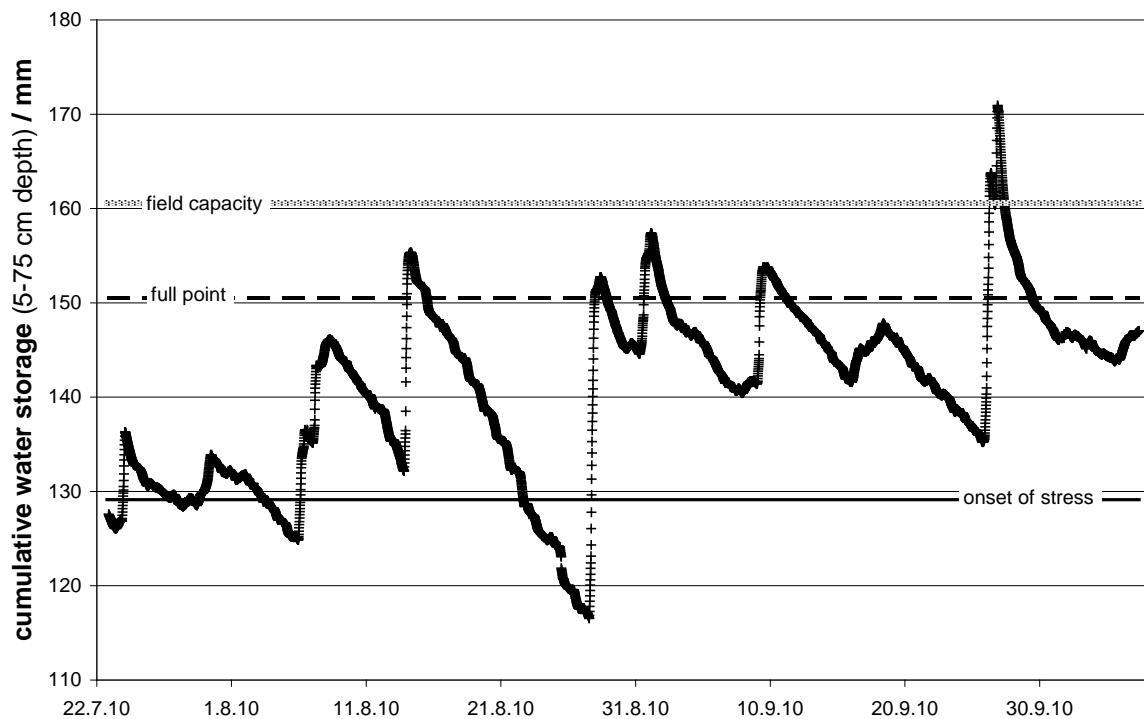


Figure 9.3: Cumulative water storage in a soil profile calculated from FDR measurements in seven depths, and thresholds for irrigation management

Soil water was below the “onset of stress”-threshold three times (Figure 9.3). However, even in the period with the biggest drop of soil water from 23rd to 27th of August, the graph shows constant steps of plant water uptake, which indicates sufficient water reserves. Hence, this situation should be verified by additional data.

Figure 9.4 shows the readings of the watermark sensors. For the juvenile grapevines the “onset of stress”-threshold was defined at 300 hPa (Kriedemann and Goodwin, 2003). This value was exceeded by two sensors at 10 and 30 cm soil depth on 24th August, while at 50 cm depth there was obviously still enough water. Nevertheless, in order not to stress the young plants, this would have been the right time to irrigate. In fact, the irrigation was started on 27th August, but had to be stopped shortly after due to beginning rainfall.

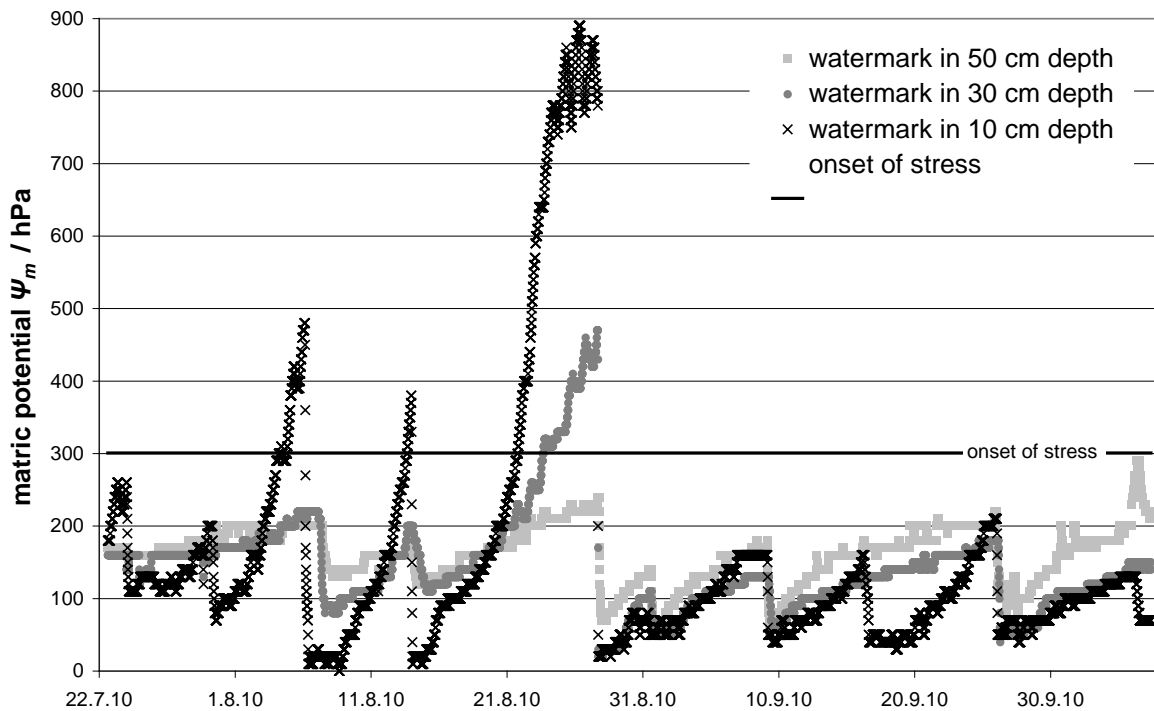


Figure 9.4: Readings of watermark sensors in three depths

9.4 Conclusions

The handling of the data as well as the remote system itself was fairly easy. The combined database of weather- and soil water data provided a sound decision support system for irrigation management. However, the thresholds for irrigation management, mainly “onset of stress”, have to be discussed in detail. Improvements are necessary mainly regarding data interpretation, since a lot of knowledge and experience is presumed from users. The irrigation system itself could not be evaluated during this first project year.

Acknowledgements

This work was supported by „Universitätsfonds der Wirtschaftskammer Wien“ in the frame of the „Wirtschaftskammerpreis 2010“ and COIN Program of the Austrian Research Promotion

Agency (FFG): Innovative Approaches to the Subsurface Drip Irrigation (SINAPSIS, PN822826). Special thanks to the staff of Adcon Telemetry GmbH, Klosterneuburg.

9.5 References

- Adcon, 2010. Information on Adcon wireless sensor networks. Adcon Telemetry GmbH, Klosterneuburg, Austria, <http://www.adcon.at>.
- Allen R.G., Pereira L.S., Raes D., Smith M. (1998): Crop Evapotranspiration: Guidelines for computing crop water requirements. In: FAO Irrigation and Drainage Paper 56, Food and Agriculture Organization of the United Nations, Rome (Italy).
- Baumer O.W. (1989): Predicting Unsaturated Hydraulic Parameters. In van Genuchten M., Th. und F.J. Leij. Indirect Methods for Estimating the Hydraulic Properties of Unsaturated Soils. Proceedings of the International Workshop on Indirect Methods for Estimating the Hydraulic Properties of Unsaturated Soils, Riverside, California, October 11-13.
- Camp C.R., Lamm F.R., Evans R.G., Phene C.J. (2000): Subsurface drip irrigation – past, present, and future. National irrigation symposium – Proceedings of the 4th Decennial Symposium, Phoenix, Arizona, USA, 363-372.
- Cepuder P., Nolz R. (2007): Irrigation management by means of soil moisture sensor technologies. In: Polish Academy of Science, Committee for Land Reclamation and Environmental Engineering in Agriculture, Journal of Water and Land Development 11: 79-90.
- Doorenbos J., Kassam A.H., Bentvelsen C.L.M., Branscheid V., Plusje J.M.G.A. (1979): Yield response to water. In: FAO Irrigation and Drainage Paper 33, Food and Agriculture Organization of the United Nations, Rome (Italy).
- Kriedemann P.E., Goodwin I. (2003): Regulated Deficit Irrigation and Partial Rootzone Drying, Irrigation Insights No. 4, Land & Water Australie, Canberra, Australien
- Paltineanu I.C., Starr J.L. (1997): Real-time soil water dynamics using mulitsensor capacitance probes: Laboratory calibration. Soil Sci. Soc. Am. J. 61: 1576-85.
- Pereira L.S., Oweis T., Zairi A. (2002): Irrigation management under water scarcity. Agr. Water Manage. 57: 175-206.
- Scanlon B.R., Jolly I., Sophocleous M., Zhang L. (2007): Global impacts of conversions from natural to agricultural ecosystems on water resources: Quantity versus quality. Water Resour. Res. 43: W03437.

10 Summary

10.1 Performance assessment of a weighing lysimeter facility and evaluation of adapted interpretation tools with respect to enhanced data management

The weighing lysimeter facility at the experimental site of the University of Natural Resources and Life Sciences, Vienna (BOKU) in Groß-Enzersdorf, Austria (48°12'N, 16°34'E; 157 m) was established in 1983 for determination of water balance components such as evapotranspiration and seepage water. In order to meet current standards, the weighing system and peripheral equipment were partly renewed, and data management was gradually adapted during the past years. In this regard, it became necessary to assess system performance and enhance data interpretation of the two large lysimeters.

Each lysimeter operates with a lever-arm-counterbalance-weighing system. Experiments have shown that the weighing system itself is subject to mechanical oscillations with more or less irregular amplitudes that are affected by disturbances, especially wind gusts. The latter proved to significantly decrease measuring accuracy. However, no linear relation was found between wind velocity and accuracy, but rather a stepwise change. The measuring accuracy for a wind velocity $<5 \text{ m}\cdot\text{s}^{-1}$ was approximately $\pm 0.4 \text{ kg}$ (equivalent to $\pm 0.14 \text{ mm}$ water ponding), at higher wind velocities the accuracy was about three times lower. A loading-unloading-experiment for evaluating the calibration delivered proper results of the measured loads. The weighing system reacted immediately to changes, but small changes (app. $\pm 0.5 \text{ kg}$) could hardly be determined due to the oscillations.

Therefore, data processing was analyzed. The applied standard procedure was that lysimeter mass was determined every 2 seconds; from raw data moving average of 64 values was computed and stored in 10-minutes-intervals. By using data from special measurements, theoretical verification was obtained to increase the accuracy by modifying the averaging process. It was shown that taking into account more values for averaging improved the accuracy, but was limited by the desired temporal resolution (measuring interval). A standard accuracy for lever-arm lysimeters with 1 m^2 surface area was found to be 0.1 mm according to literature, which seems to be an acceptable compromise for the investigated weighing lysimeter with 2.85 m^2 surface area (at normal wind conditions). Hence, an averaging of 150 values of 2-seconds-measurements and a temporal resolution (storage interval) of 30 minutes is recommended.

However, it has to be taken into account that the wind-affected inaccuracy may be about three times higher, demanding optional data processing. A natural cubic approximation spline and a basic piecewise sigmoid function were tested on a dataset of partly noisy weighing data. The sigmoid function was straightforward to fit, and it gave sound results of typical diurnal variations of evapotranspiration. However, its application was restricted to

datasets of single days without rainfall. The spline function performed generally better, except for one day (out of 28) with very noisy data. The spline-application was more user-friendly, because it could be calculated for the whole dataset in one work process. On the other hand, it was sometimes necessary to make a time-consuming adjustment to the smoothing factor. Generally, both smoothing methods provided a sound option for enhancing interpretation of noisy lysimeter weighing data. A main advantage was seen in investigations focusing on shorter than daily time intervals.

The main results of this study are transferable to similar lysimeter facilities; however, the oscillation behavior of a lysimeter system depends mainly on lysimeter size and wind conditions. Accordingly, it is recommended to adapt data processing to the local situation.

10.2 Performance assessment of approved as well as novel soil water sensors integrated into a remote monitoring network

Two types of matric potential sensors were integrated into a wireless monitoring network, calibrated and tested in the laboratory. One sensor was the well-established Watermark by Irrrometer Co., which is commonly used for soil water monitoring, particularly for irrigation scheduling. The other sensor was the MPS-1 by Decagon Devices Inc., which has a wider measuring range than the Watermark and was relatively new when the experiments started. Furthermore, two multi-sensor capacitance probes for measuring water content in different depths of a soil profile were compared at the experimental site of the University of Natural Resources and Life Sciences, Vienna (BOKU) in Groß-Enzersdorf, Austria (48°12'N, 16°34'E; 157 m). The well-known EnviroSCAN by Sentek Pty. Ltd. with its standard RT6-logger served as reference. EnviroSCAN probes are commonly used for soil water monitoring as basis for irrigation management. AquaCheck soil moisture probes by AquaCheck Soil Moisture Management operate with an identical principle and are used in the same subject areas. An AquaCheck probe was integrated into a wireless monitoring network and tested. At the time when the test started this probe represented a novel and cost-efficient alternative.

The integration of the sensors into the wireless monitoring network worked well. Three matric potential sensors of each type were connected to one analog-to-digital-interface that was connected to a Remote Terminal Unit (RTU). The AquaCheck probe was directly connected to a RTU. Data were logged, transmitted over several kilometers and made available via an Internet connection.

Six Watermark sensors were calibrated in a pressure plate apparatus in order to determine a general calibration for the sensors in combination with the interface. A function was fitted to pairs of sensor readings and equilibrium pressures. The mean 2- σ -error of the sensor measurements was 14 % in the calibration range from 10 kPa to 300 kPa. This accuracy was considered to be sufficient for several purposes, especially for irrigation management. The advantage of this general calibration function is that single sensors can be replaced easily.

However, sensor specific calibrations are recommended to improve measurement accuracy. For the MPS-1 sensor specific calibrations became essential due to very high inter-sensor-variability. Six MPS-1 were calibrated in a pressure plate apparatus, and as a basic approach a standard power function was fitted to the data pairs. Furthermore, a retention function was fitted representing a more soil physical approach. Both methods delivered proper calibrations with high accuracies. A sound alternative was found in a so-called one-point calibration after Malazian et al. (2011). Although the results were less accurate, this approach seems to be very valuable for practical application, because only one data pair (equilibrium pressure/sensor reading) is needed for calibration, which makes the method less time consuming. The factory calibration was not useful at all. After calibration, a set with three sensors of each type was installed in a thin soil layer in the laboratory in order to compare the water potential measurements during drying. Both sensor types delivered water potential measurements in a range from 10 kPa to 600 kPa. At pressures >130 kPa the Watermark sensors responded significantly slower than the MPS-1, probably due to reaching equilibrium status faster with the thin ceramic disk of the MPS-1.

EnviroSCAN probes are standard devices for measuring soil water content, thus, one served as reference for this study. However, it has to be kept in mind that also EnviroSCAN measurements may not be accurate. The AquaCheck as well the EnviroSCAN probe consisted of multiple sensors in different depths. A pairwise comparison of sensor readings in the respective depth showed considerable variations between single sensors of the AquaCheck probe despite factory normalization. Since soil type was the same within the profile, sensor normalization should be improved, or sensor-specific calibrations should be performed in order to deal with this rather unusual inter-sensor-variability of AquaCheck. Furthermore, AquaCheck readings were more overly sensitive to irrigation and rainfall, possibly due to a propensity for preferential flow in the installation method. Additionally, AquaCheck readings were correlated to EnviroSCAN water content data via specific functions for direct comparison. The modified AquaCheck graphs fitted well in a period for calibration, but diverged during an evaluation period. Further studies are recommended to explain these time-dependent variations. Additional AquaCheck probes should be tested with respect to consistency of measurements.

10.3 Performance assessment of a field weather station with respect to estimation of evapotranspiration

Data of a remote field weather station (ADCON) that are used for calculation of evapotranspiration were compared to reference data from a nearby weather station of the Austrian Central Institute for Meteorology and Geodynamics (ZAMG).

The remote station on the field plot delivered continuous data (weather and automatically calculated reference evapotranspiration ET_{ref}) that were available via internet at any time. Both datasets (ADCON and ZAMG) provided a sound basis for calculating ET_{ref} on hourly

basis. Generally, the characteristics of the respective parameters of both weather stations were similar. ET_{ref} was feasible in both cases. Nevertheless, the calculation procedures should be compared in detail in order to verify if slightly different results occurred only due to different input data.

10.4 Performance assessment of the serviceability of a sophisticated remote monitoring station for irrigation management

Data from a field station that was equipped with weather instruments and soil water sensors served as basis for irrigation management of a subsurface drip irrigation system.

The handling of the data as well as the remote system itself was fairly easy. The combined database of weather- and soil water data provided a sound decision support system for irrigation management. However, the set thresholds for irrigation management, mainly “onset of stress”, have to be discussed in detail. Further improvements are necessary mainly regarding data interpretation, since a lot of knowledge and experience is presumed from users.

11 General references

- Adcon, 2011. Information on Adcon wireless sensor networks. Adcon Telemetry GmbH, Klosterneuburg, Austria, <http://www.adcon.at>. online on Nov. 1, 2011
- Allen R.G., Pereira L.S., Raes D., Smith M., 1998. Crop Evapotranspiration: Guidelines for computing crop water requirements. In: FAO Irrigation and Drainage Paper 56, Food and Agriculture Organization of the United Nations, Rome (Italy).
- AquaCheck, 2008. AquaCheck probe Instruction manual, version 1.5, AquaCheck Pty. Ltd., 2008
- CAWMA, 2007. Water for Food, Water for Life: A Comprehensive Assessment of Water Management in Agriculture. London: Earthscan, and Colombo: International Water Management Institute.
- Centeno A., Baeza P., Lissarrague J.R., 2010. Relationship between soil and plant water status in wine grapes under various water deficit regimes. *Horttechnology* 20, 585-593.
- Cepuder P., Nolz R., 2007. Irrigation management by means of soil moisture sensor technologies. In: Polish Academy of Science, Committee for Land Reclamation and Environmental Engineering in Agriculture, *J. Water Land Dev.* 11, 79-90.
- Charlesworth P., 2005. Soil water monitoring. *Irrigation Insights* No. 1, 2nd ed. (Land and Water Australia)
- Cronje R.B., Mostert P.G., 2010. A holistic approach to improve Litchi orchard management in South Africa. In: Proc. 3rd IS on Longan, Lychee & other fruit trees in Sapindaceae family, Eds.: Qiu Dongliang et al., *ISHS 2010, Acta Hort.* 863, 433-436.
- Decagon Devices, 2009. Dielectric Water Potential Sensor MPS-1. Operator's Manual Version 3.0. Decagon Devices, Inc. 2350 NE Hopkins Court, Pullman, WA 99163.
- Doorenbos J., Kassam A.H., Bentvelsen C.L.M., Branscheid V., Plusje J.M.G.A., 1979. Yield response to water. In: FAO Irrigation and Drainage Paper 33, Food and Agriculture Organization of the United Nations, Rome (Italy).
- Doorenbos J., Pruitt W.O., 1977. Guidelines for predicting crop water requirements. In: FAO Irrigation and Drainage Paper 24, Food and Agriculture Organization of the United Nations, Rome (Italy).
- Fares A., Alva A.K., 2000. Evaluation of capacitance probe for monitoring soil moisture content in a sandy Entisol profile with citrus trees. *Irrigation Sci.* 20, 1-8.
- Feltrin R.M., de Paiva J.B.D., de Paiva E.M.C.D., Beling F. A., 2011. Lysimeter soil water balance evaluation for an experiment developed in the Southern Brazilian Atlantic Forest region. *Hydrol. Process.* 25, 2321-2328.

- Himmelbauer M., Rieckh H., Loiskandl W., 2011. Soil Water and Turfgrass Growth under defined Climate and Soil Conditions. In: Stredova H, Roznovsky J, Litschmann T (Eds.), Microclimate and mesoclimate of landscape structures and anthropogenic environment
- Huntington T.G., 2006. Evidence for intensification of the global water cycle: review and synthesis. *J. Hydrol.* 319, 83-95.
- Jones H.G., 2007. Monitoring plant and soil water status: established and novel methods revisited and their relevance to studies of drought tolerance. *J. Exp. Bot.* 58, 119-130.
- Knappe S., Haferkorn U., Meissner R., 2002. Influence of different agricultural management systems on nitrogen leaching: results of lysimeter studies. *J. Plant Nutr. Soil Sci.* 165, 73-77.
- Leib B., Jabro J., Matthews G., 2003. Field evaluation and performance comparison of soil moisture sensors. *Soil Sci.* 168, 396-408.
- Loos C., Gayler S., Priesack E., 2007. Assessment of water balance simulations for large-scale weighing lysimeters. *J. Hydrol.* 335, 259-270.
- Malazian A., Hartsough P., Kamai T., Campbell G., Cobos D., Hopmans J., 2011. Evaluation of MPS-1 soil water potential sensor. *J. Hydrol.* 402, 126-134.
- Marek T., Piccinni G., Schneider A., Howell T., Jett M., Dusek D., 2006. Weighing lysimeters for the determination of crop water requirements and crop coefficients. *Appl. Eng. Agric.* 22, 851-856.
- Murungu F.S., Chiduza C., Muchaonyerwa P., Mnkeni P.N.S., 2011. Mulch effects on soil moisture and nitrogen, weed growth and irrigated maize productivity in a warm-temperate climate of South Africa. *Soil Till. Res.*, 112, 58-65.
- Neuwirth F., Mottl W., 1983. Errichtung einer Lysimeteranlage an der agrar-meteorologischen Station in Groß-Enzersdorf. *Wetter und Leben* 35, 48-53.
- Nolz R., Kammerer G., Cepuder P., 2011. Datenmanagement der wägbaren Lysimeter in Groß-Enzersdorf. In: LFZ Raumberg-Gumpenstein (ed.): Proceedings of the 14th Lysimeter Conference, Gumpenstein, Austria, 3.-4. May 2011, 33-38.
- Pereira L.S., 1999. Higher performances through combined improvements in irrigation methods and scheduling: a discussion. *Agr. Water Manage.* 40, 153-169.
- Pereira L.S., Oweis T., Zairi A., 2002. Irrigation management under water scarcity. *Agr. Water Manage.* 57, 175-206.
- Scanlon B.R., Jolly I., Sophocleous M., Zhang L., 2007. Global impacts of conversions from natural to agricultural ecosystems on water resources: Quantity versus quality. *Water Resour. Res.* 43, W03437
- Sentek, 1997. EnviroSCAN hardware manual, version 3.0 July 1997
- Shock C.C., Feibert E.B.G., 2002. Deficit irrigation of potato. In: Food and Agricultural Organization of the United Nations (FAO) (Ed.), Deficit Irrigation Practices. Rome, Italy, 47-56.

- Steele D.D., Stegman E.C., Knighton R.E., 2000. Irrigation management for corn in the northern Great Plains, USA. *Irrigation Sci.* 19, 107-114.
- Thompson R.B., Gallardo M., Aguera T., Valdez L.C., Fernandez M.D., 2006. Evaluation of the Watermark sensor for use with drip irrigated vegetable crops. *Irrigation Sci.* 24, 185-202.
- Thompson R.B., Gallardo M., Valdez L.C., Fernandez M.D., 2007a. Determination of lower limits for irrigation management using in situ assessments of apparent crop water uptake made with volumetric soil water content sensors. *Agr. Water Manage.* 92, 13-28.
- Thompson R.B., Gallardo M., Valdez L.C., Fernandez M.D., 2007b. Using plant water status to define threshold values for irrigation management of vegetable crops using soil moisture sensors. *Agr. Water Manage.* 88, 147-158.
- van Genuchten, M.Th., 1980. A closed-form equation for predicting the hydraulic conductivity of unsaturated soils. *Soil Sci. Soc. Am. J.* 44, 892-898.
- Vellidis G., Tucker M., Perry C., Wen C., Bednarz C., 2008. A real-time wireless smart sensor array for scheduling irrigation. *Comput. Electron. Agr.* 61, 44-50.
- von Unold G., Fank J., 2008. Modular design of field lysimeters for specific application needs. *Water, Air, & Soil Pollution, Focus* 8, 233-242.
- Vaughan P.J., Trout T.J., Ayars J.E., 2007. A processing method for weighing lysimeter data and comparison to micrometeorological ETo predictions. *Agr. Water Manage.* 8, 141-146.
- Wegehenkel M., Zhang Y., Zenker T., Diestel H., 2008. The use of lysimeter data for the test of two soil-water balance models: A case study. *J. Plant Nutr. Soil Sci.* 171, 762-776.
- Xiao H., Meissner R., Seeger J., Rupp H., Borg H., 2009. Testing the precision of a weighable gravitation lysimeter. *J. Plant Nutr. Soil Sci.* 172, 194-200.

12 List of tables

Table 4.1. Exemplary computations of mass changes from weighing data and calibration factor ($m_{lys} = W_{lys} \cdot c_{lys}$), and conversion into water equivalent ($m_{lys} \cdot A_{lys}^{-1}$).....	9
Table 4.2. Overview on the experiments carried out at the lysimeter station.....	10
Table 4.3. Statistical characteristics of two selected days with different wind velocities	14
Table 4.4. Number of values for computing the average from weighing data and the respective maximum error	19
Table 5.1: Daily data of precipitation (irrigation), wind velocity, and performance of smoothing functions for the entire investigated period.....	29
Tab. 6.1: Coefficients a , and b of a standard calibration function $\psi_m = a \cdot U^b$, and coefficients of determination (R^2) for the five tested MPS-1	48
Tab. 6.2: Optimized parameters for the sensor calibration (θ_r , θ_s , α , and n) based on the retention function of the MPS-1 ($a = 0.002$ and $b = -0.833$).....	48
Tab. 6.3: Root Mean Square Error (RMSE / kPa) and Mean Relative Error (MRE / %) of five MPS-1 sensors (S1, 2, 4, 5, and 6) at six equilibrium pressures (20, 50, 100, 200, 300 and 400 kPa), for each calibration method.....	50
Table 7.1: Root mean squared error (RMSE / %) of AC versus ES for sensors in six depths in calibration period (July 2009 to December 2010), and evaluation period (January to December 2011)	64
Tab. 8.1: Mean of the respective parameters from both measuring sites for the entire period (23.7.-31.12.2010) and the first week (23.7.-31.7.2010), respectively	69
Table 9.1: Soil texture, hydraulic properties and thresholds for irrigation management.....	78

13 List of figures

Figure 4.1. Lysimeter weighing facility: a small fraction of the total mass is transmitted to an electronic load cell via a lever-arm mechanism with a counterweight.....	8
Figure 4.2: Data processing	9
Figure 4.3: Mean daily wind velocity with standard deviation (bars) in the period 1999-2009, and mean daily wind velocity 2009 (crosses), measured at the lysimeter station in Groß-Enzersdorf, Austria	12
Figure 4.4: Lysimeter weighing data and wind velocity in 10-minute-intervals in the investigated period from September 23 to October 22, 2009	13
Figure 4.5: Weighing data with smoothing function (a) on a day with low wind velocity, 2009-10-03; (b) on a day with high wind velocity, 2009-10-13.....	14
Figure 4.6: Residuals between smoothing function and weighing data in relation to wind velocity; the grey lines indicate the accuracy of the load cell (± 0.2 kg).....	15
Figure 4.7: Oscillating effect of the weighing system after manual disturbing pulse: 6 seconds in detail (a), and 10 minutes of fading (b) – the small window shows the last 3 minutes with enlarged y-axis	16
Figure 4.8: Testing the mechanical performance of the weighing facility with a stepwise loading-unloading-experiment.....	16
Figure 4.9: Evaluation of calibration and system accuracy during the loading-unloading-experiment: mass changes in kg (squares) with linear trend (thick line) and 1:1 line (thin line)	17
Figure 4.10: (a) Weighing signal: the black line displays the moving average $Y_{i,64}$ (maximum = 0.37 kg); (b) Wind velocity measured every 2 seconds 0.75 m above ground (thin grey line), measured every minute in 10 m (thin black line), and mean of 10 minutes in 10 m (thick black line)	18
Figure 5.1: Lysimeter weighing facility: via a lever-arm mechanism with a counterweight a proportional fraction of the total mass is transmitted to an electronic load cell	24
Figure 5.2: Scheme of data transmission and storage	25
Figure 5.3: Calibration of the weighing system.....	26
Figure 5.4: (a) Lysimeter weighing data, cumulated daily precipitation, and (b) wind velocity during the entire investigated period	28
Figure 5.5: Sigmoid and spline smoothing on a day without rainfall and low wind velocity ...	30
Figure 5.6: Sigmoid and spline smoothing on a day without rainfall and varying wind conditions that caused outliers in weighing data	31

Figure 5.7: Sigmoid and spline smoothing of significantly noisy weighing data	31
Figure 5.8: Hourly evapotranspiration ET on day 2009-10-13, calculated based on original data and both smoothing functions	32
Figure 5.9: Spline smoothing on a day with low rainfall and low wind velocity	32
Figure 5.10: Spline smoothing on a day with rainfall and varying wind conditions	33
Figure 5.11: Spline smoothing on a day with high wind velocity and snowfall	33
Fig. 6.1. Pressure plate apparatus with Watermark sensors (left) and MPS-1 (right)	40
Fig. 6.2. Readings of three Watermark sensors and two repetitions at several equilibrium pressures in the pressure pot (boxes = mean, bars = $2\text{-}\sigma$ -error)	45
Fig. 6.3. Watermark calibration function (line) with transformed mean $2\text{-}\sigma$ -error (thin lines) and measured data pairs (boxes).....	45
Fig. 6.4. (a) MPS-1 readings in air: Noisy output signal before modification and stable values after modification; (b) MPS-1 readings in air and water (after modification).....	46
Fig. 6.5. MPS-1 readings in the pressure plate apparatus: (a) series 1 (equilibrium pressures: 50, 100, 150, 200, 250, and 300 kPa), (b) series 2 (equilibrium pressures: 20, 50, 100, 200, 300, and 400 kPa)	47
Fig. 6.6. Consistency test of MPS-1 readings: measuring series 1 (x-axis) versus 2 (y-axis)	47
Fig. 6.7. Sensor-specific calibration functions (fitted standard function, fitted retention function and one-point calibrations) and sensor readings of five sensors at six equilibrium pressures.....	49
Fig. 6.8. Calibrated matric potentials (factory calibration, standard function, retention function, and one-point calibrations) of five sensors at six equilibrium pressures	49
Fig. 6.9. Comparison of both sensor types during three wetting-drying-cycles; Three Watermarks (WM) and three MPS-1 (S2, S3, and S6) were installed in a 6 cm soil layer. ...	51
Fig. 6.10. Calibrated matric potentials: Watermark versus MPS-1.....	51
Figure 7.1: Sensor readings from AquaCheck (ACU) and EnviroSCAN (θ_{ES}) in 10 cm.....	59
Figure 7.2: Sensor readings from AquaCheck (ACU) and EnviroSCAN (θ_{ES}) in 20 cm.....	59
Figure 7.3: Sensor readings from AquaCheck (ACU) and EnviroSCAN (θ_{ES}) in 30 cm.....	59
Figure 7.4: Sensor readings from AquaCheck (ACU) and EnviroSCAN (θ_{ES}) in 50 cm.....	60
Figure 7.5: Sensor readings from AquaCheck (ACU) and EnviroSCAN (θ_{ES}) in 70 cm.....	60
Figure 7.6: Sensor readings from AquaCheck (ACU) and EnviroSCAN (θ_{ES}) in 100 cm.....	60
Figure 7.7: Correlation between AC sensor readings and water content measured with ES in six depths (10, 20, 30, 50, 70, and 100 cm)	61

Figure 7.8: Correlation between AC and ES in all depths.....	62
Figure 7.9: Water content measured with AC and ES sensors in 10 cm	62
Figure 7.10: Water content measured with AC and ES sensors in 20 cm.....	63
Figure 7.11: Water content measured with AC and ES sensors in 30 cm.....	63
Figure 7.12: Water content measured with AC and ES sensors in 50 cm.....	63
Fig. 8.1: Measuring station with RTU, solar panel and weather instruments (photo: R. Nolz)	68
Fig. 8.2: Annual rainfall and mean annual temperature of the past 15 years	69
Fig. 8.3: Air temperature T – characteristics and correlation of both measuring sites.....	70
Fig. 8.4: Relative Humidity RH – characteristics and correlation of both measuring sites.....	70
Fig. 8.5: Air pressure p – characteristics and correlation of both measuring sites	71
Fig. 8.6: Wind velocity u_2 – characteristics and correlation of both measuring sites	71
Fig. 8.7: Solar radiation R_s – characteristics and correlation of both measuring sites.....	71
Fig. 8.8: Cumulated rainfall R of both measuring sites at the end of July	72
Fig. 8.9: Cumulated rainfall and ET_{ref} for the entire study period (23.7.-31.12.2010)	72
Figure 9.1: Measuring station with RTU, solar panel, weather sensors, FDR-probe (white cap) and three watermark sensors in 10, 30 and 50 cm depth.....	76
Figure 9.2: Air temperature and cumulative rainfall and reference evapotranspiration	77
Figure 9.3: Cumulative water storage in a soil profile calculated from FDR measurements in seven depths, and thresholds for irrigation management.....	78
Figure 9.4: Readings of watermark sensors in three depths.....	79